DYNAMIC ANALYSIS OF BEAMS AND PLATES WITH ARBITRARY SHAPES AND BOUNDARY CONDITIONS USING UNDETERMINED MULTIPLIERS

BY

MAHMOUD KAOUD

A DISSERTATION PRESENTED TO THE GRADUATE SCHOOL
OF THE UNIVERSITY OF FLORIDA IN PARTIAL FULFILLMENT OF
THE REQUIREMENTS FOR THE DEGREE OF
DOCTOR OF PHILOSOPHY

UNIVERSITY OF FLORIDA

2000

ACKNOWLEDGEMENTS

I would like to express my deep thanks and appreciation to my advisor, the chairman of the supervisory committee, professor Ali A. Seireg for his guidance, advice and support throughout the research.

I would like also to express my appreciation and thanks to the members of my Ph.D. committee, from whom I also learned during my academic journey, Professor Joseph Duffy, Professor John Ziegert, Professor Carl Crane and Professor Fazil T. Najafi for their advice, comments and suggestions.

My deep appreciation and love are to my wife for her encouragement and enduring patience throughout this study. My deep appreciation and love are also to my family who encourage me to study throughout my life.

TABLE OF CONTENTS

page

ACKNOWLODGEMENT ii

ABSTRACT vi

CHAPTERS

1. INTRODUCTION 1

Statement of The Problem 1
Review of The Literature 1
Definitions 4

2. THE PROCEDURE 6

General Formulation For the Approach 6
The Procedure of Calculating ω_n 8
The Procedure of dealing with Sinusoidal Concentrated Force 9
The Procedure of dealing with Sinusoidal Uniformly Distribution Force 10

3. APPLICATIONS TO BEAM PROBLEMS 11

Determining the Energies Using Sinusoidal Series Function 12
Determining the Energies Using Full Fourier Series Function 14

4. SAMPLE CALCULATIONS FOR BEAM PROBLEMS 16

Beam with Simple supported ends 16
Results 18
Beam with Clamped- Simple Supported ends 22
Results 26
Beam with Clamped-Clamped edges 29
Results 33
Beams with Clamped-Free edges 37
Result 42
Multi Span Beam 45
Result 47

5. APPLICATIONS TO PLATE PROBLEMS 50

6. ILLUSTRATIVE EXAMPLES 55

Plates with Simply-Supported Edges in x and y directions 55
Result 58
Plates with Two Clamped Edges in y direction and Simply Supported in the x direction 62
Result 67
Plates with One Clamped Edge in y direction at x=0 and Simply supported at the other edges 72
Result 75
Plate Clamped in All Edges 79
Result 82
Plate with Mixed Boundary Conditions 87
Result 88
Comparison with the Published Results 93

7. PLATE WITH ARBITRARILY SHAPE 95

Circular Plate 95
Result 97
Elliptical Plate 103
Result 105

8. PLATES WITH HOLES 111

Rectangular plate with Circular hole 111
Result 113

9. PLATE WITH STIFFENERS 119

Rectangular Plate with J Stiffeners 120
Result 121

10. HONEYCOMB STRUCTURE 126

Sandwich Plate with Four Stiffeners 126
Result 130

11. PLATE WITH ARBITRARY SHAPE AND BOUNDARY CONDITIONS 136

Triangular Plate with Internal Support 136
Result 139

12. BOX-STRUCTURE 146

An Open Structure with Four Rectangular Plates 146
Result 148

13. SUMMARY, CONCLUSIONS AND RECOMMENDATIONS 153

Summary 153
Conclusion 154
Recommendations 155

REFERENCES 157

BIOGRAPHICAL SKETCH 160

Abstract of Dissertation Presented to the Graduate
School of the University of Florida in Partial Fulfillment
of the Requirements for the Degree of Doctor of
Philosophy

DYNAMIC ANALYSIS OF BEAMS AND PLATES WITH ARBITRARY SHAPES AND BOUNDARY CONDITIONS USING UNDETERMINED MULTIPLIERS

By

Mahmoud Kaoud

August 2000

Chair: Professor Ali A. Seireg
Major Department: Mechanical Engineering

The study reported in this dissertation investigates the use of the undetermined multipliers approach for determining the natural frequencies, natural modes and mode shapes of general elasticity problems with complex shapes and boundary conditions.

Several cases of beams with different boundary conditions, rectangular plates with different boundary conditions, plates with stiffeners, plates with holes, circular plates and elliptical plates generated from rectangular plates, plates with arbitrary shapes and arbitrary boundary conditions, plates with arbitrary shapes and internal discrete support and box structures are investigated through the use of the presented approach.

The results show that this approach provides an excellent tool for the analysis and optimum design of complex structures.

The formulation of this method has a unified character for similar problems. The simplicity and elegance of this method is particularly evident when dealing with a class of problems with different boundary conditions.

CHAPTER 1
INTRODUCTION

Statement of The Problem

This study investigates the use of undetermined multipliers with the Rayleigh-Ritz method to find the natural frequencies of general elasticity problems with complex geometries and boundary conditions. Beams and plates cases are considered for applications.

The procedure gives excellent results and can be effectively used for the dynamic analysis of elastic structures with complex boundary conditions.

Review of The Literature

Many studies are available in the literature, which deal with finding the deflections and natural frequencies of several types of beams and plates. Analytical solutions and numerical methods such as the finite element method have been used to find the deflection and the natural frequency of the beams and plates with complex boundary conditions. Numerical methods such as the Rayleigh-Ritz method are based on the assumption of a shape function. Most of the techniques dealing with the problem assume a deflection function that satisfies all the boundary conditions.

Sheikh and Mukhopadhyay [1] have applied a spline finite strip method to determine the natural frequencies of plates and stiffened plates with edges elastically restrained against translation and rotation. The Rayleigh-Ritz method has been applied by Grossi, Arenas, and Laura [2] to generate the values of the fundamental frequency for rectangular plates with circular holes elastically restrained against rotation. A shape function that satisfies the boundary conditions is assumed. Also Chang and Liang [3] have studied the free and forced vibrations of post buckled delaminated beam-plates. The natural frequencies have been determined based on the assumption of a shape function that satisfies the boundary conditions. Three dimensional elasticity solutions for free vibrations of six types of plates were investigated by Malik and Bert [4]. The solution methodology utilizes displacement functions, which satisfy the boundary conditions. Transverse vibrations of a rectangular plate with three edges elastically restrained against rotation while the forth is free are studied by Bambill, Rossi, Jederlinic, and Rossit [5]. They found the natural frequencies using an analytical solution and the finite element method. Liew and Wang [6] have studied the vibration of a class of in-plane loaded rectangular plates with internal supports of arbitrary contour. The solutions of this problem are obtained based on the Rayleigh-Ritz method.

Little has been published on the use of undetermined multipliers with the Rayleigh-Ritz method. Al-Shareedah and Seireg [7, 8, 9] have introduced this approach and found the deflection for many types of plates. Chen [10] has also investigated the use of undetermined multipliers with the Rayleigh-Ritz method to find the deflection of different cases of beam, plate, and shell problems. These appear to be no published literature on the use of undetermined multipliers with the Rayleigh-Ritz method to find the natural frequencies of elastic structures.

Many methods have been developed to investigate this problem. Among these methods, the most widely used are the Galerkin method [1], The finite difference method, the finite element method [7, 8], and the Rayleigh-Ritz method [10].

The Galerkin method provides a solution to the differential equations, and is applicable whether the transformation into a variational problem is possible or not. In other words this method can apply an approximate solution without the construction of the functional (the potential energy). Its limitations make it more difficult to apply than the Rayleigh-Ritz method [10].

The finite difference method is a purely numerical technique. The equations of motion have to be known for the structure that is to be investigated. The finite difference method is based on the argument that a derivative can be approximately replaced by a difference [11]. It is an approximate numerical procedure based on the use of approximate expressions for the derivatives of the deflection, which appear in the fundamental differential equations.

The finite element method is a very popular approach. Knowing a solution of a simple element, a shell or a plate can be assumed to be assembled from these elements. This is done by mathematically enforcing continuity and equilibrium conditions at the element node points [11]. The finite element method based on matrix-displacement analysis is extremely well suited to the computerized solution of plates and beams. Computer solutions based on the finite element method are more general and flexible than those using other numerical techniques. Arbitrary geometry, loads and boundary conditions can be handled with ease and several computer programs are available. A very large number of very small elements give a virtually continuous structures [12].

This method, however, has some disadvantages, the most important being the extensive preprocessing and post processing efforts that are required. Another disadvantage is that it is necessary to choose a very fine mesh in regions with steep stress gradients. This leads to the construction and solution of a large number of equations with a large number of unknowns. In some cases, if there is no efficient computing machine, the finite element method cannot be practically used.

The Rayleigh method consists of choosing arbitrarily a deflected shape, involving an undetermined coefficients, and using this expression for the deflection. This method allows approximate solutions to be obtained for cases involving complex boundary conditions, which make the differential equation formulation difficult or impossible to use. The boundary conditions can often be satisfied by choosing the right deflection function [12].

Definitions

SS	Beam of Simple –Simple supported edges
CS	Beam of Clamped –Simple supported edges
CC	Beam of Clamped –Clamped edges
CF	Beam of Clamped –Free edges
SSS	Multi span Beam Simply supported
SSSS	Plate of Simply Supported at all four edges
CSCS	Plate Clamped at edge x=0 and x=a and Simply supported at edges y=0, and y=b
CCCC	Plate Clamped at all four edges

CSSS	Plate Clamped at edge x=0 and Simply supported at edges where x=a, y=0, and y=b
Mix.B.C	Mixed boundary condition plate, which it is, clamped for 1/3 the width at the middle of each edge and simply supported at the remaining edges
ω	Forced Frequency
ω_n	Natural Frequency
λ	Frequency parameter of beam or plate with distributed mass
Ω	Frequency parameter of massless beam with a concentrated mass
w	Deflection
p_0	The amplitude of the applied distributed load
F_0	The amplitude of the applied concentrated force
l	The length of the beam
a	The length of the plate along x-axis
b	The width of the plate along y-axis
N	The number of approximation in the assumed function

CHAPTER 2
THE PROCEDURE

General Formulation For the Approach

Although classical theories are very successful in the analysis of many structural elements, including beams, plates, and shells, there are still many problems in these categories that are difficult to be solved by the classical methods which require the assumption of a function that satisfies all the boundary conditions. For some cases it is difficult to find a function that satisfies all conditions as in the case of a multi-span beam (a beam with many internal supports) or a plate with complex geometry or mixed boundary conditions.

The method proposed in this thesis is to use the Rayleigh-Ritz method together with the Lagrangian multiplier approach in a way that the assumed function may not necessary satisfy all the boundary conditions. The unsatisfied boundary conditions can be forced to be satisfied by using this approach.

The Rayleigh-Ritz method can be applied to find the fundamental natural frequency of all continuous systems. By assuming a harmonic function

$$w(x,t) = \sum_{n=1}^{N} a_n \Phi_n(x) \sin(\omega t) \tag{2.1}$$

the maximum of the kinetic energy T and the total potential energy U can be found. The total potential energy consists of the strain energy U_e and the potential of external work W. The total energy is

$$\prod = U - T \tag{2.2}$$

Since the potential energy is

$$U = U_e - W \tag{2.3}$$

then equation 2.2 becomes

$$\prod = U_e - W - T \tag{2.4}$$

Hence

$$\prod = \prod(a_1, a_2, a_3, \ldots\ldots., a_N) \tag{2.5}$$

Consider a problem subjected to the following unsatisfied constraints:

$$G_i(a_1, a_2, a_3, \ldots\ldots\ldots., a_N) = 0 \tag{2.6}$$

where i=1,2,3… I_c and I_c is the number of unsatisfied constraints. From equation 2.5 and equation 2.6 the Lagrangian function L can be expressed as follows:

$$L(a_1, a_2, a_3, \ldots\ldots., a_N, \lambda_1, \lambda_2, \lambda_3, \ldots\ldots., \lambda_{I_c}) =$$

$$\prod(a_1, a_2, a_3, \ldots\ldots., a_N) + \sum_{i=1}^{I_c} \lambda_i G_i(a_1, a_2, a_3, \ldots\ldots., a_N) \tag{2.7}$$

The partial derivatives of L with respect to all coefficients must equal to zero:

$$\frac{\partial L}{\partial a_n} = 0, \ \frac{\partial L}{\partial \lambda_i} = 0 \tag{2.8}$$

where $n = 1,2,3,\ldots.,N$ and $i = 1,2,3,\ldots.,I_c$. Equations 2.8 can then be solved to evaluate a_n.

The Procedure of Calculating ω_n

The procedure of calculating the natural frequency is based upon determining the deflection function and plotting its maximum value versus the forced frequency. The steps of this procedure can be repeated for any structure problem to find its natural frequency and its natural modes. These steps are as follows:

1- First the deflection is assumed as a finite series function.

2- The expressions for the strain energy, the external work and the kinetic energy can be formulated by substituting the assumed function in the energy expressions.

3- Next, the expressions for the unsatisfied constraints are obtained for any structure problems. The smaller the number of the unsatisfied constraints, the faster the convergence. Therefore, choosing a function that satisfies most of the constraints will speed the convergence.

4- The energy expressions and the unsatisfied constraints multiplied by λ_i are added together to form the Lagrangian function given in equation 2.7. The Lagrangian function will be expressed in terms of the displacement coefficients and the undetermined multipliers.

5- Taking the derivative of L with respect to the displacement coefficients a_n and the undetermined parameters λ_i, and equating them to zero, a number of equations can be obtained. The number of equations obtained are $N + I_c$.

6- These equations are then solved simultaneously to give the coefficients $a_1, a_2, a_3, \ldots, a_N$.

7- By substituting these coefficients in the assumed function the deflection function at the specified forced frequency can be found.

8- The inverse of the maximum deflection at any specific forced frequency obtained from the deflection function obtained in step 7 can be plotted versus the forced frequency. The value of the inverse of maximum absolute deflection, normalized to the static value for different forced frequencies, changes from unity at $\omega=0$ and approaches zero when resonance occurs.

The Procedure of Dealing with Sinusoidal Concentrated Force

In case of the beam, the driving force is chosen to be in the form of

$$F(t) = F_o \sin(\omega t) \tag{2.10}$$

where F_o represents the amplitude of the applied force and ω denotes the forced frequency. The external potential energy is expressed as

$$W = F_o w\big|_{x=a} \tag{2.11}$$

where a is the distance of the concentrated force along the x-axis.

In case of the plate the external potential energy is expressed as

$$W = F_o w\big|_{x=\bar{a},y=\bar{b}} \tag{2.12}$$

where F_o is the concentrated force at $x=\bar{a}$ and $y=\bar{b}$ where $\bar{a}$ and $\bar{b}$ are the coordinates of the point of application of the concentrated force.

The Procedure of Dealing with Sinusoidal Uniform Distribution Force

In case of the beam, the distributed force per unit length is chosen to be in the form

$$p(t) = p_o \sin(\omega t) \tag{2.13}$$

where p_o represents the amplitude of the applied distributed force per unit length and ω denotes the forced frequency. The external potential energy is expressed as

$$W = \int_0^a p_o w dx \tag{2.14}$$

where a is the distance over which the distributed force is applied. In case of the plate, the external potential energy is expressed as

$$W = \int_0^{\bar{b}} \int_0^{\bar{a}} p_o w dx dy \tag{2.15}$$

where p_o is the uniformly distributed force per unit area over the region defined by $x = \bar{a}$ and $y = \bar{b}$.

CHAPTER 3
APPLICATIONS TO BEAM PROBLEMS

To use this approach in beam problems, four expressions are needed to be found. These are as follows:

1. The strain energy.
2. The external potential energy.
3. The kinetic energy.
4. The boundary conditions.

For all examples discussed below, Fourier series functions are used because they can satisfy a wide variety of boundary conditions. The strain energy of the beam is

$$U_e = \frac{EI}{2} \int_0^l (w''(x))^2 \, dx \tag{3.1}$$

where the bending rigidity EI is assumed to be constant. The external potential energy is determined according to the type of load. Two types of load are used in this study. One is the concentrated force and its potential energy is expressed in equation 2.11. The other is the uniform distributed force and its potential energy is expressed in equation 2.14. The kinetic energy of the beam is

$$T = \frac{\gamma}{2} \int_0^l (\omega w(x))^2 \, dx \tag{3.2}$$

The boundary conditions at any point in the beam can be any of the following:

1. The deflection $w(x) = 0$ (3.3)

   The slope $\frac{dw(x)}{dx} = 0$ (3.4)

2. The moment $M(x) = 0$ (3.5)

$$M(x) = -EI\frac{d^2w(x)}{dx^2} \tag{3.6}$$

$$EI\frac{d^2w(x)}{dx^2} = 0 \tag{3.7}$$

3. The shear force $V(x) = 0$ (3.8)

$$V(x) = -EI\frac{d^3w(x)}{dx^3} \tag{3.9}$$

$$-EI\frac{d^3w(x)}{dx^3} = 0 \tag{3.10}$$

In the following examples, two types of assumed functions are used. These two types of functions are a Sinusoidal Series function and the Full Fourier Series function.

Determining the Energies Using Sinusoidal Series Function

The first type is

$$w(x) = \sum_{1}^{\infty} a_n \sin(\frac{n\pi}{l}x) \tag{3.11}$$

The Nth approximation of this function is simply a truncated Fourier series, and it gets closer to $w(x)$ as N increases. It is as

$$w_N(x) = \sum_1^N a_n \sin(\frac{n\pi}{l}x) \tag{3.12}$$

The strain energy using this assumed function of equation 3.12 and equation 3.1, can be written in the following form

$$U_e = \frac{EI\pi^4}{4l^3}\sum_1^N n^4 a_n^2 \tag{3.13}$$

The kinetic energy using equation 3.12 and equation 3.2, can take the following form

$$T = \frac{\gamma\omega^2 l}{4}\sum_1^N a_n^2 \tag{3.14}$$

If we consider a concentrated mass M supported on the beam, the kinetic energy due to that mass should be added to equation 3.14. The kinetic energy due to the concentrated mass is

$$T_M = \frac{\omega^2}{2} M w^2(l_m) \tag{3.15}$$

Using equation 3.12, equation 3.15 becomes

$$T_M = \frac{\omega^2}{2} M \sum_1^N a_n^2 \sin^2(\frac{n\pi l_m}{l}) \tag{3.16}$$

where l_m is location of the concentrated mass. Therefore equation 3.14 can take the following form

$$T = \frac{\omega^2}{2}\sum_1^N a_n^2 (\frac{\gamma l}{2} + M\sin^2(\frac{n\pi l_m}{l})) \tag{3.17}$$

The external potential energy for the concentrated force at x=a, using equation 3.12 and equation 2.11, is

$$W = Fw_{x=a} = F_0 \sum_{1}^{N} a_n \sin(\frac{n\pi a}{l}) \tag{3.18}$$

And the external potential energy for the uniformly distributed force along the distance a, using equation 3.12 and equation 2.14, is

$$W = \int_0^a p_o w(x) dx = p_o \sum_{1}^{N} a_n \frac{l}{n\pi}(1 - \cos(\frac{n\pi a}{l})) \tag{3.19}$$

Determining the Energies Using Full Fourier Series Function

The other type of function used in these examples is

$$w(x) = a_0 + \sum_{n=1}^{\infty} a_n \cos(\frac{n\pi x}{l}) + \sum_{m=1}^{\infty} b_m \sin(\frac{m\pi x}{l}) \tag{3.20}$$

The Nth approximation of this function, which becomes closer to $w(x)$ as N increases is

$$w(x) = a_0 + \sum_{n=1}^{N} a_n \cos(\frac{n\pi x}{l}) + \sum_{m=1}^{N} b_m \sin(\frac{m\pi x}{l}) \tag{3.21}$$

Using this assumed function of equation 3.21 the strain energy can be determined from equation 3.1 as

$$U_e = \frac{EI\pi^4}{4l^3}[\sum_{1}^{N} n^4 a_n^2 + \sum_{1}^{N} m^4 b_m^2 +$$

$$\sum_{n=1}^{N}\sum_{\substack{m=1\\ n\neq m}}^{N} a_n b_m \frac{4n^2 m^3}{\pi(n^2-m^2)}(\cos(n\pi)\cos(m\pi)-1) \tag{3.22}$$

The kinetic energy using equation 3.21 and equation 3.2, can be written in the following form

$$T=\frac{\gamma\omega^2 l}{4}[2a_0^2+\sum_{n=1}^{N}a_n^2+\sum_{m=1}^{N}(b_m^2-4a_0 b_m\frac{1}{m\pi}(1-\cos(m\pi)))+$$

$$\sum_{n=1}^{N}\sum_{\substack{m=1\\ m\neq n}}^{N}\frac{4a_n b_m m(\cos(m\pi)\cos(n\pi)-1)}{\pi(n^2-m^2)}] \tag{3.23}$$

Also, the kinetic energy due to the concentrated mass at location $x=l_m$ can be found using the assumed function of equation 3.21. It is then added to equation 3.23 to determine the total kinetic energy.

The external potential energy for the concentrated force at the position x=a, using equation 3.21 and equation 2.11, is

$$W=Fw_{x=a}=F_0[a_0+\sum_{n=1}^{N}a_n\cos(\frac{n\pi a}{l})+\sum_{m=1}^{N}b_m\sin(\frac{m\pi a}{l})] \tag{3.24}$$

And the external potential energy for the uniformly distributed load along the distance a, using equation 3.21 and equation 2.14, is

$$W=\int_0^a pw dx=\int_0^a p_0[a_0+\sum_{n=1}^{N}a_n\cos(\frac{n\pi x}{l})+\sum_{m=1}^{N}b_m\sin(\frac{m\pi x}{l})]dx \tag{3.25}$$

$$W=p_0[a_0 a+\sum_1^N a_n\frac{l}{n\pi}\sin(\frac{n\pi a}{l})-\sum_1^N b_m\frac{l}{m\pi}\cos(\frac{m\pi a}{l})] \tag{3.26}$$

CHAPTER 4
SAMPLE CALCULATIONS FOR BEAM PROBLEMS

The examples discussed below are considered to illustrate the proposed approach in this study. The effectiveness of the approach will be seen during these examples. In these illustrations, the fundamental natural frequency as well as the natural modes will be determined.

Beam with Simple Supported Ends

Consider a beam simply supported at the ends as in figure 4.1. The beam may be subjected either to a concentrated force or t a uniform distributed load.

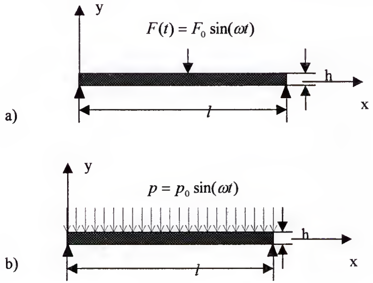

Figure. 4.1 simply supported beam with a) concentrated force b) uniform distribution load.

The boundary conditions of this case are

$$w(x) = 0 \qquad \text{At } x = 0 \text{ and } x = l \tag{4.1}$$

$$M(x) = 0 \qquad \text{At } x = 0 \text{ and } x = l \tag{4.2}$$

The assumed function for this case is as in equation 3.12. All the boundary conditions are satisfied in this case and there are no unsatisfied constraints to be dealt with for this case.

The strain energy of the beam is the same as that in equation 3.13. The kinetic energy of the beam is given in equation 3.14. In case of applying a concentrated force at the middle of the beam as in figure 4.1a, the external potential energy is determined from equation 3.15.

Considering the case of concentrated force at $x = l/2$. The total potential energy is

$$U = U_e - W \tag{4.3}$$

Substituting equation 3.23 and equation 3.21 into equation 4.3 gives the following:

$$U = \frac{EI\pi^4}{4l^3}\sum_1^N n^4 a_n^2 - p_0 \sum_1^N a_n \sin(\frac{n\pi a}{l}) \tag{4.4}$$

Since the constraints are satisfied the Lagrange function of equation 2.7 becomes

$$L = U - T \tag{4.5}$$

$$L = \frac{EI\pi^4}{4l^3}\sum_1^N n^4 a_n^2 - p_0 \sum_1^N a_n \sin(\frac{n\pi a}{l}) - \frac{\gamma\omega^2 l}{4}\sum_1^N a_n^2 \tag{4.6}$$

Taking the partial derivatives of equation 4.6 with respect to a_n and setting them equal to zero gives

$$\frac{\partial L}{\partial a_n} = 0 \tag{4.7}$$

$$\frac{EI\pi^4}{2l^3} n^4 a_n - p_0 \sin(\frac{n\pi a}{l}) - \frac{\gamma\omega^2 l}{2} a_n = 0 \tag{4.8}$$

Thus an expression for the parameter a_n is obtained as

$$a_n = \frac{2l^3 p_0 \sin(\frac{n\pi a}{l})}{EI\pi^4 n^4 - \gamma\omega^2 l^4} \tag{4.9}$$

Equation 4.9 is substituted into equation 3.12 to give the following equation:

$$w(x) = \sum_1^N \frac{2l^3 p_0 \sin(\frac{n\pi a}{l})}{EI\pi^4 n^4 - \gamma\omega^2 l^4} \sin(\frac{n\pi}{l} x) \tag{4.10}$$

Figure 4.2 and table 4.4 show the natural frequency, while the coefficients of the deflection function are shown in table 4.5.

In case of including a concentrated mass on the beam, the kinetic energy due to the concentrated mass will be added to the kinetic energy of equation 3.14.

Results

The result of this case is based upon finding the natural frequency and the modes of three types of loads. One is using a beam that has its own mass with no concentrated mass. The second type is to consider a beam that has its own mass and also a concentrated mass of 50kg. The last type is a beam that does not have a mass but has a concentrated mass of 50kg. The results of the first and third types are compared to the published results, which are shown in tables 4.1 and 4.3.

Table 4.4 shows the values of forced frequency parameter λ for N terms. The table shows the convergence as N increases for the three types of beam. Table 4.5 shows the normal modes of the three types of beam. It is clear from the table that the odd numbers in Fourier series have the effect since the even numbers go to zero.

The calculated natural frequency for the beam that has its own mass only without concentrated mass is 9.8696, which is closer to the published one, which it is 9.869604. Also, the calculated natural frequency for the beam that has a concentrated mass without its own mass is 9.92827, which is closer to the published one, which it is 9.928203.

Table 4.1 The published λ parameter [13] for the beam cases without concentrated mass where $\lambda = \omega_n \sqrt{EI / l^4 \gamma}$

	SS	FF	CC	CF	CS	SF
βl	π	4.730041	4.730041	1.875104	3.926602	3.926602
$\lambda = (\beta l)^2$	9.869604	22.373288	22.373288	3.516015	15.418203	15.418203

Table 4.2 The published stiffness k [14] for the beam.

	SS	CC	CF	CS
k	$\frac{48EI}{l^3}$	$\frac{192EI}{l^3}$	$\frac{3EI}{l^3}$	$\frac{768EI}{7l^3}$

Since $\omega_n = \sqrt{\frac{k}{M}}$ and assuming $\Omega = \omega_n \sqrt{\frac{Ml^3}{EI}}$ therefore table 4.2 can be converted to table 4.3, which defines the frequency parameter for the massless beam with a concentrated mass.

Table 4.3 The Ω parameter for the massless beam cases with a concentrated mass. It is obtained from Table 4.2, where $\Omega = \omega_n \sqrt{Ml^3 / EI}$ and M is the added mass

	SS	CC	CF	CS
Ω	6.92820323	13.8564065	1.73205081	10.4744587

Table 4.4 The λ and Ω values of SS Beam with three cases of mass distribution subjected to a concentrated force where $\lambda = \omega_n \sqrt{\gamma l^4 / EI}$, $\Omega = \omega_n \sqrt{Ml^3 / EI}$, and M is the added mass.

Beam without M				Beam with M				Massless beam with M			
N	λ	N		N	λ	N	λ	N	Ω	N	Ω
2	9.8696	12	9.8696	2	2.94171	12	2.92403	2	6.97886	12	6.92853
3	9.8696	13	9.8696	3	2.92672	13	2.92398	3	6.93618	13	6.92841
4	9.8696	14	9.8696	4	2.92672	14	2.92398	4	6.93618	14	6.92841
5	9.8696	15	9.8696	5	2.92479	15	2.92396	5	6.9307	15	6.92834
6	9.8696	16	9.8696	6	2.92479	16	2.92396	6	6.9307	16	6.92834
7	9.8696	17	9.8696	7	2.92429	17	2.92395	7	6.92928	17	6.9283
8	9.8696	18	9.8696	8	2.92429	18	2.92395	8	6.92928	18	6.9283
9	9.8696	19	9.8696	9	2.92411	19	2.92394	9	6.92876	19	6.92827
10	9.8696	20	9.8696	10	2.92411	20	2.92394	10	6.92876	20	6.92827
11	9.8696			11	2.92403			11	6.92853		

Table 4.5 Coefficients of SS Beam for three cases of mass distribution subjected to a concentrated force, and M is the added mass.

Beam without M				Beam with M				Massless beam with M			
n	a_n / a_1	n	a_n / a_1	n	a_n / a_1	n	a_n / a_1	n	a_n / a_1	n	a_n / a_1
1	1	11	1.36E-13	1	1	11	-6.23E-05	1	1	11	-6.83E-05
2	0	12	0	2	0	12	0	2	0	12	0
3	2.49E-11	13	-6.99E-14	3	-1.13E-02	13	3.19E-05	3	-1.23E-02	13	3.50E-05
4	0	14	0	4	0	14	0	4	0	14	0
5	-3.20E-12	15	3.94E-14	5	1.46E-03	15	-1.80E-05	5	1.60E-03	15	-1.98E-05
6	0	16	0	6	0	16	0	6	0	16	0
7	8.31E-13	17	-2.39E-14	7	-3.80E-04	17	1.09E-05	7	-4.16E-04	17	1.20E-05
8	0	18	0	8	0	18	0	8	0	18	0
9	-3.04E-13	19	1.53E-14	9	1.39E-04	19	-7.00E-06	9	1.52E-04	19	-7.67E-06
10	0	20	0	10	0	20	0	10	0	20	0

Table 4.6 Coefficients of SS Beam for three cases of mass distribution subjected to uniformly distributed load, and M is the added mass.

Beam without M				Beam with M				Massless beam with M			
n	a_n/a_1	n	a_n/a_1	n	a_n/a_1	n	a_n/a_1	n	a_n/a_1	n	a_n/a_1
1	1	11	-1.24E-14	1	1	11	-6.23E-05	1	1	11	-6.83E-05
2	0	12	0	2	0	12	0	2	0	12	0
3	-8.31E-12	13	-5.37E-15	3	-1.13E-02	13	3.19E-05	3	-1.23E-02	13	3.50E-05
4	0	14	0	4	0	14	0	4	0	14	0
5	-6.40E-13	15	-2.63E-15	5	1.46E-03	15	-1.80E-05	5	1.60E-03	15	-1.98E-05
6	0	16	0	6	0	16	0	6	0	16	0
7	-1.19E-13	17	-1.41E-15	7	-3.80E-04	17	1.09E-05	7	-4.16E-04	17	1.20E-05
8	0	18	0	8	0	18	0	8	0	18	0
9	-3.38E-14	19	-8.06E-16	9	1.39E-04	19	-7.00E-06	9	1.52E-04	19	-7.67E-06
10	0	20	0	10	0	20	0	10	0	20	0

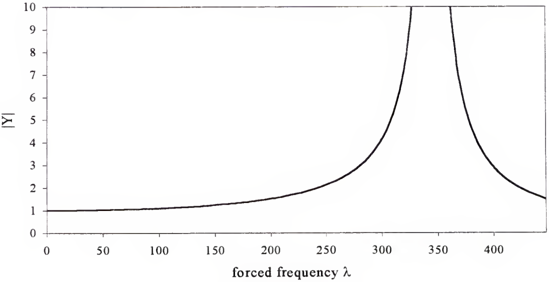

Figure 4.2 Maximum Absolute deflection versus forced frequency for a simply supported beam without M subjected to a uniformly distributed load for N=20.

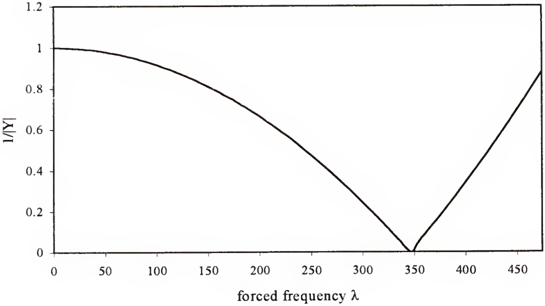

Figure 4.3 The inverse of the normalized maximum absolute deflection versus forced frequency for a simply supported beam without mass subjected to a uniformly distributed load for N=20.

Beam with Clamped-Simple Supported Ends

Consider a clamped-supported beam subjected to a concentrated force at the middle as shown in figure 4.4. Assume the deflection function to be as in equation 3.2. The strain energy, the external potential energy and the kinetic energy are given in equations 3.13, 3.14, and 3.15. The boundary conditions in this case are

$$w(x) = 0 \text{ at } x = 0 \text{ and } x = l \tag{4.11}$$

$$\frac{dw(x)}{dx} = 0 \text{ at x=0} \tag{4.12}$$

$$M(x) = 0 \text{ at x=L} \tag{4.13}$$

a)

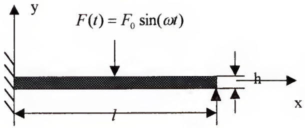

b)

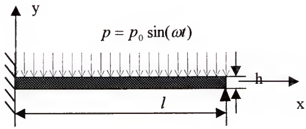

Figure 4.4 A beam clamped at one end and simply support at the other end.

The boundary conditions in this case are not all satisfied by the deflection function. The unsatisfied constraint, which corresponds to the boundary condition of equation 4.12, is

$$g_1 = \sum_{1}^{N} a_n \frac{n\pi}{l} \tag{4.14}$$

Applying the equations 3.13, 3.14, 3.15,and 4.14 into the Lagrangian function gives

$$L = \frac{EI\pi^4}{4}\sum_1^N n^4 a_n^2 - p_0 \sum_1^N a_n \sin(\frac{n\pi a}{l}) - \frac{\gamma\omega^2 l}{4}\sum_1^N a_n^2 + \lambda_1 \sum_1^N a_n n \qquad (4.15)$$

Taking the derivatives of the Lagrangian function, equation 4.15, with respect to a_n gives:

$$\frac{\partial L}{\partial a_n} = 0 \qquad (4.16)$$

Equation 4.15 and equation 4.16 give

$$a_n = \frac{2l^3 (p_0 \sin(\frac{n\pi a}{l}) - \lambda_1 \frac{n\pi}{l})}{EI\pi^4 n^4 - \gamma\omega^2 l^4} \qquad (4.17)$$

Taking the derivatives of the Lagrangian with respect to λ_1 gives

$$\frac{\partial L}{\partial \lambda_1} = 0 \qquad (4.18)$$

$$\sum_1^N a_n \frac{n\pi}{l} = 0 \qquad (4.19)$$

The undetermined multiplier λ_1 can be found by substituting equation 4.17 into equation 4.19:

$$\sum_1^N \frac{nlp_0 \sin(\frac{n\pi a}{l})}{EI\pi^4 n^4 - \gamma\omega^2 l^4} - \lambda_1 \sum_1^N \frac{n^2 \pi}{EI\pi^4 n^4 - \gamma\omega^2 l^4} = 0 \qquad (4.20)$$

The undetermined multiplier λ_1 is found as:

$$\lambda_1 = \frac{\sum_{1}^{N} \dfrac{nlp_0 \sin(\frac{n\pi a}{l})}{EI\pi^4 n^4 - \gamma\omega^2 l^4}}{\sum_{1}^{N} \dfrac{n^2\pi}{EI\pi^4 n^4 - \gamma\omega^2 l^4}} \tag{4.21}$$

The undetermined multiplier can now be readily found. By substituting its value into equation 4.17 the values of the displacement parameters can be found. Equation 4.17 is substituted into equation 3.12 to give the following equation:

$$w(x) = \sum_{1}^{N} \frac{2l^3 (p_0 \sin(\frac{n\pi a}{l}) - \lambda_1 \frac{n\pi}{l})}{EI\pi^4 n^4 - \gamma\omega^2 l^4} \sin(\frac{n\pi}{l} x) \tag{4.22}$$

The natural frequency can be found from figure 4.5 or table 4.8. If the beam is subjected to a uniformly distributed load as in figure 4.4b, equation 3.16 will be used in conjunction with equations 3.13 and 3.14 to give the Lagrangian function:

$$L = \frac{EI\pi^4}{4l^3} \sum_{1}^{N} n^4 a_n^2 - p_o \sum_{1}^{N} a_n \frac{l}{n\pi}(1 - \cos(n\pi)) -$$

$$\frac{\gamma\omega^2 l}{4} \sum_{1}^{N} a_n^2 + \lambda_1 \sum_{1}^{N} a_n \frac{n\pi}{l} \tag{4.23}$$

To find a_n and λ_1, the same steps used in the previous case are followed. The expressions for a_n and λ_1 are determined respectively as follows:

$$a_n = \frac{2l^3 (p_0 \frac{l}{n\pi}(1 - \cos(n\pi)) - \lambda_1 \frac{n\pi}{l})}{EI\pi^4 n^4 - \gamma\omega^2 l^4} \tag{4.24}$$

$$\lambda_1 = \frac{\sum_1^N \frac{p_0 \frac{l^2}{\pi}(1-\cos(n\pi))}{EI\pi^4 n^4 - \gamma\omega^2 l^4}}{\sum_1^N \frac{n^2\pi}{EI\pi^4 n^4 - \gamma\omega^2 l^4}} \tag{4.25}$$

The deflection function takes the form

$$w(x) = \sum_1^N \frac{2l^3 (p_0 \frac{l}{n\pi}(1-\cos(n\pi)) - \lambda_1 \frac{n\pi}{l})}{EI\pi^4 n^4 - \gamma\omega^2 l^4} \sin(\frac{n\pi}{l} x) \tag{4.26}$$

The natural frequency can be found as previously discussed by plotting the inverse of the maximum absolute deflection versus the forced frequency and determining the frequency where it approaches zero.

Results

Table 4.7 shows the fundamental frequency for 20 term approximations and table 4.8 shows the corresponding displacement parameters. As in the previous case, three types of beams have been investigated. The results are compared to the published results, in tables 4.1 and 4.3. For the case of a beam without a concentrated mass, the difference is 2.1% for 20 terms. The difference can be reduced by increasing N. The convergence rate is illustrated in table 4.7. Comparing the obtained values of λ and Ω to the published results, the difference is found to be 2%. This difference can be further reduced by adding more terms. The corresponding normal modes are shown in table 4.8

Table 4.7 The λ and Ω values of CS Beam with three cases of mass disrtibution subjected to a concentrated force where $\lambda = \omega_n \sqrt{\gamma l^4 / EI}$, $\Omega = \omega_n \sqrt{M l^3 / EI}$ and M is the added mass.

Beam without M				Beam with M				Massless beam with M			
N	λ	N	λ	N	λ	N	λ	N	Ω	N	Ω
2	19.7392	12	15.9658	2	6.50601	12	4.58919	2	15.6052	12	10.8332
3	17.9797	13	15.9217	3	5.14267	13	4.57936	3	12.1291	13	10.8106
4	17.2388	14	15.8842	4	4.92413	14	4.5687	4	11.6157	14	10.7856
5	16.8298	15	15.8519	5	4.86064	15	4.55762	5	11.4762	15	10.7592
6	16.5705	16	15.8237	6	4.78345	16	4.54967	6	11.2944	16	10.7405
7	16.3916	17	15.799	7	4.70784	17	4.54386	7	11.1113	17	10.7271
8	16.2607	18	15.7772	8	4.67026	18	4.53768	8	11.0231	18	10.7126
9	16.1607	19	15.7577	9	4.6501	19	4.53126	9	10.9773	19	10.6974
10	16.082	20	15.7402	10	4.62749	20	4.52633	10	10.9243	20	10.6858
11	16.0183			11	4.60412			11	10.8682		

Table 4.8 Deflection coefficients of CS Beam for three cases of mass distribution subjected to a concentrated force, M is the added mass.

Beam without M				Beam with M				Massless beam with M			
n	a_n / a_1	n	a_n / a_1	n	a_n / a_1	n	a_n / a_1	n	a_n / a_1	n	a_n / a_1
1	1	11	-0.00116	1	1	11	-1.32E-03	1	1	11	-0.00116
2	-0.2294	12	-0.00089	2	-0.19577	12	-8.94E-04	2	-0.2294	12	-0.00089
3	-0.059017	13	-0.0007	3	-8.63E-02	13	-6.22E-04	3	-0.05902	13	-0.0007
4	-0.024358	14	-0.00056	4	-2.42E-02	14	-5.63E-04	4	-0.02436	14	-0.00056
5	-0.012398	15	-0.00046	5	-8.63E-03	15	-5.04E-04	5	-0.0124	15	-0.00046
6	-0.00716	16	-0.00038	6	-7.16E-03	16	-3.77E-04	6	-0.00716	16	-0.00038
7	-0.004505	17	-0.00031	7	-5.48E-03	17	-2.87E-04	7	-0.0045	17	-0.00031
8	-0.003016	18	-0.00026	8	-3.02E-03	18	-2.65E-04	8	-0.00302	18	-0.00026
9	-0.002118	19	-0.00023	9	-1.76E-03	19	-2.43E-04	9	-0.00212	19	-0.00023
10	-0.001544	20	-0.00019	10	-0.00155	20	-1.93E-04	10	-0.00154	20	-0.00019

Table 4.9 Deflection coefficients of CS Beam for three cases of mass distribution subjected to uniform distributed load and M is the added mass.

Beam without M				Beam with M				Massless beam with M			
n	a_n/a_1	n	a_n/a_1	n	a_n/a_1	n	a_n/a_1	n	a_n/a_1	n	a_n/a_1
1	1	11	-1.16E-03	1	1	11	-1.32E-03	1	1	11	-0.00133
2	-0.2294	12	-8.93E-04	2	-0.19577	12	-8.94E-04	2	-0.19307	12	-0.00089
3	-0.059017	13	-0.0007	3	-0.0863	13	-6.22E-04	3	-0.08862	13	-0.00061
4	-0.024358	14	-0.00056	4	-0.02417	14	-5.63E-04	4	-0.02413	14	-0.00056
5	-0.012398	15	-0.00046	5	-0.00863	15	-5.04E-04	5	-0.00829	15	-0.00051
6	-0.00716	16	-0.00038	6	-0.00716	16	-3.77E-04	6	-0.00715	16	-0.00038
7	-0.004505	17	-0.00031	7	-0.00548	17	-2.87E-04	7	-0.00556	17	-0.00028
8	-0.003016	18	-0.00026	8	-0.00302	18	-2.65E-04	8	-0.00302	18	-0.00026
9	-0.002118	19	-0.00023	9	-0.00176	19	-2.43E-04	9	-0.00173	19	-0.00024
10	-0.001544	20	-0.00019	10	-0.00155	20	-1.93E-04	10	-0.00154	20	-0.00019

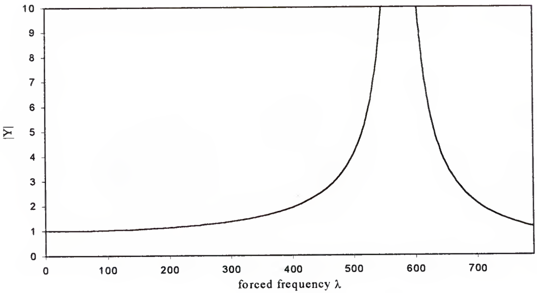

Figure 4.5 CS beam without added mass subjected to uniform distributed force for different forced frequencies at N=20

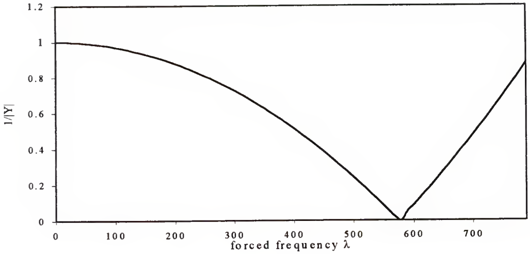

Figure 4.6 The inverse of normalized maximum absolute deflection vs. forced frequency for CS beam without mass subjected to a uniformly distributed load for different forced frequencies at N=20

Beam with Clamped-Clamped Edges

Consider a case of beam clamped at both ends and subjected to a force in the middle as in figure 4.7a. The beam length is l. The beam will be studied for three cases of mass distribution. The first case is the beam with its own mass only. The second case is considering a concentrated mass on the beam in addition to its own mass. The third case is neglecting the mass of the beam and considering only a concentrated mass on the beam. The boundary conditions for this problem are

$$w(x) = 0 \text{ at } x = 0 \text{ and } x = l \tag{4.27}$$

$$\frac{dw(x)}{dx} = 0 \text{ at } x = 0 \text{ and } x = l \tag{4.28}$$

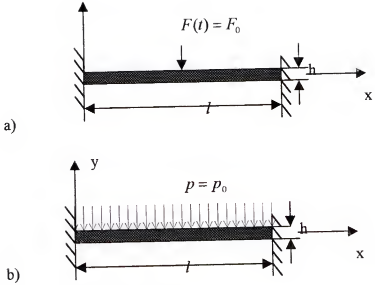

Figure 4.7 Clamped Beam for both ends

Let us assume equation 3.12 to be the deflection function of this case. Since this function has already satisfied the requirement of zero deflection at both ends of the beam, the boundary conditions of equation 4.28 constitute the only constraints needed for this case. The unsatisfied constraints are

$$g_1 = \sum_{1}^{N} a_n \frac{n\pi}{l} \tag{4.29}$$

$$g_2 = \sum_{1}^{N} a_n \frac{n\pi}{l} \cos(n\pi) \tag{4.30}$$

The Lagrangian function takes the following form:

$$L = U - T + \sum \lambda_i g_i \qquad (4.31)$$

Substituting equations 3.13, 3.14, 3.15, 4.29, and 4.30 into equation 4.31 gives

$$L = \frac{EI\pi^4}{4l^3}\sum_1^N n^4 a_n^2 - p_0 \sum_1^N a_n \sin(\frac{n\pi a}{l}) - \frac{\gamma\omega^2 l}{4}\sum_1^N a_n^2 + \lambda_1 \sum_1^N a_n \frac{n\pi}{l} +$$

$$\lambda_2 \sum_1^N a_n \frac{n\pi}{l}\cos(n\pi) \qquad (4.32)$$

Now taking the derivative of Lagrangian function of equation 4.32 with respect to a_n gives

$$a_n = \frac{2l^3(p_0 \sin(\frac{n\pi a}{l}) - \lambda_1 \frac{n\pi}{l} - \lambda_2 \frac{n\pi}{l}\cos(n\pi))}{EI\pi^4 n^4 - \gamma\omega^2 l^4} \qquad (4.33)$$

$$\frac{\partial L}{\partial \lambda} = 0 \qquad (4.34)$$

Taking derivative of Lagrangian function of equation 4.32 with respect to λ_1 and λ_2 gives the following equations:

$$\sum_1^N a_n n = 0 \qquad (4.35)$$

$$\sum_1^N a_n n \cos(n\pi) = 0 \qquad (4.36)$$

Following the same procedure used in the previous case, one can find

$$\sum_1^N \frac{nlp_0 \sin(\frac{n\pi a}{l})}{EI\pi^4 n^4 - \gamma\omega^2 l^4} - \lambda_1 \sum_1^N \frac{n^2\pi}{EI\pi^4 n^4 - \gamma\omega^2 l^4} -$$

$$\lambda_2 \sum_1^N \frac{n^2\pi\cos(n\pi)}{EI\pi^4 n^4 - \gamma\omega^2 l^4} = 0 \tag{4.37}$$

$$\sum_1^N \frac{nlp_0 \sin(\frac{n\pi a}{l})\cos(n\pi)}{EI\pi^4 n^4 - \gamma\omega^2 l^4} - \lambda_1 \sum_1^N \frac{n^2\pi\cos(n\pi)}{EI\pi^4 n^4 - \gamma\omega^2 l^4} -$$

$$\lambda_2 \sum_1^N \frac{n^2\pi\cos^2(n\pi)}{EI\pi^4 n^4 - \gamma\omega^2 l^4} = 0 \tag{4.38}$$

Solving equation 4.37 and equation 4.38 for λ_1 and λ_2 and substituting their values into equation 4.33, the coefficient a_n can be obtained. Then the calculated a_n can be substituted into equation 3.12 to give the following equation:

$$w(x) = \sum_1^N \frac{2l^3(p_0 \sin(\frac{n\pi a}{l}) - \lambda_1 \frac{n\pi}{l} - \lambda_2 \frac{n\pi}{l}\cos(n\pi))}{EI\pi^4 n^4 - \gamma\omega^2 l^4} \sin(\frac{n\pi}{l}x) \tag{4.39}$$

The natural frequency can be found from figure 4.9 or table 4.10. Now, consider that the beam is subjected to a uniformly distributed load as in figure 4.7b. The only difference from the above case is the external work as given in equation 3.16. Substituting equations 3.13, 3.14, 3.16, 4.29, and 4.30 into equation 4.31 gives

$$L = \frac{EI\pi^4}{4l^3}\sum_1^N n^4 a_n^2 - p_0 \sum_1^N a_n \frac{l}{n\pi}(1-\cos(n\pi)) - \frac{\gamma\omega^2 l}{4}\sum_1^N a_n^2 +$$

$$\lambda_1 \sum_1^N a_n \frac{n\pi}{l} + \lambda_2 \sum_1^N a_n \frac{n\pi}{l}\cos(n\pi) \tag{4.40}$$

The same procedure is used and the displacement function parameters are found to be:

$$a_n = \frac{2l^3(p_0 \frac{l}{n\pi}(1-\cos(n\pi)) - \lambda_1 \frac{n\pi}{l} - \lambda_2 \frac{n\pi}{l}\cos(n\pi))}{EI\pi^4 n^4 - \gamma\omega^2 l^4} \tag{4.41}$$

The undetermined parameters are found by substituting the displacement parameter into equation 4.29 and equation 4.30 and solving the resulting equations. By substituting their values into equation 4.41 one can calculate a_n. The calculated a_n can be substituted into equation 3.12 to give the following equation:

$$w(x) = \sum_{1}^{N} \frac{2l^3(p_0 \frac{l}{n\pi}(1-\cos(n\pi))}{EI\pi^4 n^4 - \gamma\omega^2 l^4}\sin(\frac{n\pi}{l}x) -$$

$$\frac{\lambda_1 \frac{n\pi}{l} + \lambda_2 \frac{n\pi}{l}\cos(n\pi))}{EI\pi^4 n^4 - \gamma\omega^2 l^4}\sin(\frac{n\pi}{l}x) \tag{4.42}$$

Results

The fundamental frequency result is shown in table 4.10. The table shows the convergence for the three types of beams as N increases. The difference between the calculated frequency and the published one for the beam without concentrated mass is 4.4%. However, the difference can be reduced by increasing N. Also the difference between the calculated frequency and the published one for the massless beam with concentrated mass is 3.2% and the difference can be reduced also by increasing N. The corresponding normal modes are shown in table 4.11 for the three types of beams. The study is undertaken using the concentrated force and also the uniform distributed load as given in tables 4.10-4.13. The same result is obtained for both types of loading as would be expected.

Table 4.10 The λ and Ω values of CC Beam with three cases of mass distribution subjected to a concentrated force where $\lambda = \omega_n \sqrt{\gamma l^4 / EI}$, $\Omega = \omega_n \sqrt{Ml^3 / EI}$ and M is the added mass.

Beam without mass				Beam with mass				Massless beam with mass			
N	λ	N	λ	N	λ	N	λ	N	Ω	N	Ω
3	29.6088	12	24.1047	3	7.09608	12	6.247	3	16.5518	12	14.632
4	29.6088	13	23.8275	4	7.09608	13	6.20199	4	16.5518	13	14.5306
5	26.4085	14	23.8275	5	6.7544	14	6.20199	5	15.8065	14	14.5306
6	26.4085	15	23.6267	6	6.7544	15	6.15634	6	15.8065	15	14.4249
7	25.1698	16	23.6267	7	6.43939	16	6.15634	7	15.0704	16	14.4249
8	25.1698	17	23.4746	8	6.43939	17	6.13029	8	15.0704	17	14.3659
9	24.5122	18	23.4746	9	6.34318	18	6.13029	9	14.8555	18	14.3659
10	24.5122	19	23.3554	10	6.34318	19	6.10379	10	14.8555	19	14.3047
11	24.1047	20	23.3554	11	6.247	20	6.10379	11	14.632	20	14.3047

Table 4.11 Deflection coefficients of CC Beam for three cases of mass distribution subjected to a concentrated force and M is the added mass.

Beam without M				Beam with M				Massless beam with M			
n	a_n / a_1	n	a_n / a_1	n	a_n / a_1	n	a_n / a_1	n	a_n / a_1	n	a_n / a_1
1	1	11	-0.00346	1	1	11	-0.00338	1	1	11	-3.38E-03
2	0	12	0	2	0	12	0	2	0	12	0
3	-0.18302	13	-0.00209	3	-0.20993	13	-0.00169	3	-0.21184	13	-1.66E-03
4	3.82E-18	14	0	4	0	14	0	4	0	14	0
5	-0.037131	15	-0.00136	5	-0.02512	15	-0.0013	5	-0.02426	15	-1.30E-03
6	0	16	0	6	1.31E-18	16	0	6	1.31E-18	16	0
7	-0.013442	17	-0.00094	7	-0.01384	17	-0.00077	7	-0.01388	17	-7.62E-04
8	0	18	8.20E-20	8	0	18	-6.14E-18	8	5.54E-19	18	0
9	-0.006315	19	-0.00067	9	-0.00488	19	-0.00063	9	-0.00477	19	-6.28E-04
10	0	20	0	10	-2.82E-19	20	0	10	0	20	0

Table 4.12 The λ and Ω values of CC Beam with three cases of mass distribution subjected to uniformly distributed load where $\lambda = \omega_n \sqrt{\gamma l^4 / EI}$, $\Omega = \omega_n \sqrt{M l^3 / EI}$ and M is the added mass.

Beam without M				Beam with M				Massless beam with M			
N	λ	N	λ	N	λ	N	λ	N	Ω	N	Ω
3	29.6088	12	24.1047	3	7.09608	12	6.247	3	16.5518	12	14.632
4	29.6088	13	23.8275	4	7.09608	13	6.20199	4	16.5518	13	14.5306
5	26.4085	14	23.8275	5	6.7544	14	6.20199	5	15.8065	14	14.5306
6	26.4085	15	23.6267	6	6.7544	15	6.15634	6	15.8065	15	14.4249
7	25.1698	16	23.6267	7	6.43939	16	6.15634	7	15.0704	16	14.4249
8	25.1698	17	23.4746	8	6.43939	17	6.13029	8	15.0704	17	14.3659
9	24.5122	18	23.4746	9	6.34318	18	6.13029	9	14.8555	18	14.3659
10	24.5122	19	23.3554	10	6.34318	19	6.10379	10	14.8555	19	14.3047
11	24.1047	20	23.3554	11	6.247	20	6.10379	11	14.632	20	14.3047

Table 4.13 Coefficients of CC Beam for three cases of concentrated mass distribution subjected to a uniform distributed load . M is the added mass.

Beam without M				Beam with M				Massless beam with M			
n	a_n / a_1	n	a_n / a_1	n	a_n / a_1	n	a_n / a_1	n	a_n / a_1	n	a_n / a_1
1	1	11	-3.46E-03	1	1	11	-3.38E-03	1	1	11	-3.38E-03
2	0	12	0	2	0	12	0	2	0	12	0
3	-0.18302	13	-2.09E-03	3	-0.20993	13	-1.69E-03	3	-0.21184	13	-1.66E-03
4	3.82E-18	14	0	4	0.e	14	0	4	0	14	-1.03E-19
5	-0.037131	15	-1.36E-03	5	-0.02512	15	-1.30E-03	5	-0.02426	15	-1.30E-03
6	0	16	0	6	1.31E-18	16	0	6	1.31E-18	16	0
7	-0.013442	17	-9.36E-04	7	-0.01384	17	-7.74E-04	7	-0.01388	17	-7.62E-04
8	-1.20E-16	18	0	8	0	18	4.83E-20	8	0	18	0
9	-0.006315	19	-6.71E-04	9	-4.88E-03	19	-6.30E-04	9	-4.77E-03	19	-6.28E-04
10	0	20	0	10	0	20	0	10	0	20	0

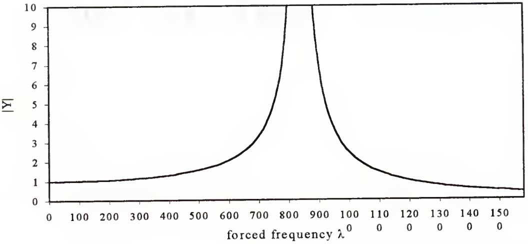

Figure 4.8 CC beam without added mass subjected to uniformly distributed load for different forced frequencies at N=30

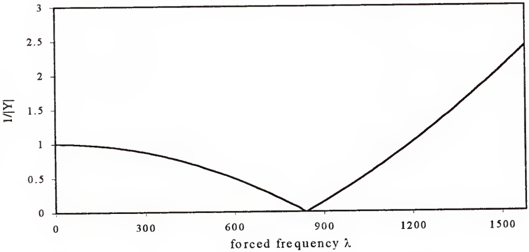

Figure 4.9 The inverse of normalized maximum absolute deflection vs. forced frequency for CC beam without added mass subjected to a uniformly distributed load for different forced frequencies at N=30

Beams with Clamped-Free Edges

In this case we consider a cantilever beam as in figure 4.10. We will use in this example a function with sine and cosine series as in equation 3.21. The strain energy stored in this beam for this assumed function is given in equation 3.22 while its kinetic energy is given in equation 3.23

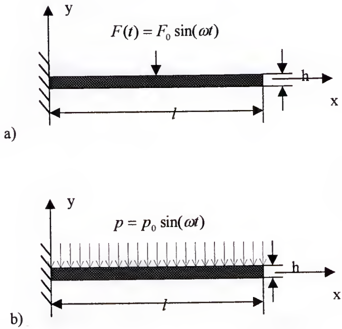

Figure 4.10 Clamped free edges beam

In case of subjecting the beam to a force at $x = l$ as in figure 4.10a, the external work will be as expressed in equation 3.24. The boundary conditions of the beam at the clamped edge are

$$w(x) = 0 \text{ at } x = 0 \tag{4.43}$$

$$\frac{dw(x)}{dx} = 0 \text{ at } x = 0 \tag{4.44}$$

The boundary conditions of the beam at the free end are

$$M(x) = 0 \text{ at } x = l \tag{4.45}$$

$$V(x) = 0 \text{ at } x = l \tag{4.46}$$

Since equation 3.21 is the assumed function, some boundary conditions are not satisfied. Therefore the unsatisfied constraints are

$$g_1 = a_0 + \sum_1^N a_n \tag{4.47}$$

$$g_2 = \sum_1^N b_m \frac{m\pi}{l} \tag{4.48}$$

$$g_3 = EI \sum_1^N a_n \frac{n^2\pi^2}{l^2} \cos(n\pi) \tag{4.49}$$

$$g_4 = EI \sum_1^N b_m \frac{m^3\pi^3}{l^3} \cos(m\pi) \tag{4.50}$$

Substituting these equations into the Lagrangian function gives

$$L = \frac{EI\pi^4}{4l^3}[\sum_1^N n^4 a_n^2 + \sum_1^N m^4 b_m^2 +$$

$$\sum_{n=1}^N \sum_{\substack{m=1 \\ n \neq m}}^N a_n b_m \frac{4n^2 m^3}{\pi(n^2 - m^2)}(\cos(n\pi)\cos(m\pi) - 1)]$$

$$-\frac{\gamma\omega^2 l}{4}[2a_0^2 + \sum_{n=1}^N a_n^2 + \sum_{m=1}^N (b_m^2 - 4a_0 b_m \frac{1}{m\pi}(1 - \cos(m\pi))) +$$

$$\sum_{n=1}^{N}\sum_{\substack{m=1\\ m\neq n}}^{N}\frac{4a_n b_m m(\cos(m\pi)\cos(n\pi)-1)}{\pi(n^2-m^2)}]$$

$$-F_0[a_0+\sum_{n=1}^{N}a_n\cos(\frac{n\pi a}{l})+\sum_{m=1}^{N}b_m\sin(\frac{m\pi a}{l})]+\sum_{1}^{4}\lambda_i g_i \qquad (4.51)$$

To minimize the energy, the derivatives of equation 4.51 with respect to the different parameters are equated to zero.

$$\frac{\partial L}{\partial a_0}=0,\ \frac{\partial L}{\partial a_n}=0,\ \frac{\partial L}{\partial b_m}=0 \text{ And } \frac{\partial L}{\partial \lambda_i}=0 \qquad (4.52)$$

where the number of unsatisfied constraints $i=1,2,3,4$. The first derivative in equation 4.52, which is the derivative of equation 4.51 with respect to a_0 takes the following form:

$$-\gamma\omega^2 l+\gamma\omega^2 l\sum_{1}^{N}b_m\frac{1}{m\pi}(1-\cos(m\pi))-F_0+\lambda_1=0 \qquad (4.53)$$

The second derivative in equation 4.52, which is the derivative of equation 4.51 with respect to a_n becomes

$$\frac{EI\pi^4}{2l^3}n^4 a_n+\sum_{\substack{m=1\\ n\neq m}}^{N}(\frac{EI\pi^4}{l^3}n^2m^3b_m-\gamma\omega^2 l b_m m)\frac{\cos(n\pi)\cos(m\pi)-1}{\pi(n^2-m^2)}-$$

$$\frac{\gamma\omega^2 l}{2}a_n-F_0\cos(n\pi)+\lambda_1+\lambda_3 EI\frac{n^2\pi^2}{l^2}\cos(n\pi)=0 \qquad (4.54)$$

The third derivative in equation 4.52, which is the derivative of equation 4.51 with respect to b_m, is

$$\frac{EI\pi^4}{4l^3}(2m^4 b_m + \sum_{\substack{n=1\\n\neq m}}^{N} a_n \frac{4n^2m^3}{\pi(n^2-m^2)}(\cos(n\pi)\cos(m\pi)-1)) -$$

$$\frac{\gamma\omega^2 l}{2}(b_m - 2a_0\frac{1}{m\pi}(1-\cos(m\pi)) + \sum_{\substack{n=1\\n\neq m}}^{N} \frac{2a_n m(\cos(m\pi)\cos(n\pi)-1)}{\pi(n^2-m^2)})$$

$$-F_o\sin(\frac{n\pi a}{l}) + \lambda_2\frac{m\pi}{l} + \lambda_4 EI\frac{m^3\pi^3}{l^3}\cos(m\pi) = 0 \tag{4.55}$$

The last derivative in equation 4.52, which is the derivative of equation 4.51 with respect to the undetermined parameter, λ_i takes the following forms:

$$a_0 + \sum_1^N a_n = 0 \tag{4.56}$$

$$\sum_1^N b_m \frac{m\pi}{l} = 0 \tag{4.57}$$

$$EI\sum_1^N a_n \frac{n^2\pi^2}{l^2}\cos(n\pi) = 0 \tag{4.58}$$

$$EI\sum_1^N b_m \frac{m^3\pi^3}{l^3}\cos(m\pi) = 0 \tag{4.59}$$

It can be seen that equations 4.56 to 4.59 are the same of equations 4.47 to 4.50 respectively. Equations 4.53 to 4.55 can be solved to find the displacement parameters a_0, a_n, and b_m in terms of λ_1, λ_2, λ_3, and λ_4. The undetermined parameters λ_1, λ_2, λ_3, and λ_4 are found by simultaneously solving e 4.56 to 4.59. Applying λ_1, λ_2, λ_3, and λ_4 into equations 4.53 to 4.55, the displacement parameters a_0, a_n, and b_m can be found as numerical values.

Next, consider a uniformly distributed load is applied to the beam as in figure 4.10b. The Lagrangian function becomes

$$L=\frac{EI\pi^4}{4l^3}[\sum_1^N n^4a_n^2+\sum_1^N m^4b_m^2+$$

$$\sum_{n=1}^N\sum_{\substack{m=1\\n\neq m}}^N a_nb_m\frac{4n^2m^3}{\pi(n^2-m^2)}(\cos(n\pi)\cos(m\pi)-1)]$$

$$-\frac{\gamma\omega^2 l}{4}[2a_0^2+\sum_{n=1}^N a_n^2+\sum_{m=1}^N(b_m^2-4a_0b_m\frac{1}{m\pi}(1-\cos(m\pi)))+$$

$$\sum_{n=1}^N\sum_{\substack{m=1\\m\neq n}}^N\frac{4a_nb_mm(\cos(m\pi)\cos(n\pi)-1)}{\pi(n^2-m^2)}]$$

$$-p_0[a_0\frac{l}{2}+\sum_{n=1}^N a_n\frac{l}{n\pi}\sin(\frac{n\pi}{2})+$$

$$\sum_{m=1}^N b_m\frac{l}{m\pi}(1-\cos(\frac{m\pi}{2}))]+\sum_1^4\lambda_i g_i \tag{4.60}$$

Taking the derivative of equation 4.60 with respect to a_0 gives

$$\gamma\omega^2 l+\gamma\omega^2 l\sum_1^N b_m\frac{1}{m\pi}(1-\cos(m\pi))+p_0\frac{l}{2}+\lambda_1=0 \tag{4.61}$$

Taking the derivative of equation 4.60 with respect to a_n gives

$$\frac{EI\pi^4}{2l^3}n^4a_n+\sum_{\substack{m=1\\n\neq m}}^N(\frac{EI\pi^4}{l^3}n^2m^3b_m-\gamma\omega^2 lb_mm)\frac{\cos(n\pi)\cos(m\pi)-1}{\pi(n^2-m^2)}-$$

$$\frac{\gamma\omega^2 l}{2} a_n - p_0 \frac{l}{n\pi}\sin(\frac{n\pi}{2}) + \lambda_1 + \lambda_3 EI \frac{n^2\pi^2}{l^2}\cos(n\pi) = 0 \qquad (4.62)$$

Taking the derivative of equation 4.60 with respect to b_m gives

$$\frac{EI\pi^4}{4l^3}(2m^4 b_m + \sum_{\substack{n=1\\ n\neq m}}^{N} a_n \frac{4n^2 m^3}{\pi(n^2 - m^2)}(\cos(n\pi)\cos(m\pi) - 1)) -$$

$$\frac{\gamma\omega^2 l}{2}(b_m - 2a_0 \frac{1}{m\pi}(1 - \cos(m\pi)) + \sum_{\substack{n=1\\ n\neq m}}^{N} \frac{2a_n m(\cos(m\pi)\cos(n\pi) - 1)}{\pi(n^2 - m^2)}) -$$

$$p_0 \frac{l}{m\pi}(1 - \cos(\frac{m\pi}{2})) \quad + \lambda_2 \frac{m\pi}{l} + \lambda_4 EI \frac{m^3\pi^3}{l^3}\cos(m\pi) = 0 \qquad (4.63)$$

The undetermined parameters, which are found, previously can be substituted into equations 4.61 to 4.63. The resulting equations can be solved simultaneously to give the values of a_0, a_n, and b_m.

Result

The fundamental frequency result is shown in table 4.14. The table shows the convergence for the three types of beams as N increases. The study is undertaken using the concentrated force and also the uniform distributed load. The calculated parameters are compared to the published result as in tables 4.1 and 4.3. The difference between the calculated frequency and the published one for the beam without concentrated mass is 0.0001%. Also the difference between the calculated frequency and the published one for the massless beam with concentrated mass is 0.0005%. The corresponding normal modes are shown in tables 4.15 and 4.16 for the three types of beams.

Table 4.14 The λ and Ω values of CF Beam with three cases of mass distribution subjected to a concentrated force where $\lambda = \omega_n \sqrt{\gamma l^4 / EI}$, $\Omega = \omega_n \sqrt{M l^3 / EI}$ and M is the added mass.

Beam without M				Beam with M				Massless beam with M			
N	λ	N	λ	N	λ	N	λ	N	Ω	N	Ω
2		6	3.51607	2	4.70073	6	1.69366	2	4.9348	6	1.7322
3	4.20536	7	3.51602	3	2.17219	7	1.69354	3	2.22918	7	1.73208
4	3.55295	8	3.51602	4	1.72134	8	1.69353	4	1.761	8	1.73206
5	3.51743			5	1.69508			5	1.73369		

Table 4.15 Deflection Coefficients of CF Beam for three cases of mass distribution subjected to a concentrated force, M is the added mass.

Beam without M				Beam with M				Massless beam with M			
n	a_n / a_0	n	b_n / a_0	n	a_n / a_0	n	b_n / a_0	n	a_n / a_0	n	b_n / a_0
1	-0.97986	1	-0.50371	1	-0.83498	1	-0.76	1	-0.82941	1	-0.76979
2	-0.13694	2	0.2738	2	-0.35682	2	0.25928	2	-0.36525	2	0.2587
3	0.11598	3	0.049454	3	0.11584	3	0.20934	3	0.11582	3	0.21547
4	0.018823	4	-0.047701	4	0.11167	4	-0.05167	4	0.11523	4	-0.051816
5	-0.017122	5	-66.343e-4	5	-0.020657	5	-0.049714	5	-0.02079	5	-0.051364
6	-19.535e-4	6	49.526e-4	6	-0.017279	6	68.314e-4	6	-0.017866	6	69.026e-4
7	10.299e-4	7	4.22e-4	7	16.687e-4	7	42.178e-4	7	16.93e-4	7	43.632e-4
8	5.0538e-5	8	-1.1764e-4	8	5.5504e-4	8	-2.309e-4	8	5.7436e-4	8	-2.3522e-4

Table 4.16 Deflection Coefficients of CF Beam for three cases of mass distribution subjected to uniformly distributed load. M is the added mass.

Beam without mass				Beam with mass				Massless beam with mass			
n	a_n / a_0	n	b_n / a_0	n	a_n / a_0	n	b_n / a_0	n	a_n / a_0	n	b_n / a_0
1	-0.97986	1	-0.50371	1	-0.77486	1	-0.70339	1	-0.71187	1	-0.76536
2	-0.13694	2	0.2738	2	-0.38701	2	0.18625	2	-0.46407	2	0.15954
3	0.11598	3	0.049454	3	0.06894	3	0.21852	3	0.0546	3	0.27071
4	0.018823	4	-0.047701	4	0.1193	4	-0.024149	4	0.15033	4	-0.016962
5	-0.017122	5	-66.343e-4	5	-68.009e-4	5	-0.054919	5	-0.0036461	5	-0.069832
6	-19.535e-4	6	49.526e-4	6	-0.020559	6	12.702e-4	6	-0.026305	6	1.4282e-4
7	10.299e-4	7	4.22e-4	7	7.4177e-5	7	55.327e-4	7	-2.1891e-4	7	71.111e-4
8	5.0538e-5	8	-1.1764e-4	8	9.1578e-4	8	2.0745e-5	8	11.83e-4	8	6.3239e-5

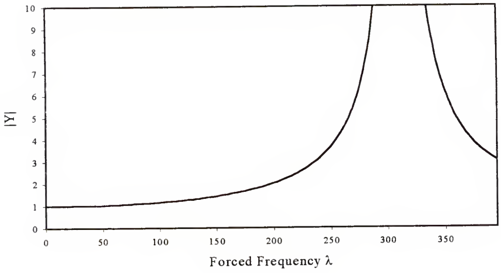

Figure 4.11 The normalized maximum absolute deflection vs. forced frequency for CF beam without mass distribution subjected to uniformly distributed load for different forced frequencies at N=10

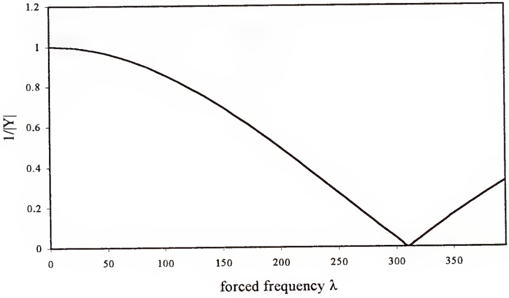

Figure 4.12 The inverse of normalized maximum absolute deflection vs. forced frequency for CF beam without mass distribution subjected to uniform distributed load for different forced frequencies at N=10

Multi Span Beam

The proposed method can be applied to different types of beam support conditions such as multi-span beams as in figure 4.12. The beam is simply supported at the two ends and has intermediate support at x= x_s

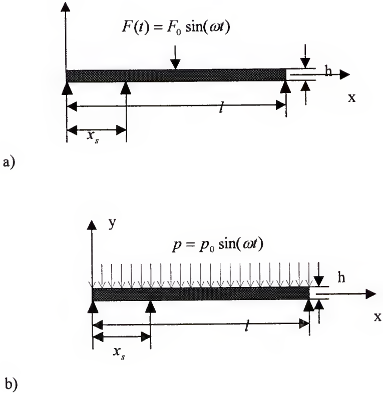

Figure 4.12 Multi span beam a) subjected to concentrated force; b) uniformly distributed load.

By using the same series of equation 3.21, the formulation for strain energy, kinetic energy, and external potential energy for either a concentrated force or a uniform distributed load will be the same as in equations 3.22, 3.23, and 3.24

This case has five boundary conditions at the two ends and at the intermediate position. By using the function assumed in equation 3.21 all theses conditions are not satisfied. The boundary conditions for both ends are that the deflection should be equal to zero and the moment should be equal to zero. Not all these boundary conditions are satisfied by the assumed function. Therefore the unsatisfied constraints for the end where $x = 0$ are the deflection and the moment. These unsatisfied constraints are given below respectively:

$$g_1 = a_0 + \sum_1^N a_n \tag{4.64}$$

$$g_3 = EI \sum_1^N a_n \frac{n^2 \pi^2}{l^2} \tag{4.65}$$

Also the unsatisfied constraints for the end where $x = l$ are the deflection and the moment as given below respectively:

$$g_2 = a_0 + \sum_1^N a_n \cos(n\pi) \tag{4.66}$$

$$g_4 = EI \sum_1^N a_n \frac{n^2 \pi^2}{l^2} \cos(n\pi) \tag{4.67}$$

The intermediate support, which it is at $x = x_s$ as in figure 4.12, will constrain the deflection of the beam at this position. This constraint is also unsatisfied. Therefore, this constraint should be enforced to be satisfied. The unsatisfied constraint at this position is expressed as:

$$g_5 = a_0 + \sum_{n=1} a_n \cos(\frac{n\pi x_s}{l}) + \sum_{m=1} b_m \sin(\frac{m\pi x_s}{l}) \tag{4.68}$$

Using the same procedure as in the previous section the displacement parameters can be found. Hence, the natural frequency can be calculated. The results of the fundamental frequency and the normalized coefficients of deflection (normal mode) are shown in table 4.17 and table 4.18 respectively.

Result

The fundamental frequency result is shown in table 4.17. The table shows the convergence for the three types of beams as N increases. The convergence occurs very fast for the three types of beams. The study is undertaken using the concentrated force and also the uniform distributed load. Also, figure 4.14 shows that the natural frequency is found when 1/|Y| becomes approaches zero.

The fundamental frequency for the beam without concentrated mass is found to be 23.6058 for eight approximation terms. Also the fundamental frequency for the beam with concentrated mass is found to be 7.32855 for the same number of terms. The fundamental frequency for the massless beam with concentrated mass is found to be 17.3528 for the same terms.

The corresponding normal modes are shown in tables 4.18 and 4.19 for the three types of beams.

Table 4.17 The λ values of SSS Beam with three cases of mass distribution subjected to a concentrated force where $\lambda = \omega_n \sqrt{\gamma l^4 / EI}$, $\Omega = \omega_n \sqrt{Ml^3 / EI}$ and M is the added mass.

Beam without M				Beam with M				Massless beam with M			
N	λ	N	λ	N	λ	N	λ	N	Ω	N	Ω
3	23.7352	6	23.6145	3	7.47879	6	7.33478	3	17.7446	6	17.369
4	23.6777	7	23.6104	4	7.3668	7	7.33345	4	17.4497	7	17.3654
5	23.6307	8	23.6058	5	7.33735	8	7.32855	5	17.375	8	17.3528

Table 4.18 Deflection Coefficients of SSS Beam for three cases of mass distribution subjected to a concentrated force and M is the added mass.

Beam without M				Beam with M				Massless beam with M			
n	a_n / a_0	n	b_n / a_0	n	a_n / a_0	n	b_n / a_0	n	a_n / a_0	n	b_n / a_0
1	0.11467	1	-1.6793	1	0.05583	1	-1.7929	1	0.053649	1	-1.7968
2	-1.4802	2	-0.30074	2	-1.4863	2	-0.12771	2	-1.4865	2	-0.12149
3	-0.19468	3	0.9944	3	-0.094786	3	1.0049	3	-0.091083	3	1.0053
4	0.57251	4	0.15421	4	0.58337	4	0.075081	4	0.58378	4	0.072148
5	0.09513	5	-0.26423	5	0.046316	5	-0.27317	5	0.044507	5	-0.2735
6	-0.095334	6	-0.043981	6	-0.10092	6	-0.021415	6	-0.10113	6	-0.020578
7	-0.015118	7	0.024145	7	-7.3604e-3	7	0.026369	7	-0.0070729	7	0.026451
8	0.0030086	8	0.0029351	8	3.8182e-3	8	0.001429	8	0.0038482	8	0.0013731

Table 4.19 Deflection Coefficients of SSS Beam for three cases of mass distribution subjected to uniformly distributed load and M is the added mass.

Beam without M				Beam with M				Massless beam with M			
n	a_n / a_0	n	b_n / a_0	n	a_n / a_0	n	b_n / a_0	n	a_n / a_0	n	b_n / a_0
1	0.11467	1	-1.6793	1	0.05583	1	-1.7929	1	0.053649	1	-1.7968
2	-1.4802	2	-0.30074	2	-1.4863	2	-0.12771	2	-1.4865	2	-0.12149
3	-0.19468	3	0.9944	3	-0.094786	3	1.0049	3	-0.091083	3	1.0053
4	0.57251	4	0.15421	4	0.58337	4	0.075081	4	0.58378	4	0.072148
5	0.09513	5	-0.26423	5	0.046316	5	-0.27317	5	0.044507	5	-0.2735
6	-0.095334	6	-0.043981	6	-0.10092	6	-0.021415	6	-0.10113	6	-0.020578
7	-0.015118	7	0.02414	7	-7.3604E-3	7	0.026369	7	-7.0729E-3	7	0.026451
8	0.0030086	8	0.0029351	8	0.0038182	8	0.001429	8	0.0038482	8	0.0013731

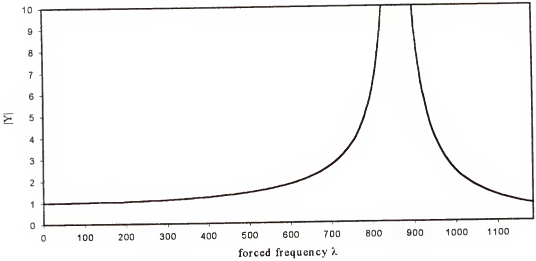

Figure 4.13 SSS beam without added mass supported at x_s=0.25 subjected to a concentrated force at the middle for N=8

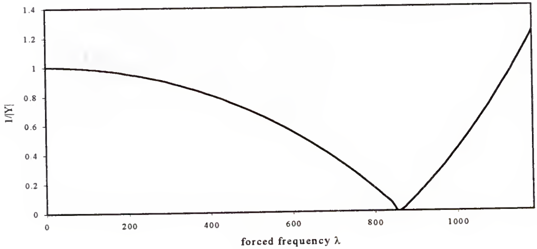

Figure 4.14 The inverse of normalized maximum absolute deflection vs. forced frequency for SSS beam without added mass supported at x_s=0.25 and subjected to a concentrated force at the middle for N=8

CHAPTER 5
APPLICATIONS TO PLATE PROBLEMS

The energy of the plate is the sum of the strain energy, the external potential energy, and the kinetic energy. These energies would be known if the deflection function is known. Assuming a rectangular plate with dimensions a, b, we can assume a double Fourier sine series of N and M terms to represent the deflection function:

$$w(x,y)=\sum_{m=1}^{M}\sum_{n=1}^{N}A_{mn}\sin(\frac{n\pi}{a}x)\sin(\frac{m\pi}{b}y) \qquad (5.1)$$

This function may not satisfy all the boundary conditions of the considered plate. In such case, it should be forced to satisfy the remaining boundary conditions on each point on the boundaries. For simplicity, N and M will be taken the same throughout the study such that M=N. The strain energy of the plate is obtained by performing the integration of the strain energy density of the plate over the entire plate. The strain energy is formulated as

$$Ue=\frac{D}{2}\int_0^b\int_0^a[(w_{xx}+w_{yy})^2-2(1-\nu)(w_{xx}w_{yy}-w_{xy}^2)]dxdy \qquad (5.2)$$

where ν is Poisson's ratio and the symbol D is the flexural rigidity of the plate, which is defined as:

$$D=\frac{Eh^3}{12(1-\nu^2)} \qquad (5.3)$$

where h is the thickness of the plate. Using equations 5.1 and 5.3 the second term in the integral vanishes for orthogonal deflection functions. The strain energy becomes

$$Ue = \sum\sum \frac{abD}{8}[(\frac{n\pi}{a})^2 + (\frac{m\pi}{b})^2]^2 A_{mn}^2 = \sum\sum Q_{mn} A_{mn}^2 \tag{5.4}$$

where $Q_{mn} = \frac{abD}{8}[(\frac{n\pi}{a})^2 + (\frac{m\pi}{b})^2]^2$ (5.5)

If a load p(x,y) acts on the surface of the plate, the work done by the load is

$$W = \int_A p(x,y)w(x,y)dA \tag{5.6}$$

$$W = \int_0^b \int_0^a p(x,y)w(x,y)dxdy \tag{5.7}$$

By applying equation 5.1 to equation 5.7 the external work becomes

$$W = \sum\sum A_{mn} S_{mn} \tag{5.8}$$

where $S_{mn} = \int_0^b \int_0^a p_0(x,y)\sin(\frac{n\pi}{a}x)\sin(\frac{m\pi}{b}y)dxdy$ (5.9)

and p_0 is the distributed load. After integration, equation 5.9 takes the following form

$$S_{mn} = \frac{ab}{nm\pi^2} p_0[\cos(n\pi) - 1][\cos(m\pi) - 1] \tag{5.10}$$

The kinetic energy of the plate is

$$T = \frac{\rho h}{2} \int_0^b \int_0^a [\omega w(x,y)]^2 dxdy \tag{5.11}$$

Equation 5.11 becomes

$$T = \sum_{n}^{N} \sum_{m=1}^{N} A_{mn}^2 \omega^2 \frac{\rho abh}{8} \tag{5.12}$$

Equation 5.12 may be simplified to the following form

$$T = \sum_{n}^{N} \sum_{m=1}^{N} A_{mn}^2 \overline{\omega}^2 \tag{5.13}$$

where $\overline{\omega}^2 = \omega^2 \dfrac{\rho abh}{8}$ (5.14)

The terms in the above equations, a, b, ω, and ρ represent the length, the width, the forced frequency, and the density per unit area of the plate respectively. The boundary conditions at the edges of the plate can be categorized as follows:

1. Clamped edges along which w and $\partial w / \partial n$ vanish.
2. Simply Supported edges along which w and M_n vanish.
3. Free edges along which M_n and V_n vanish.

In the above expressions, n is a direction that represents x or y, and M_n and V_n represent the bending moment and the shear force, respectively, in the assigned direction n, M_x, M_y, V_x and V_y are defined as:

$$M_x = -D(\partial^2 w / \partial x^2 + \nu \partial^2 w / \partial y^2) \tag{5.15}$$

$$M_y = -D(\partial^2 w / \partial y^2 + \nu \partial^2 w / \partial x^2) \tag{5.15}$$

$$V_x = -D[\frac{\partial^3 w}{\partial x^3} + (2-\nu)\frac{\partial^3 w}{\partial x \partial y^2}] \tag{5.16}$$

$$V_y = -D[\frac{\partial^3 w}{\partial y^3} + (2-\nu)\frac{\partial^3 w}{\partial x^2 \partial y}] \tag{5.17}$$

The advantage of the undetermined multiplier method is that it is easy to use in the case of plate as in the beam case. Each edge of the plate is divided into a chosen finite number of points. The chosen function should satisfy the boundary conditions at all these finite points. As the number of points reach infinity, the actual boundary conditions will be exactly satisfied. In most practical cases a relatively small number of points is all that is nessary to achieve reasonable accuracy. The undetermined multipliers for the constraints at the edge parallel to the x-axis are λ_i, while the undetermined multipliers for the constraints at the edge parallel to the y-axis are μ_j. The constraints on the boundaries can be represented by the functions G_i and H_j. The constraints for the edges parallel to the x-axis are G_i, while those parallel to the y-axis are H_j. The Lagrangian function is

$$L = U - W - T + \sum_{1}^{I} \lambda_i G_i + \sum_{1}^{J} \mu_j H_j \tag{5.18}$$

The constants $A_{1,1}, A_{1,2}, \ldots\ldots, A_{mn}$ can be evaluated by minimizing the energy function in conjunction with the enforced constraints. The minimization is performed by taking the partial derivatives of the Lagrangian function for all the coefficients. Taking the partial derivative of the Lagrangian function with respect A_{mn} and equating it to zero, the resulting equations give the deflection parameters in terms of the undetermined multipliers λ_i, μ_i, ...

$$\frac{\partial L}{\partial A_{mn}} = 0 \tag{5.19}$$

Also, taking derivatives of the Lagrangian function with respect λ_i, μ_i, ... And equating them to zero, the resulting equations give the parameters λ_i, μ_i, ...

$$\frac{\partial L}{\partial \lambda_i} = 0, \frac{\partial L}{\partial \mu_j} = 0 \tag{5.20}$$

where $i = 1,2,3,.....,I$ and $j = 1,2,3,.....J$. By substituting the undetermined multipliers into the displacement parameter A_{mn}, those parameters can be found.

CHAPTER 6
ILLUSTRATIVE EXAMPLES

Plates with Simply Supported Edges in x and y Directions

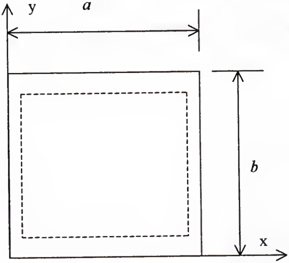

Figure 6.1 Rectangular plate clamped at all sides and subjected to a uniformly distributed load

Consider a rectangular plate with dimensions a and b as shown in figure 6.1. The plate is simply supported at all edges. The boundary conditions for this case are zero deflection and zero moment at all edges. The deflection and the moment for all edges are given respectively as following

$$w(0,y)=0 \tag{6.1}$$

$$w(x,0)=0 \tag{6.2}$$

$$w(a,y)=0 \tag{6.3}$$

$$w(x,b)=0 \tag{6.4}$$

$$M_x(0,y)=0 \tag{6.5}$$

$$M_y(x,0)=0 \tag{6.6}$$

$$M_x(a,y)=0 \tag{6.7}$$

$$M_y(x,b)=0 \tag{6.8}$$

Equations 6.2, 6.4, 6.6, and 6.8 can be written in the following forms

$$w=0 \quad \frac{\partial^2 w}{\partial x^2}=0 \quad \text{at } (x=0 \text{ and } x=a) \tag{6.9}$$

Equations 6.1, 6.3, 6.5, and 6.7 can be also written in the following forms

$$w=0 \quad \frac{\partial^2 w}{\partial y^2}=0 \quad \text{at } (y=0 \text{ and } x=b) \tag{6.10}$$

Since all the boundary conditions are satisfied by the assumed function of equation 5.1 there are no unsatisfied constraints. In this case the Lagrangian function is in its simple form

$$L=U-W-T \tag{6.11}$$

The strain energy, the external potential energy, and the kinetic energy are described in equations 5.4, 5.8, and 5.13. Substituting these equations into equation 6.11 gives

$$L=\sum_{1}^{N}\sum_{1}^{N}Q_{mn}A_{mn}^{2}-\sum_{1}^{N}\sum_{1}^{N}A_{mn}S_{mn}-\sum_{n}^{N}\sum_{m=1}^{N}A_{mn}^{2}\varpi^{2} \tag{6.12}$$

To minimize the energy, the partial derivative of L with respect to A_{mn} is taken and set equal to zero:

$$\frac{\partial L}{\partial A_{mn}}=0 \tag{6.13}$$

From equation 6.12 and equation 6.13, we obtain

$$2\sum_{n=1}^{N}\sum_{m=1}^{N}Q_{mn}A_{mn}-\sum_{n=1}^{N}\sum_{m=1}^{N}S_{mn}-2\sum_{n=1}^{N}\sum_{m=1}^{N}A_{mn}\varpi^{2}=0 \tag{6.14}$$

Equation 6.14 creates N by M equations. If N=20 and M=N, then 400 equations will be created. Solving 400 equations directly may need considerable time. However, the solution of these equations can be accomplished by simplifying equation 6.14. This equation can take the following simple form:

$$2Q_{mn}A_{mn}-S_{mn}-2A_{mn}\varpi^{2}=0 \tag{6.15}$$

From equation 6.15, the displacement parameter is

$$A_{mn}=\frac{S_{mn}}{2(Q_{mn}-\varpi^{2})} \tag{6.16}$$

Using equation 6.16 the displacement parameters can be found by substituting for n=1, 2, . . ., N and m=1, 2, . . ., M. Using a computer the result will be obtained within a few seconds. The natural frequency data is shown in figures 6.1-6.4 and Tables 6.1 and 6.2.

Result

Tables 6.1 and 6.2 show the displacement parameter for the square simple supported plate at N=15. The tables show that the significant terms are the odd terms for both n and m. The even terms for n and m are very close to zero. Tables 6.12 and 6.13 show the result of the natural frequency parameters for different numbers of terms. The tables show the fast convergence as increasing N. The published result for this case is shown in tables 6.11. Comparing the calculated result with the published result show that the difference is very close to zero.

It can be seen from figures 6.4 and 6.5 that the values of the natural frequency parameters are found when 1/|Y| approaches zero.

Table 6.1 The displacement parameters of SSSS square plate without added mass subjected to a concentrated force (a=b=3)

	m							
n	1	2	3	4	5	6	7	8
1	1223.2	4.71E-21	-8.41E-06	-6.94E-22	1.20E-06	2.17E-22	-3.23E-07	-9.37E-23
2	4.71E-21	2.02E-37	-5.99E-22	-6.11E-38	1.18E-22	2.28E-38	-3.52E-23	-1.05E-38
3	-8.41E-06	-5.99E-22	2.52E-06	3.18E-22	-7.01E-07	-1.47E-22	2.40E-07	7.42E-23
4	-6.94E-22	-6.11E-38	3.18E-22	4.75E-38	-1.18E-22	-2.69E-38	4.68E-23	1.51E-38
5	1.20E-06	1.18E-22	-7.01E-07	-1.18E-22	3.23E-07	7.98E-23	-1.48E-07	-4.99E-23
6	2.17E-22	2.28E-38	-1.47E-22	-2.69E-38	7.98E-23	2.10E-38	-4.11E-23	-1.45E-38
7	-3.23E-07	-3.52E-23	2.40E-07	4.68E-23	-1.48E-07	-4.11E-23	8.41E-08	3.10E-23
8	-9.37E-23	-1.05E-38	7.42E-23	1.51E-38	-4.99E-23	-1.45E-38	3.10E-23	1.18E-38
9	1.20E-07	1.37E-23	-9.97E-08	-2.10E-23	7.19E-08	2.17E-23	-4.78E-08	-1.88E-23
10	4.85E-23	5.60E-39	-4.16E-23	-9.00E-39	3.16E-23	9.82E-39	-2.23E-23	-9.00E-39
11	-5.42E-08	-6.33E-24	4.78E-08	1.05E-23	-3.79E-08	-1.20E-23	2.79E-08	1.16E-23
12	-2.82E-23	-3.32E-39	2.53E-23	5.67E-39	-2.08E-23	-6.73E-39	1.59E-23	6.72E-39
13	2.79E-08	3.30E-24	-2.55E-08	-5.78E-24	2.14E-08	7.06E-24	-1.70E-08	-7.28E-24
14	1.78E-23	2.12E-39	-1.65E-23	-3.77E-39	1.42E-23	4.72E-39	-1.15E-23	-5.01E-39
15	-1.58E-08	-1.89E-24	1.47E-08	3.40E-24	-1.29E-08	-4.35E-24	1.08E-08	4.73E-24

Table 6.2 The displacement parameters of SSSS square plate without added mass subjected to a concentrated force (Continuation of table 6.1)

n	m						
	9	10	11	12	13	14	15
1	1.20E-07	4.85E-23	-5.42E-08	-2.82E-23	2.79E-08	1.78E-23	-1.58E-08
2	1.37E-23	5.60E-39	-6.33E-24	-3.32E-39	3.30E-24	2.12E-39	-1.89E-24
3	-9.97E-08	-4.16E-23	4.78E-08	2.53E-23	-2.55E-08	-1.65E-23	1.47E-08
4	-2.10E-23	-9.00E-39	1.05E-23	5.67E-39	-5.78E-24	-3.77E-39	3.40E-24
5	7.19E-08	3.16E-23	-3.79E-08	-2.08E-23	2.14E-08	1.42E-23	-1.29E-08
6	2.17E-23	9.82E-39	-1.20E-23	-6.73E-39	7.06E-24	4.72E-39	-4.35E-24
7	-4.78E-08	-2.23E-23	2.79E-08	1.59E-23	-1.70E-08	-1.15E-23	1.08E-08
8	-1.88E-23	-9.00E-39	1.16E-23	6.72E-39	-7.28E-24	-5.01E-39	4.73E-24
9	3.08E-08	1.51E-23	-1.98E-08	-1.17E-23	1.29E-08	9.02E-24	-8.62E-09
10	1.51E-23	7.57E-39	-1.01E-23	-6.10E-39	6.83E-24	4.84E-39	-4.68E-24
11	-1.98E-08	-1.01E-23	1.38E-08	8.45E-24	-9.60E-09	-6.89E-24	6.74E-09
12	-1.17E-23	-6.10E-39	8.45E-24	5.25E-39	-6.05E-24	-4.40E-39	4.36E-24
13	1.29E-08	6.83E-24	-9.60E-09	-6.05E-24	7.07E-09	5.19E-24	-5.20E-09
14	9.02E-24	4.84E-39	-6.89E-24	-4.40E-39	5.19E-24	3.86E-39	-3.90E-24
15	-8.62E-09	-4.68E-24	6.74E-09	4.36E-24	-5.20E-09	-3.90E-24	3.99E-09

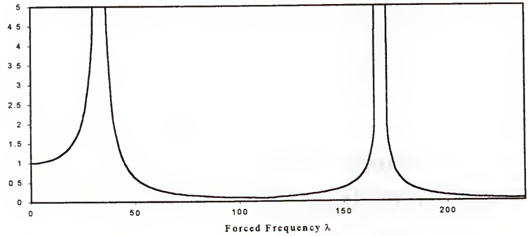

Figure 6.2 Maximum deflection vs. forced frequency for SSSS Plate without added mass and a concentrated force at the middle.

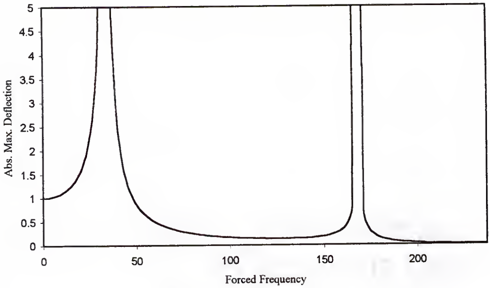

Figure 6.3 Maximum deflection vs. forced frequency for SSSS Plate without added mass at the middle and subjected to uniformly distributed load.

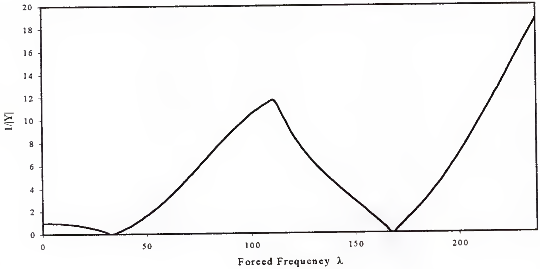

Figure 6.4 Inverse of maximum deflection vs. forced frequency for SSSS Plate without added mass and subjected to a concentrated force at the middle.

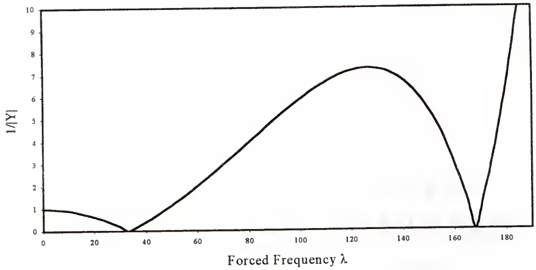

Figure 6.5 Inverse of maximum absolute deflection vs. forced frequency for SSSS Plate without added mass and subjected to uniformly distributed load on the entire surface.

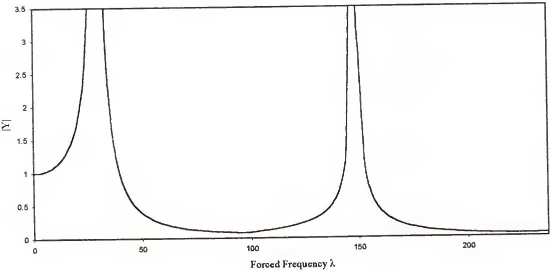

Figure 6.6 Maximum absolute deflection vs. forced frequency for SSSS Plate with 50kg mass and concentrated force at the middle

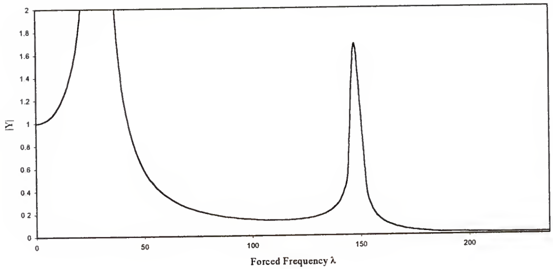

Figure 6.7 Maximum absolute deflection vs. forced frequency for SSSS Plate with 50kg mass at the middle and subjected to uniformly distributed load.

Plates with Two Clamped Edges in y Direction and Simply Supported in the x Direction

The previous case does not require the use of multipliers since all boundary conditions are satisfied. In the present case, the plate is simply support at two edges while clamped at the other two as shown in figure 6.8. The boundary conditions are

$$w(x,y)=0 \quad \frac{\partial w(x,y)}{\partial x}=0 \text{ at } (x=0 \text{ and } x=a) \tag{6.16}$$

$$w(x,y)=0 \quad M_y(x,y)=0 \text{ at } (y=0 \text{ and } y=b) \tag{6.17}$$

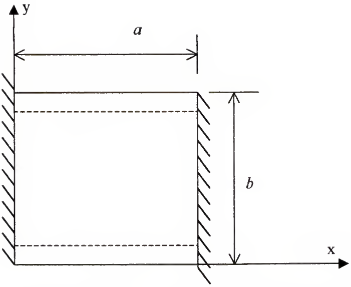

Figure 6.8 Rectangular plate with clamped edges along the y-axis, and simple support along x-axis.

The assumed function is considered as equation 5.1. The strain energy will take the same form as equation 5.4 while the kinetic energy will take the same form as equation 5.13. The external work due to the uniformly distributed load through the entire plate also is the same fas in equation 5.8.

Since we use the same function of equation 5.1 it is found that deflection boundary conditions along all edges are satisfied by the assumed function. The moment boundary conditions on the edges along the x-axis are also satisfied. The slope boundary conditions at x=0 and x=a along the y-axis are not satisfied. Therefore the unsatisfied constrains at x=0 are

$$G_i = w_x(0, y_i) = \sum\sum A_{mn} \frac{n\pi}{a} \sin(\frac{m\pi}{b} y_i) \tag{6.18}$$

where $i = 1,2,\ldots,I$ and I is the number of discrete points along y-axis at x=0. Equation 6.18 can be simplified in the following form

$$G_i = \sum_{m=1}^{N}\sum_{n=1}^{N} A_{mn}\overline{G}_{mni} \tag{6.19}$$

where $\overline{G}_{mni} = \frac{n\pi}{a}\sin(\frac{m\pi}{b}y_i)$ (6.20)

The other unsatisfied constrains at x=a are

$$H_j = w_x(0,y_j) = \sum_{m=1}^{N}\sum_{n=1}^{N} A_{mn}\frac{n\pi}{a}\cos(n\pi)\sin(\frac{m\pi}{b}y_j) \tag{6.21}$$

where $j = 1,2,\ldots\ldots,J$ and J is the number of discrete points along y-axis at x=a. Equation 6.21 can be simplified in the following form

$$H_i = \sum_{m=1}^{N}\sum_{n=1}^{N} A_{mn}\overline{H}_{mnj} \tag{6.22}$$

where $\overline{H}_{mnj} = \frac{n\pi}{a}\cos(n\pi)\sin(\frac{m\pi}{b}y_j)$ (6.23)

In this case, the Lagrange multipliers are used. The Lagrangian function becomes

$$L = U - W - T + \sum_{1}^{I}\lambda_i G_i + \sum_{1}^{J}\mu_j H_j \tag{6.24}$$

$$L = \sum_{n=1}^{N}\sum_{m=1}^{N} Q_{mn}A_{mn}^2 - \sum_{n=1}^{N}\sum_{m=1}^{N} A_{mn}S_{mn} - \sum_{n=1}^{N}\sum_{m=1}^{N} A_{mn}^2\varpi^2 +$$

$$\sum_{i=1}^{I}\lambda_i \sum_{n=1}^{N}\sum_{m=1}^{N} A_{mn}\overline{G}_{mni} + \sum_{j=1}^{J}\mu_j \sum_{n=1}^{N}\sum_{m=1}^{N} A_{mn}\overline{H}_{mnj} \tag{6.25}$$

The energy terms are the same as in the previous case. Taking partial derivatives of equation 6.25 with respect to A_{mn} gives the following

$$\frac{\partial L}{\partial A_{mn}} = 0 \tag{6.26}$$

$$2\sum_{n=1}^{N}\sum_{m=1}^{N} Q_{mn}A_{mn} - \sum_{n=1}^{N}\sum_{m=1}^{N} S_{mn} - 2\sum_{n=1}^{N}\sum_{m=1}^{N} A_{mn}\overline{\omega}^2 + \sum_{i=1}^{I}\lambda_i \sum_{n=1}^{N}\sum_{m=1}^{N} \overline{G}_{mni} +$$

$$\sum_{j=1}^{J}\mu_j \sum_{n=1}^{N}\sum_{m=1}^{N} \overline{H}_{mnj} = 0 \tag{6.27}$$

Simplifying equation 6.27 gives

$$\sum_{n=1}^{N}\sum_{m=1}^{N} [2A_{mn}(Q_{mn} - \overline{\omega}^2) - S_{mn} + \sum_{i=1}^{I}\lambda_i\overline{G}_{mn} + \sum_{j}^{J}\mu_j\overline{H}_{mnj}] = 0 \tag{6.28}$$

Solving equation 6.28 may require extensive computing for large numbers N and M terms. For example, if N=20 and M=20 then 400 equations need to be solved, which requires too much time. Instead, equation 6.28 can take a simple form so that it can be solved rapidly. The simple form of equation 6.28 is the following

$$2A_{mn}(Q_{mn} - \overline{\omega}^2) - S_{mn} + \sum_{i=1}^{I}\lambda_i\overline{G}_{mn} + \sum_{j}^{J}\mu_j\overline{H}_{mnj} = 0 \tag{6.29}$$

Then the displacement parameters can be determined from

$$A_{mn} = \frac{1}{2(Q_{mn} - \overline{\omega}^2)}\left[S_{mn} - \sum_{1}^{I}\lambda_i\overline{G}_{mni} - \sum_{1}^{J}\mu_j\overline{H}_{mnj}\right] \tag{6.30}$$

Taking the derivative of equation 6.25 with respect to λ_i gives the same form as equation 6.19. Also taking the derivative of equation 6.25 with respect to μ_j gives the same form as equation 6.22.

To simplify equation 6.30 let

$$\overline{Q}_{mn} = \frac{1}{2(Q_{mn} - \varpi^2)} \tag{6.31}$$

Then equation 6.30 becomes

$$A_{mn} = \overline{Q}_{mn}\left[S_{mn} - \sum_{1}^{I} \lambda_i \overline{G}_{mni} - \sum_{1}^{J} \mu_j \overline{H}_{mnj} \right] \tag{6.32}$$

From equation 6.19 and equation 6.32 we obtain

$$\sum_{m=1}^{N} \sum_{n=1}^{N} \overline{Q}_{mn}\left[S_{mn} - \sum_{1}^{I} \lambda_i \overline{G}_{mni} - \sum_{1}^{J} \mu_j \overline{H}_{mnj} \right] \overline{G}_{mn\bar{i}} = 0 \tag{6.33}$$

Expanding equation 6.33 yields

$$\sum_{m=1}^{N} \sum_{n=1}^{N} \overline{Q}_{mn} S_{mn} \overline{G}_{mn\bar{i}} - \sum_{1}^{I} \lambda_i \sum_{m=1}^{N} \sum_{n=1}^{N} \overline{Q}_{mn} \overline{G}_{mni} \overline{G}_{mn\bar{i}} -$$

$$\sum_{1}^{J} \mu_j \sum_{m=1}^{N} \sum_{n=1}^{N} \overline{Q}_{mn} \overline{H}_{mnj} \overline{G}_{mn\bar{i}} = 0 \tag{6.34}$$

where $\bar{i} = 1,2,.......I$. Equation 6.34 produces I simultaneous equations. From equation 6.22 and equation 6.32 we get

$$\sum_{m=1}^{N} \sum_{n=1}^{N} \overline{Q}_{mn}\left[S_{mn} - \sum_{1}^{I} \lambda_i \overline{G}_{mni} - \sum_{1}^{J} \mu_j \overline{H}_{mnj} \right] \overline{H}_{mn\bar{j}} = 0 \tag{6.35}$$

Expanding equation 6.35 gives

$$\sum_{m=1}^{N}\sum_{n=1}^{N}\overline{Q}_{mn}S_{mn}\overline{H}_{mn\bar{j}} - \sum_{1}^{I}\lambda_i \sum_{m=1}^{N}\sum_{n=1}^{N}\overline{Q}_{mn}\overline{G}_{mni}\overline{H}_{mn\bar{j}} -$$

$$\sum_{1}^{J}\mu_j \sum_{m=1}^{N}\sum_{n=1}^{N}\overline{Q}_{mn}\overline{H}_{mnj}\overline{H}_{mn\bar{j}} \qquad (6.36)$$

where $\bar{j} = 1,2,3,\ldots\ldots.J$

Equation 6.36 gives J simultaneous equations. Solving these I+J equations yields the parameters λ_i and μ_j. Taking the undetermined multipliers resulted from solving equations 6.34 and 6.36 and apply them to equation 6.32 produces the values of A_{mn}. The same procedure can be applied for all the following examples in this study.

Result

Tables 6.3-6.4 show the displacement parameters for a square plate without added mass for N=15. Tables 6.12 and 6.13 show respectively the natural frequency parameters for a square plate without added mass and a square plate with added mass of 50kg. The tables show the convergence as N increases. Table 6.11 shows the published results for a square plate without an added mass. Figures 6.11 and 6.12 show the inverse of the maximum absolute deflection versus the forced frequency. The figures are built up by finding the inverse of the normalized maximum absolute deflection for incremental change in the forced frequency. The figures show that the natural frequency parameter is determined when 1/|Y| approaches zero. Table 6.14 shows the comparison of the calculated result with the published result. The comparison shows that the difference is 1.5% for 15 terms. The difference can be further reduced as N increases.

Table 6.3 The displacement parameters of CSCS square plate without added mass subjected to a concentrated force

	m							
n	1	2	3	4	5	6	7	8
1	1214.3	-1.68E-13	-194.58	-1.93E-14	-44.3	-6.19E-15	-16.609	-2.57E-15
2	-1.16E-13	-3.55E-14	-3.94E-14	-9.99E-15	-1.23E-14	-3.40E-15	-5.15E-15	-1.69E-15
3	-8.56E-06	-1.88E-15	2.82E-06	-9.76E-16	-5.85E-07	-2.98E-16	2.97E-07	-2.26E-16
4	1.58E-14	2.69E-15	2.12E-14	2.07E-15	1.37E-14	1.23E-15	7.42E-15	6.59E-16
5	1.21E-06	3.52E-15	-7.01E-07	3.51E-15	3.26E-07	2.35E-15	-1.47E-07	1.48E-15
6	-1.43E-15	1.17E-30	-2.89E-15	1.39E-30	-2.62E-15	1.03E-30	-1.89E-15	7.48E-31
7	-3.24E-07	-9.93E-16	2.40E-07	-1.32E-15	-1.48E-07	-1.25E-15	8.35E-08	-8.72E-16
8	-2.19E-15	-2.28E-16	-5.40E-15	-3.29E-16	-5.97E-15	-3.31E-16	-5.23E-15	-2.57E-16
9	1.16E-07	4.17E-17	-1.10E-07	6.40E-17	5.98E-08	4.40E-17	-5.90E-08	5.72E-17
10	-2.43E-16	1.81E-16	-6.33E-16	2.91E-16	-7.70E-16	4.23E-16	-1.00E-15	2.91E-16
11	0.39736	7.70E-17	1.0498	1.28E-16	1.387	2.93E-16	1.4321	1.41E-16
12	4.24E-16	-7.32E-32	1.14E-15	-1.25E-31	1.56E-15	-6.60E-32	1.67E-15	-1.48E-31
13	-0.20459	-3.01E-17	-0.55982	-5.27E-17	-0.78544	-1.22E-16	-0.87079	-6.65E-17
14	-6.39E-17	-5.64E-17	-1.40E-16	-1.00E-16	-2.40E-16	-1.17E-16	-2.40E-16	-1.33E-16
15	-1.53E-08	-5.73E-18	1.62E-08	-1.04E-17	-1.07E-08	-8.83E-18	1.33E-08	-1.44E-17

Table 6.4 The displacement parameters of CSCS square plate without added mass subjected to a concentrated force (Continuation of table 6.3)

	m						
n	9	10	11	12	13	14	15
1	-7.922	-6.20E-16	-4.371	-8.01E-16	-2.6596	-3.72E-16	-1.7362
2	-1.92E-15	-1.00E-15	-1.58E-15	-4.94E-16	-7.24E-16	-3.01E-16	-5.05E-16
3	-6.96E-08	-3.04E-16	6.55E-08	-5.14E-17	-1.43E-08	-8.59E-17	2.22E-08
4	4.41E-15	4.47E-16	2.69E-15	2.58E-16	1.69E-15	2.14E-16	1.22E-15
5	7.26E-08	9.63E-16	-3.74E-08	6.11E-16	2.17E-08	4.19E-16	-1.27E-08
6	-1.28E-15	5.78E-31	-8.68E-16	3.30E-31	-6.01E-16	1.19E-31	-4.28E-16
7	-4.82E-08	-6.77E-16	2.76E-08	-4.84E-16	-1.72E-08	-3.21E-16	1.06E-08
8	-4.15E-15	-2.46E-16	-3.06E-15	-1.53E-16	-2.28E-15	-1.25E-16	-1.74E-15
9	2.15E-08	1.10E-16	-2.71E-08	2.38E-17	7.27E-09	4.70E-17	-1.30E-08
10	-7.71E-16	3.01E-16	-5.30E-16	2.63E-16	-4.49E-16	1.78E-16	-3.07E-16
11	1.304	1.35E-16	1.1104	2.06E-16	0.91377	1.26E-16	0.74066
12	1.58E-15	-2.15E-31	1.39E-15	-5.15E-32	1.18E-15	-3.70E-32	9.81E-16
13	-0.85127	-4.99E-17	-0.77319	-1.04E-16	-0.67265	-9.48E-17	-0.57118
14	-2.51E-16	-1.17E-16	-2.63E-16	-1.09E-16	-2.44E-16	-9.39E-17	-1.43E-16
15	-6.01E-09	-3.42E-17	9.24E-09	-8.83E-18	-2.93E-09	-2.04E-17	6.00E-09

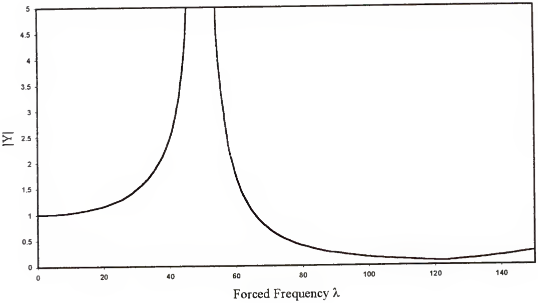

Figure 6.9 Maximum absolute deflection vs. forced frequency for CSCS Plate without added mass and subjected to a concentrated force at the middle

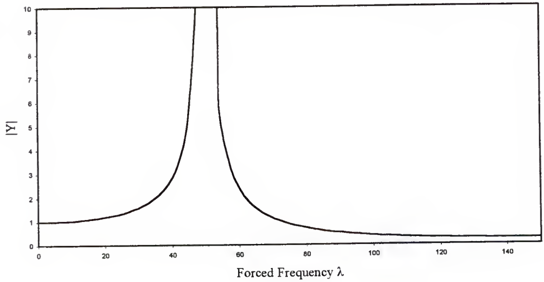

Figure 6.10 Maximum absolute deflection vs. forced frequency for CSCS Plate without added mass at the middle and subjected to uniformly distributed load.

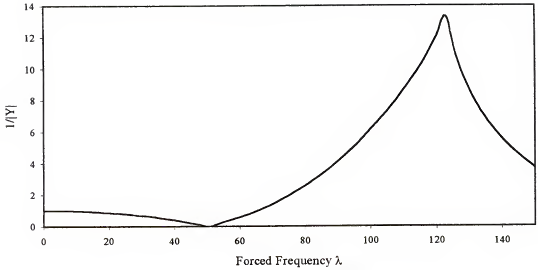

Figure 6.11 The inverse of normalized maximum deflection vs. forced frequency for CSCS Plate without added mass and subjected to a concentrated force at the middle.

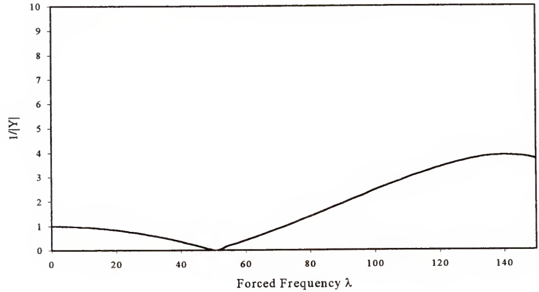

Figure 6.12 The inverse of normalized maximum deflection vs. forced frequency for CSCS Plate without added mass and subjected to uniformly distributed load on the entire surface

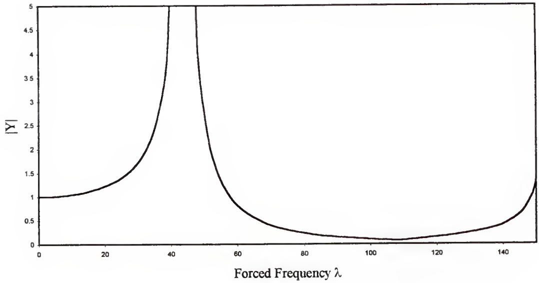

Figure 6.13 The normalized maximum absolute deflection vs. forced frequency for CSCS Plate with 50kg mass and a concentrated force at the middle.

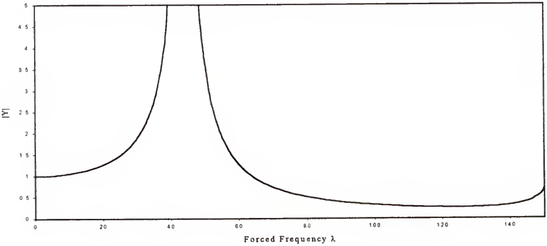

Figure 6.14 The normalized maximum absolute deflection vs. forced frequency for CSCS Plate with 50kg mass at the middle and subjected to uniformly distributed load.

Plates with One Clamped Edge in y Direction at x=0 and Simply Supported at the Other Edges

Consider a rectangular plate with three edges simply supported and clamped at the fourth edge as shown in figure 5.3

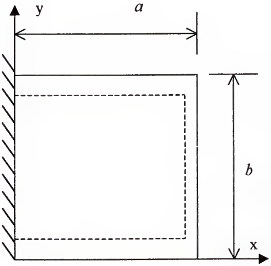

Figure 6.15 Rectangular plate clamped at one edge and simply supported at the other edges

Using the same assumed function as in equation 5.1, the formulations of the strain energy, the external potential energy, and the kinetic energy are the same as in equations 5.4, 5.8, and 5.13 respectively.

The boundary conditions are

$$w(0,y)=0\,,\; w(a,y)=0\,,\; \frac{\partial w(0,y)}{\partial x}=0\,,\; M_x(a,y)=0 \tag{6.37}$$

$$w(x,y)=0 \quad M_y(x,y)=0 \text{ at } (y=0 \text{ and } y=b) \tag{6.38}$$

The boundary conditions, however, are not all satisfied by the assumed deflection function. The unsatisfied constraint is

$$G_i = w_x(0,y_i) = \sum_1^N \sum_1^N A_{mn} \frac{n\pi}{a} \sin(\frac{m\pi}{b} y_i) \tag{6.39}$$

$$G_i = \sum_{m=1}^N \sum_{n=1}^N A_{mn} \overline{G}_{mni} \tag{6.40}$$

where

$$\overline{G}_{mni} = \frac{n\pi}{a} \sin(\frac{m\pi}{b} y_i) \tag{6.41}$$

The Lagrangian function is

$$L = U - W - T + \sum_1^I \lambda_i G_i \tag{6.42}$$

$$L = \sum_1^N \sum_1^N Q_{mn} A_{mn}^2 - \sum_1^N \sum_1^N A_{mn} S_{mn} - \sum_n^N \sum_{m=1}^N A_{mn}^2 \overline{\omega}^2 +$$

$$\sum_1^I \lambda_i \sum_1^N \sum_1^N A_{mn} \overline{G}_{mni} \tag{6.43}$$

Taking the derivative of L with respect to A_{mn} and making it equal to zero gives an equation in term of A_{mn} as in the following form:

$$\frac{\partial L}{\partial A_{mn}} = 0 \tag{6.44}$$

From which:

$$A_{mn} = \frac{1}{2(Q_{mn} - \overline{\omega}^2)} \left[S_{mn} - \sum_{1}^{I} \lambda_i \overline{G}_{mni} \right] \tag{6.45}$$

Let

$$\overline{Q}_{mn} = \frac{1}{2(Q_{mn} - \overline{\omega}^2)} \tag{6.46}$$

Then equation 6.45 becomes:

$$A_{mn} = \overline{Q}_{mn} \left[S_{mn} - \sum_{1}^{I} \lambda_i \overline{G}_{mni} \right] \tag{6.47}$$

Taking the derivative of L with respect to λ_i and making it equal to zero gives an equation in term of λ_i as in the following form:

$$\frac{\partial L}{\partial \lambda_i} = 0 \tag{6.48}$$

From which:

$$\sum_{m=1}^{N} \sum_{n=1}^{N} A_{mn} \overline{G}_{mni} = 0 \tag{6.49}$$

$$\sum_{m=1}^{N} \sum_{n=1}^{N} \overline{Q}_{mn} \left[S_{mn} - \sum_{i=1}^{I} \lambda_i \overline{G}_{mni} \right] \overline{G}_{mn\bar{i}} = 0 \tag{6.50}$$

Equation 6.50 gives I simultaneous equations. Solving these equations gives λ_i. Substituting λ_i into equation 6.47 Gives A_{mn}

Result

The displacement parameters are shown in tables 6.5 and 6.6 for a square plate without a concentrated mass with N=15. The result in the tables show a fast convergence at N=15. Comparing the calculated result with the published result shown in table 6.14 gives a difference of 0.74%. Figures 6.18 and 6.19 show the inverse of normalized maximum absolute deflection versus the forced frequency. The value of the natural frequency parameter can be obtained as 1/|Y| approaches zero.

Table 6.5 The displacement parameters of CSSS square plate without added concentrated mass subjected to a concentrated force.

	m							
n	1	2	3	4	5	6	7	8
1	592.75	-112.84	-34.464	-15.282	-8.0716	-4.7618	-3.0363	-2.0513
2	-1.27E-14	-8.40E-15	-4.15E-15	-2.48E-15	-1.26E-15	-8.49E-16	-5.36E-16	-4.23E-16
3	-8.43E-06	1.59E-07	2.66E-06	8.39E-08	-6.45E-07	3.86E-08	2.67E-07	1.95E-08
4	1.19E-15	1.72E-15	1.46E-15	1.33E-15	1.08E-15	6.69E-16	5.70E-16	4.23E-16
5	1.21E-06	1.05E-09	-7.01E-07	1.04E-09	3.24E-07	7.06E-10	-1.47E-07	4.42E-10
6	-2.61E-16	-4.46E-16	-5.29E-16	-5.27E-16	-4.79E-16	-4.12E-16	-3.45E-16	-2.85E-16
7	-3.24E-07	-3.12E-10	2.40E-07	-4.15E-10	-1.48E-07	-3.63E-10	8.38E-08	-2.74E-10
8	-2.98E-16	-5.45E-16	-7.34E-16	-7.88E-16	-7.60E-16	-7.82E-16	-6.95E-16	-6.15E-16
9	1.18E-07	-3.60E-09	-1.05E-07	-5.52E-09	6.61E-08	-5.69E-09	-5.32E-08	-4.94E-09
10	-5.71E-17	-1.08E-16	-1.58E-16	-1.73E-16	-2.02E-16	-2.03E-16	-2.30E-16	-1.73E-16
11	0.072715	0.13853	0.19211	0.23064	0.25384	0.26341	0.2621	0.25293
12	7.75E-17	1.49E-16	2.09E-16	2.55E-16	2.85E-16	3.02E-16	3.06E-16	3.01E-16
13	-0.03744	-0.07231	-0.10246	-0.12646	-0.14375	-0.15448	-0.15937	-0.15944
14	-6.30E-18	-1.22E-17	-1.61E-17	-2.17E-17	-2.77E-17	-2.51E-17	-2.50E-17	-2.89E-17
15	-1.56E-08	4.95E-10	1.55E-08	8.94E-10	-1.19E-08	1.14E-09	1.20E-08	1.24E-09

Table 6.6 The displacement parameters of CSSS square plate without added concentrated mass subjected to concentrated force (Continuation of table 6.5)

	m						
n	9	10	11	12	13	14	15
1	-1.4493	-1.0612	-0.79987	-0.61765	-0.48675	-0.39033	-0.31776
2	-1.67E-16	-1.95E-16	-1.54E-16	-1.24E-16	-6.03E-17	-7.52E-17	-5.16E-17
3	-8.53E-08	1.09E-08	5.62E-08	6.66E-09	-2.02E-08	4.33E-09	1.83E-08
4	3.84E-16	2.68E-16	1.92E-16	1.41E-16	1.32E-16	1.07E-16	8.28E-17
5	7.22E-08	2.80E-10	-3.77E-08	1.84E-10	2.16E-08	1.25E-10	-1.28E-08
6	-2.34E-16	-1.92E-16	-1.59E-16	-1.32E-16	-1.10E-16	-9.26E-17	-7.84E-17
7	-4.80E-08	-1.97E-10	2.78E-08	-1.41E-10	-1.71E-08	-1.02E-10	1.07E-08
8	-5.58E-16	-4.47E-16	-4.13E-16	-3.61E-16	-2.99E-16	-2.62E-16	-2.30E-16
9	2.63E-08	-3.96E-09	-2.33E-08	-3.08E-09	1.02E-08	-2.37E-09	-1.07E-08
10	-1.65E-16	-1.58E-16	-1.29E-16	-1.26E-16	-1.04E-16	-1.17E-16	-9.11E-17
11	0.23866	0.22154	0.20323	0.18488	0.16724	0.15073	0.13556
12	2.90E-16	2.74E-16	2.55E-16	2.36E-16	2.16E-16	1.97E-16	1.80E-16
13	-0.1558	-0.14952	-0.14151	-0.13252	-0.12311	-0.11369	-0.10454
14	-2.74E-17	-3.09E-17	-2.69E-17	-2.34E-17	-2.71E-17	-1.96E-17	-1.70E-17
15	-7.37E-09	1.23E-09	7.94E-09	1.14E-09	-4.11E-09	1.03E-09	4.95E-09

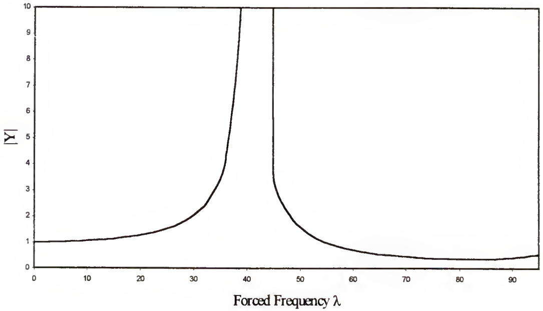

Figure 6.16 Maximum deflection vs. forced frequency for CSSS Plate without added mass and subjected to a concentrated force at the middle.

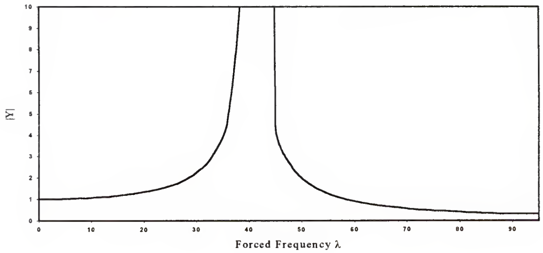

Figure 6.17 Maximum absolute deflection vs. forced frequency for CSSS Plate without added mass at the middle and subjected to uniformly distributed load.

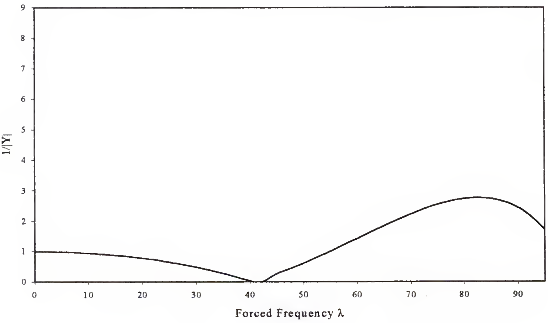

Figure 6.18 The inverse of normalized maximum deflection vs. forced frequency for CSSS Plate without added mass and subjected to a concentrated force at the middle.

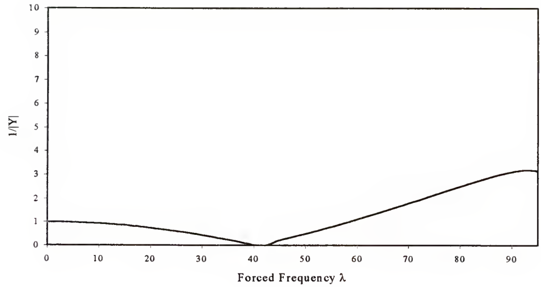

Figure 6.19 The inverse of normalized maximum deflection vs. forced frequency for CSSS Plate without added mass and subjected to uniformly distributed load on the entire surface.

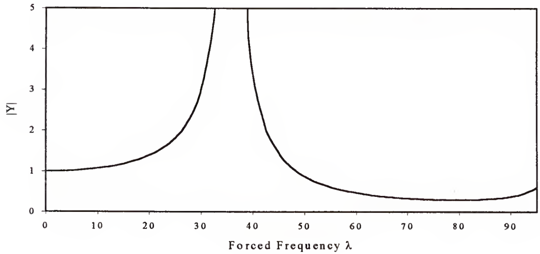

Figure 6.20 Normalized maximum of the absolute deflection vs. forced frequency for CSSS Plate with 50kg mass and subjected to a concentrated force at the middle

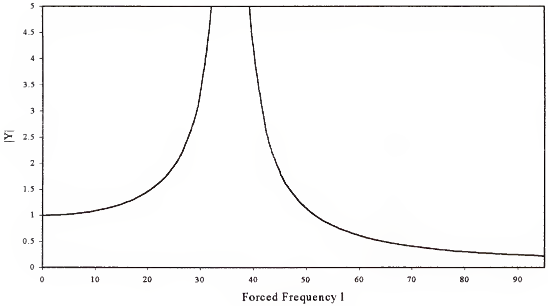

Figure 6.21 Normalized maximum of absolute deflection vs. forced frequency for CSSS Plate with 50kg mass at the middle and subjected to uniformly distributed load.

Plate Clamped in All Edges

In this case, using the same function as in equation 5.1 the strain energy, the kinetic energy and the external work will have the same forms as in chapter 5. The boundary conditions in this example are the deflection and the slope should equal zero for all four edges. However, the deflection boundary conditions are satisfied, the slope boundary conditions are not satisfied. Hence four boundary conditions are not satisfied.

The four unsatisfied constraints are

$$G_i = w_x(0, y_i) = \sum\sum A_{mn} \frac{n\pi}{a} \sin(\frac{m\pi}{b} y_i) \qquad 0 \le y_i \le b \qquad (6.51)$$

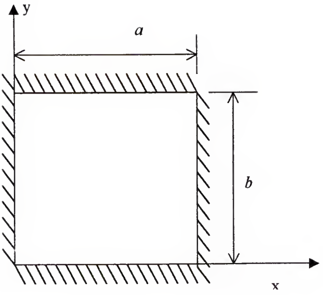

Figure 6.22 Rectangular plate with clamped edges

where $i=1,2,\ldots,I$ and I is the number of discrete points at the edge along y-axis at $x=0$.

$$H_j = w_x(a,y_j) = \sum_{m=1}^{N}\sum_{n=1}^{N} A_{mn}\frac{n\pi}{a}\cos(n\pi)\sin(\frac{m\pi}{b}y_j) \quad 0 \le y_j \le b \quad (6.52)$$

where $j=1,2,\ldots,J$ and J is the number of discrete points at the edge along y-axis at $x=a$.

$$E_k = w_y(x_k,0) = \sum\sum A_{mn}\frac{m\pi}{b}\sin(\frac{n\pi}{a}x_k) \qquad 0 \le x_k \le a \qquad (6.53)$$

where $k=1,2,\ldots,K$ and K is the number of discrete points at the edge along x-axis at $y=0$.

$$Z_l = w_y(x_l,b) = \sum\sum A_{mn}\frac{m\pi}{b}\sin(\frac{n\pi}{a}x_l)\cos(m\pi) \quad 0 \le x_l \le a \quad (6.54)$$

where $l = 1,2,\ldots,L$ and L is the number of discrete points at the edge along x-axis at $y = b$.

To simplify the above equations, we define the following:

$$\overline{G}_{mni} = \frac{n\pi}{a}\sin(\frac{m\pi}{b}y_i) \tag{6.55}$$

$$\overline{H}_{mnj} = \frac{n\pi}{a}\cos(n\pi)\sin(\frac{m\pi}{b}y_j) \tag{6.56}$$

$$\overline{E}_k = \frac{m\pi}{b}\sin(\frac{n\pi}{a}x_k) \tag{6.57}$$

$$\overline{Z}_l = \frac{m\pi}{b}\sin(\frac{n\pi}{a}x_l)\cos(m\pi) \tag{6.58}$$

After simplification, equations 6.55 to 6.58 take the following forms:

$$G_i = \sum_{m=1}^{N}\sum_{n=1}^{N} A_{mn}\overline{G}_{mni} \tag{6.59}$$

$$H_i = \sum_{m=1}^{N}\sum_{n=1}^{N} A_{mn}\overline{H}_{mnj} \tag{6.60}$$

$$E_k = \sum_{m=1}^{N}\sum_{n=1}^{N} A_{mn}\overline{E}_k \tag{6.61}$$

$$Z_l = \sum_{m=1}^{N}\sum_{n=1}^{N} A_{mn}\overline{Z}_l \tag{6.62}$$

The Lagrangian function and its partial derivatives, which are equated to zero, are as follows

$$L = U - W - T + \sum_{i=1}^{I} \lambda_i G_i + \sum_{j=1}^{J} \mu_j H_j + \sum_{k=1}^{K} \eta_k E_k + \sum_{l=1}^{L} \zeta_l Z_l \tag{6.63}$$

$$\frac{\partial L}{\partial A_{mn}} = 0, \; \frac{\partial L}{\partial \lambda_i} = 0, \; \frac{\partial L}{\partial \mu_j} = 0, \; \frac{\partial L}{\partial \eta_k} = 0, \; \frac{\partial L}{\partial \zeta_l} = 0 \tag{6.64}$$

Using the same procedure as in the previous cases the displacement parameter A_{mn} and the natural frequency ω_n can be found.

Result

Tables 6.7 and 6.8 show the displacement parameters for the clamped square plate without added concentrated mass at N=15. The table shows that the odd terms of n and m are the significant ones. The even terms are close to zero. Therefore using the odd numbers only is all that is necessary with the assumed function. Figures 6.25 and 6.26 show that the value of the natural frequency parameter can be found as 1/|Y| approaches zero. Tables 6.12 and 6.13 show the convergence rate as N increases. A published result for the natural frequency is shown in table 6.11. The calculated result with 15 terms is λ=36.6999 where $\lambda = \omega_n a^2 \sqrt{\rho / D}$. The published result is λ=35.9852. Comparison of the calculated result with the published result is shown in table 6.14. The difference between the calculated and published result for the square plate without an added concentrated mass is 2% for 15 terms only and 6 discrete points at each edge. The difference can be further reduced by increasing N.

Table 6.7 The displacement parameters of CCCC plate without added concentrated mass subjected to a concentrated force at the middle.

	m							
n	1	2	3	4	5	6	7	8
1	3138	6.06E-13	-497.65	1.00E-13	-115.48	1.72E-14	-43.662	8.07E-15
2	1.28E-13	-3.00E-14	-1.46E-13	-5.06E-14	-3.82E-14	-6.82E-15	-2.30E-14	-1.43E-15
3	-497.65	-1.38E-13	65.211	4.92E-16	16.394	-9.55E-15	6.4859	-1.13E-14
4	8.03E-14	1.71E-14	2.80E-14	-1.85E-14	2.56E-14	2.24E-15	4.36E-15	4.33E-15
5	-115.48	-1.09E-14	16.394	3.54E-14	2.5055	1.23E-14	0.22808	1.52E-15
6	9.10E-15	5.69E-15	2.09E-15	-1.27E-14	2.60E-15	1.84E-29	-5.00E-15	3.13E-15
7	-43.662	-2.17E-14	6.4859	-2.57E-15	0.22808	-9.97E-15	-0.90934	-1.33E-14
8	5.93E-15	1.83E-15	-6.22E-15	-7.35E-15	-4.72E-15	-5.42E-16	-1.03E-14	2.06E-15
9	-21.182	-6.34E-15	2.5014	4.93E-15	-1.0024	-4.76E-16	-1.7295	-4.95E-15
10	3.48E-15	1.67E-15	-1.01E-15	-3.22E-15	3.47E-16	6.83E-16	-4.20E-15	2.68E-15
11	-10.369	-4.31E-15	4.9352	1.48E-15	3.9406	-1.52E-15	3.4991	-4.96E-15
12	2.09E-15	8.24E-16	3.24E-15	-2.68E-15	4.55E-15	8.58E-31	2.33E-15	1.45E-15
13	-7.4727	-1.85E-15	-0.07675	2.00E-15	-1.8339	-1.35E-16	-2.4421	-2.64E-15
14	1.02E-15	2.71E-16	-2.86E-16	-1.98E-15	-4.19E-16	-1.90E-16	-2.48E-15	8.36E-16
15	-4.4633	-1.56E-15	1.1085	8.91E-16	0.41928	-6.68E-16	0.1899	-2.71E-15

Table 6.8 The displacement parameters of CCCC plate without mass subjected to a concentrated force at the middle (Continuation of table 6.7)

	m						
n	9	10	11	12	13	14	15
1	-21.182	3.07E-15	-10.369	3.29E-15	-7.4727	1.38E-15	-4.4633
2	-9.34E-15	-2.28E-15	-6.03E-15	-9.89E-16	-2.76E-15	-7.78E-16	-2.15E-15
3	2.5014	-3.95E-15	4.9352	1.23E-15	-0.07675	-1.57E-15	1.1085
4	4.35E-15	3.58E-16	1.76E-15	4.70E-16	2.21E-15	4.35E-16	1.38E-15
5	-1.0024	3.24E-15	3.9406	7.11E-15	-1.8339	1.51E-15	0.41928
6	-2.20E-15	-3.90E-16	-2.15E-15	1.98E-31	-1.22E-16	1.34E-16	-2.56E-16
7	-1.7295	-7.18E-15	3.4991	3.47E-16	-2.4421	-3.55E-15	0.1899
8	-6.41E-15	-8.95E-16	-5.94E-15	-2.50E-16	-2.71E-15	-6.23E-17	-2.46E-15
9	-2.3134	-1.71E-15	2.4928	3.72E-15	-2.9221	-1.02E-15	-0.21605
10	-2.24E-15	3.61E-16	-2.41E-15	4.24E-16	-7.73E-16	4.53E-16	-1.01E-15
11	2.4928	-2.73E-15	5.7934	2.44E-15	0.36673	-1.86E-15	2.2419
12	2.80E-15	-2.42E-16	2.06E-15	-3.76E-30	2.84E-15	1.25E-16	2.15E-15
13	-2.9221	-1.06E-15	0.36673	2.85E-15	-3.5094	-7.04E-16	-1.2076
14	-1.96E-15	-5.35E-16	-2.19E-15	-1.77E-16	-1.12E-15	-7.83E-17	-1.03E-15
15	-0.21605	-1.59E-15	2.2419	1.80E-15	-1.2076	-1.17E-15	0.49946

Table 6.7 The displacement parameters of CCCC plate without added concentrated mass subjected to a concentrated force at the middle.

	m							
n	1	2	3	4	5	6	7	8
1	3138	6.06E-13	-497.65	1.00E-13	-115.48	1.72E-14	-43.662	8.07E-15
2	1.28E-13	-3.00E-14	-1.46E-13	-5.06E-14	-3.82E-14	-6.82E-15	-2.30E-14	-1.43E-15
3	-497.65	-1.38E-13	65.211	4.92E-16	16.394	-9.55E-15	6.4859	-1.13E-14
4	8.03E-14	1.71E-14	2.80E-14	-1.85E-14	2.56E-14	2.24E-15	4.36E-15	4.33E-15
5	-115.48	-1.09E-14	16.394	3.54E-14	2.5055	1.23E-14	0.22808	1.52E-15
6	9.10E-15	5.69E-15	2.09E-15	-1.27E-14	2.60E-15	1.84E-29	-5.00E-15	3.13E-15
7	-43.662	-2.17E-14	6.4859	-2.57E-15	0.22808	-9.97E-15	-0.90934	-1.33E-14
8	5.93E-15	1.83E-15	-6.22E-15	-7.35E-15	-4.72E-15	-5.42E-16	-1.03E-14	2.06E-15
9	-21.182	-6.34E-15	2.5014	4.93E-15	-1.0024	-4.76E-16	-1.7295	-4.95E-15
10	3.48E-15	1.67E-15	-1.01E-15	-3.22E-15	3.47E-16	6.83E-16	-4.20E-15	2.68E-15
11	-10.369	-4.31E-15	4.9352	1.48E-15	3.9406	-1.52E-15	3.4991	-4.96E-15
12	2.09E-15	8.24E-16	3.24E-15	-2.68E-15	4.55E-15	8.58E-31	2.33E-15	1.45E-15
13	-7.4727	-1.85E-15	-0.07675	2.00E-15	-1.8339	-1.35E-16	-2.4421	-2.64E-15
14	1.02E-15	2.71E-16	-2.86E-16	-1.98E-15	-4.19E-16	-1.90E-16	-2.48E-15	8.36E-16
15	-4.4633	-1.56E-15	1.1085	8.91E-16	0.41928	-6.68E-16	0.1899	-2.71E-15

Table 6.8 The displacement parameters of CCCC plate without mass subjected to a concentrated force at the middle (Continuation of table 6.7)

	m						
n	9	10	11	12	13	14	15
1	-21.182	3.07E-15	-10.369	3.29E-15	-7.4727	1.38E-15	-4.4633
2	-9.34E-15	-2.28E-15	-6.03E-15	-9.89E-16	-2.76E-15	-7.78E-16	-2.15E-15
3	2.5014	-3.95E-15	4.9352	1.23E-15	-0.07675	-1.57E-15	1.1085
4	4.35E-15	3.58E-16	1.76E-15	4.70E-16	2.21E-15	4.35E-16	1.38E-15
5	-1.0024	3.24E-15	3.9406	7.11E-15	-1.8339	1.51E-15	0.41928
6	-2.20E-15	-3.90E-16	-2.15E-15	1.98E-31	-1.22E-16	1.34E-16	-2.56E-16
7	-1.7295	-7.18E-15	3.4991	3.47E-16	-2.4421	-3.55E-15	0.1899
8	-6.41E-15	-8.95E-16	-5.94E-15	-2.50E-16	-2.71E-15	-6.23E-17	-2.46E-15
9	-2.3134	-1.71E-15	2.4928	3.72E-15	-2.9221	-1.02E-15	-0.21605
10	-2.24E-15	3.61E-16	-2.41E-15	4.24E-16	-7.73E-16	4.53E-16	-1.01E-15
11	2.4928	-2.73E-15	5.7934	2.44E-15	0.36673	-1.86E-15	2.2419
12	2.80E-15	-2.42E-16	2.06E-15	-3.76E-30	2.84E-15	1.25E-16	2.15E-15
13	-2.9221	-1.06E-15	0.36673	2.85E-15	-3.5094	-7.04E-16	-1.2076
14	-1.96E-15	-5.35E-16	-2.19E-15	-1.77E-16	-1.12E-15	-7.83E-17	-1.03E-15
15	-0.21605	-1.59E-15	2.2419	1.80E-15	-1.2076	-1.17E-15	0.49946

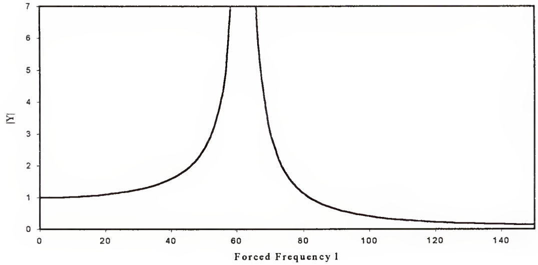

Figure 6.23 Normalized maximum absolute deflection vs. forced frequency for CCCC Plate without added mass and subjected to a concentrated force at the middle.

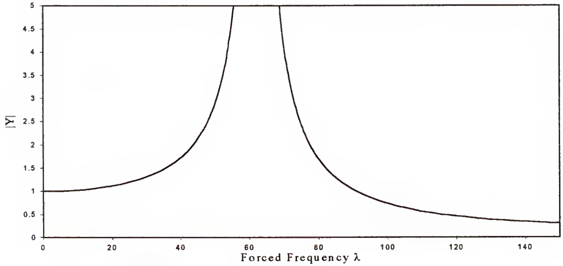

Figure 6.24 Normalized maximum absolute deflection vs. forced frequency for CCCC Plate without added mass at the middle and subjected to uniformly distributed load.

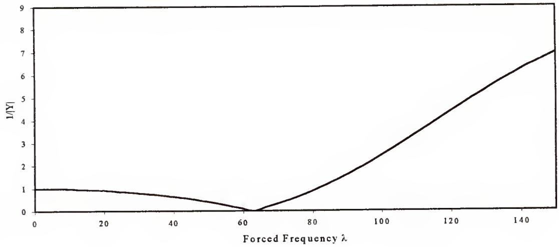

Figure 6.25 The inverse of normalized maximum absolute deflection vs. forced frequency for CCCC Square Plate without added mass and subjected to a concentrated force at the middle.

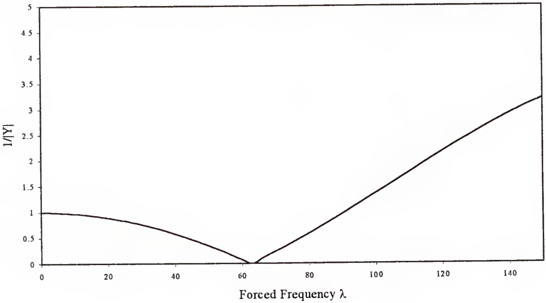

Figure 6.26 The inverse of normalized maximum absolute deflection vs. forced frequency for CCCC Square Plate without added mass and subjected to uniformly distributed load on the entire surface.

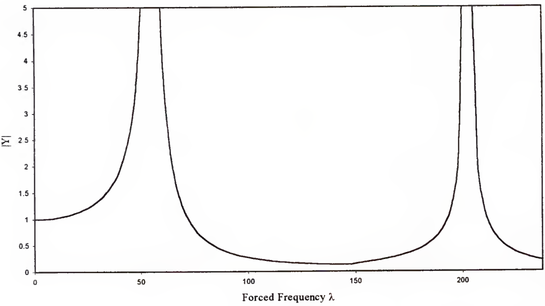

Figure 6.27 Normalized maximum absolute deflection vs. forced frequency for CCCC Plate with 50kg mass and subjected to a concentrated force at the middle.

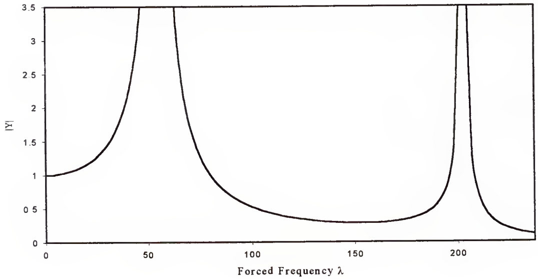

Figure 6.28 Normalized maximum absolute deflection vs. forced frequency for CCCC Plate with 50kg mass at the middle and subjected to uniformly distributed load.

Plate with Mixed Boundary Conditions

The problem of a plate with mixed boundary conditions is difficult to solve by classical plate theory since it needs a function that satisfies all the mixed boundary conditions.

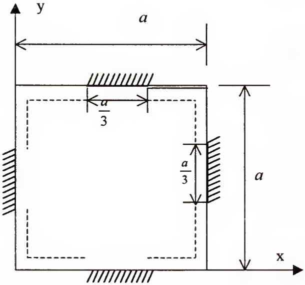

Figure 6.29 Rectangular plate with mixed boundary conditions.

Therefore, only numerical approaches are used to solve this type of problems, such as the finite element method. However, such problems can be readily solved using the present approach since it is based on forcing the unsatisfied boundary condition to be satisfied.

Consider a plate, which has mixed boundary conditions as in figure 6.29. The plate is clamped at x=0 for $b/3 \le y \le 2b/3$, and clamped at x=a for $b/3 \le y \le 2b/3$, clamped at y=0 for $a/3 \le x \le 2a/3$, and clamped at y=b for $a/3 \le x \le 2a/3$. The remaining edges are simply supported. Since the same approximation function of equation 5.1 is used, the only unsatisfied constraints are those related to the slope. Therefore, the constraints are the same as those in equations 6.51 to 6.54 with some limitations on the distances. Equation 6.51 is limited by $b/3 \le y_i \le 2b/3$, equation 6.52 is limited by $b/3 \le y_j \le 2b/3$, equation 6.53 is limited by $a/3 \le x_k \le 2a/3$, and equation 6.54 is limited by $a/3 \le x_l \le 2a/3$. The procedure used is the same as in the previous case. The parameter A_{mn} can be found and accordingly, the natural frequency can also be found by using the previous procedure.

Result

The result shows that the proposed approach can readily handle a plate with mixed boundary conditions. Table 6.9 and 6.10 show the result of the displacement parameters. Tables 6.12 and 6.13 show the fundamental frequency for a square plate of mixed boundary conditions. The convergence can be seen in the tables as N increases. Figures 6.30 to 6.33 and table 6.12 show that the fundamental frequency of this case is 37.7039 at N=15. The fundamental frequency at N=54 is 34.792. From table 6.11, the published result is 33.9. Table 6.14 shows the comparison of the calculated and the published result. The comparison shows that the difference is 2.6%. This difference can be further reduced by increasing N. Also, table 6.13 and figures 6.34 and 6.35 show the fundamental frequency for a square plate with mixed boundary conditions and with an added mass at the middle of the plate. Its fundamental frequency obtained from the table is 32.9086 at N=15.

Table 6.9 The displacement parameters of Mixed B.C. case 1 of square plate without an added concentrated mass and subjected to a concentrated force at the middle.

	m							
n	1	2	3	4	5	6	7	8
1	-589.3	0	89.194	2.33E-15	22.357	-2.21E-15	8.9212	5.45E-16
2	5.61E-14	-4.54E-14	2.01E-14	-1.27E-14	4.36E-15	-2.05E-15	1.69E-15	-2.63E-15
3	89.194	4.86E-15	-28.021	4.19E-15	-7.2765	-3.11E-15	-2.1612	1.78E-15
4	0	7.80E-16	4.29E-15	7.44E-16	5.41E-16	3.18E-15	6.78E-16	-5.42E-16
5	22.357	2.55E-15	-7.2765	3.43E-15	-1.4425	-1.87E-15	0.42098	2.32E-15
6	-4.00E-15	1.33E-15	-1.60E-15	1.23E-15	-3.33E-15	3.35E-15	-2.09E-15	6.02E-17
7	8.9212	5.38E-16	-2.1612	1.64E-15	0.42098	-1.68E-15	1.4042	1.74E-15
8	5.71E-16	-1.57E-15	2.80E-15	-2.31E-15	2.13E-15	-6.98E-16	2.15E-15	-2.44E-15
9	4.0349	-8.34E-17	-1.6848	7.04E-16	-0.37747	-1.55E-15	0.429	1.06E-15
10	-2.95E-16	2.78E-16	3.04E-16	4.03E-16	-3.47E-16	1.53E-15	-1.63E-16	2.24E-17
11	2.1895	3.08E-16	-1.0807	8.98E-16	-0.36803	-4.96E-16	0.17747	1.34E-15
12	-2.86E-16	-8.24E-17	2.39E-16	-2.12E-16	-6.32E-17	5.13E-16	0	-5.28E-16
13	1.3909	-8.04E-17	-0.51993	2.46E-16	-0.02035	-7.72E-16	0.37797	5.87E-16
14	-1.55E-17	-1.35E-16	1.59E-16	-3.61E-16	1.23E-17	8.07E-17	5.01E-17	-7.12E-16
15	0.89421	5.74E-17	-0.38528	3.31E-16	-0.06993	-3.40E-16	0.21102	6.55E-16

Table 6.10 The displacement parameters of Mixed B.C. of square plate without added mass and subjected to a concentrated force (Continuation of table 6.9)

	m						
n	9	10	11	12	13	14	15
1	4.0349	-2.44E-16	2.1895	-9.80E-17	1.3909	-5.72E-17	0.89421
2	1.23E-15	-7.24E-16	3.32E-16	-5.49E-16	4.20E-16	-4.53E-16	1.55E-16
3	-1.6848	7.60E-17	-1.0807	-2.48E-17	-0.51993	-1.43E-17	-0.38528
4	1.06E-15	8.50E-16	-1.20E-16	2.35E-16	3.82E-16	1.00E-17	7.26E-17
5	-0.37747	3.66E-16	-0.36803	2.29E-16	-0.02035	1.11E-16	-0.06993
6	-8.59E-16	1.24E-15	-1.35E-15	5.50E-16	-3.79E-16	2.12E-16	-5.42E-16
7	0.429	1.49E-16	0.17747	6.51E-17	0.37797	-2.51E-17	0.21102
8	2.12E-15	-6.94E-16	8.17E-16	-8.34E-16	1.24E-15	-8.14E-16	6.27E-16
9	-0.13846	-9.18E-17	-0.22632	-1.18E-16	0.070238	-1.41E-16	-0.01293
10	2.58E-16	1.01E-15	-4.31E-16	4.95E-16	2.00E-16	2.33E-16	-1.37E-16
11	-0.22632	3.82E-16	-0.29275	2.94E-16	-0.01853	2.21E-16	-0.07909
12	3.20E-16	3.03E-16	-2.57E-16	1.22E-31	2.58E-16	-1.56E-16	-5.61E-17
13	0.070238	-8.31E-17	-0.018531	-1.26E-16	0.17733	-1.17E-16	0.092187
14	3.01E-16	-3.43E-17	-1.44E-16	-2.60E-16	2.93E-16	-3.64E-16	-9.59E-18
15	-0.01293	1.48E-16	-0.079088	9.91E-17	0.092187	6.45E-17	0.029894

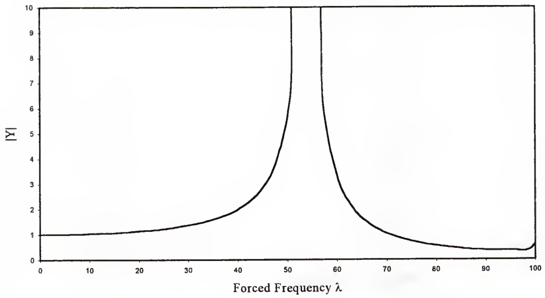

Figure 6.30 Normalized maximum absolute deflection vs. forced frequency for Mixed B.C. Square Plate without added mass and subjected to a concentrated force at the middle.

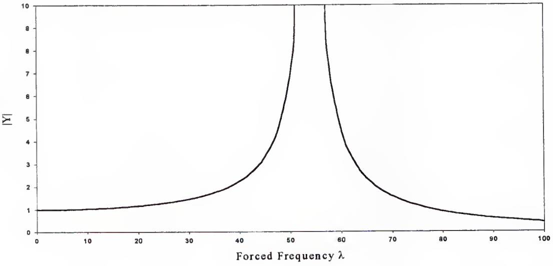

Figure 6.31 Normalized maximum absolute deflection vs. forced frequency for Mixed B.C. Square Plate without added mass at the middle and subjected to uniformly distributed load.

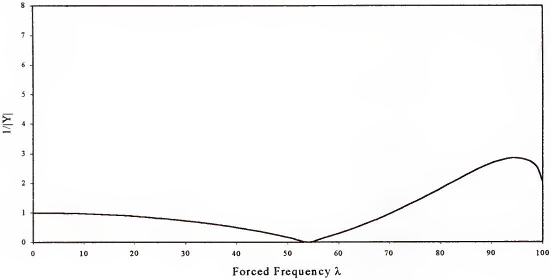

Figure 6.32 The inverse of maximum absolute deflection vs. forced frequency for Mixed B.C. Square Plate without added mass and subjected to a concentrated force at the middle.

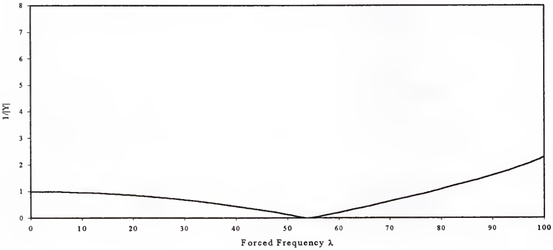

Figure 6.33 The inverse of normalized maximum absolute deflection vs. forced frequency for Mixed B.C. Square Plate without added mass and subjected to uniformly distributed load on the entire surface.

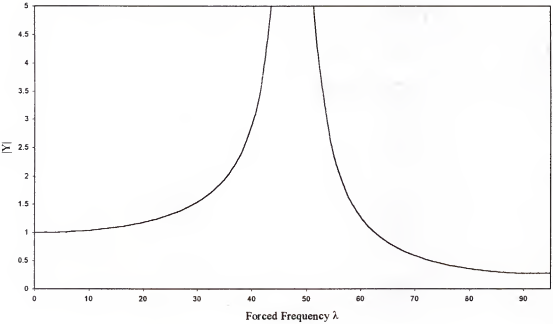

Figure 6.34 Normalized maximum absolute deflection vs. forced frequency for Mixed B.C. Plate with 50kg mass and subjected to a concentrated force at the middle.

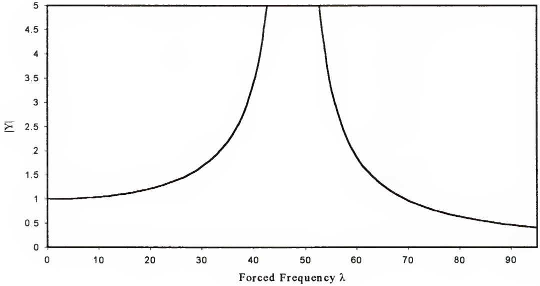

Figure 6.35 Normalized maximum absolute deflection vs. forced frequency for Mixed B.C. Plate with 50kg mass and subjected to uniformly distributed load.

Comparison with the Published Results

The following tables include the natural frequency parameters for all the previously investigated cases. The results are compared to the published data and are found to be in excellent agreement. Table 6.11 shows the published results. Tables 6.12 and 6.13 show the calculated results. Table 6.14 shows the comparison between the calculated and the published results.

Table 6.11 Published results [15] for the parameter λ of the natural frequencies for square plate cases without added mass where $\lambda = \omega_n a^2 \sqrt{\rho / D}$

CSCS	CSSS	CCCC	SSSS	Mix.B.C
28.946	23.646	35.9852	19.74	33.9

Table 6.12 The parameter λ of the natural frequencies for plate cases without added mass

N	λ					
	CCCC	CSCS	CSSS	SSSS	CFCF	Mixed B.C.
7	40.6989	31.7431	24.6287	19.7392	31.7632	40.6434
8	40.6989	31.7431	24.4923	19.7392	31.7632	40.6434
9	39.4470	31.0712	24.3890	19.7392	31.0812	39.2117
10	39.4470	31.0712	24.3080	19.7392	31.0812	39.2117
11	38.1645	30.3030	24.1347	19.7392	30.3043	38.2827
12	38.1645	30.3030	24.0685	19.7392	30.3043	38.2827
13	37.2180	29.6951	23.9295	19.7392	29.6979	37.7039
14	37.2180	29.6951	23.8719	19.7392	29.6979	37.7039
15	36.6999	29.3901	23.8207	19.7392	29.3919	37.7039

Table 6.13 The parameter λ of the natural frequencies for plate cases with 50kg mass at the middle

N	λ					
	CCCC	CSCS	CSSS	SSSS	CFCF	Mixed B.C.
7	35.9044	28.0037	21.8543	17.4139	28.0214	35.8554
8	35.9044	28.0037	21.7251	17.4139	28.0214	35.8554
9	34.8000	27.4109	21.6275	17.4139	27.4197	34.5925
10	34.8000	27.4109	21.5512	17.4139	27.4197	34.5925
11	33.6686	26.7332	21.3883	17.4139	26.7344	33.7728
12	33.6686	26.7332	21.3263	17.4139	26.7344	33.7728
13	32.8336	26.1969	21.1962	17.4139	26.1994	33.2623
14	32.8336	26.1969	21.1425	17.4139	26.1994	33.2623
15	32.3765	25.9279	21.0948	17.4139	25.9294	32.9086

Table 6.14 Comparison between the calculated and the published results for the parameter λ of the natural frequencies for square plate cases without added mass where $\lambda = \omega_n a^2 \sqrt{\rho / D}$

	CSCS	CSSS	CCCC	SSSS	Mix.B.C
Calculated	29.3901	23.8207	36.6999	19.7392	34.792
Published [15]	28.946	23.646	35.9852	19.74	33.9
Difference %	1.5	0.74	2.0	0.0	2.6

CHAPTER 7
PLATE WITH ARBITRARY SHAPE

It is often difficult to find a deflection function that represents the deflection surface of plates with arbitrary shapes, which satisfies the boundary conditions. This task becomes prohibitively difficult when the boundaries of the plates are arbitrarily mixed. Using the proposed approach, it is relatively easy to solve this kind of problem.

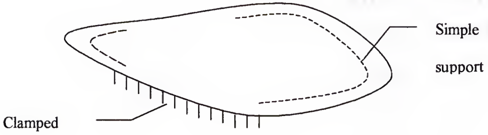

Figure 7.1 Plate with arbitrarily shape and boundary support

Circular Plate

As an illustration, we will consider the case of a circular plate with clamped edges. The solution can be obtained from consideration of a square plate with circular internal clamped boundary conditions. The radius of the plate is half the width of the square plate. The circular plate is assumed to be subjected to a uniform distributed load in this case.

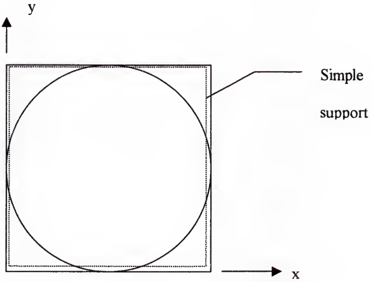

Figure 7.2 Generating a solution for a circular plate with fixed edges from a rectangular plate clamped at the circular boundary.

The deflection function of the rectangular plate is assumed to be the same as in equation 5.1. The strain energy and the kinetic energy for the plate will be the same as in equations 5.4 and 5.12. The external work will be due to the uniformly distributed load on the circular area. Since it is difficult to make double integration to find the external work on the circular surface, a numerical integration can be used. First the integration along one axis can be performed. Then the numerical integration along the other axis can be performed. The integration in this study is done by the computer using Simpson's rule.

The boundary conditions are that the deflections and the slope at the boundary are zeros. These boundary conditions are unsatisfied constraints in the rectangular plate. The unsatisfied constraints due to the deflection boundary condition take the following form:

$$G_i = w(x_i, y_i) = \sum_{m=1}^{M} \sum_{n=1}^{N} A_{mn} \sin(\frac{n\pi x}{a}) \sin(\frac{m\pi y}{b}) \tag{7.1}$$

The unsatisfied constraint due to the slope boundary condition is

$$G_{i+I} = \cos(\theta)\frac{\partial w}{\partial x} + \sin(\theta)\frac{\partial w}{\partial y} \tag{7.2}$$

Using the assumed deflection function, equation 7.2 becomes

$$G_{i+I} = \sum_{m=1}^{M} \sum_{n=1}^{N} A_{mn}[\cos(\theta_i)\frac{\pi n}{a}\cos(\frac{n\pi x_i}{a})\sin(\frac{m\pi_i y}{b}) +$$

$$\sin(\theta_i)\frac{m\pi}{b}\sin(\frac{n\pi x_i}{a})\cos(\frac{m\pi y_i}{b})] \tag{7.3}$$

where $i = 1,2,3,\ldots\ldots\ldots\ldots I$ and I is the number of the selected discrete points on the circular boundary. The total number of equations are $2I$. The same approach as in the previous cases is applied and the natural frequencies can be readily obtained.

Result

The approach is based upon forcing the unsatisfied boundary conditions to be satisfied. Choosing a function that satisfies most of the boundary conditions speeds the process time. The problem solved in this example is a rectangular plate with a/b=1, used to generate a circular plate with r=0.5a. The number of discrete points used along the boundary is 20. Figure 7.3 shows the inverse of the maximum absolute deflection $1/|Y|$ verses the forcing frequency. The natural frequency is obtained when $1/|Y|$ approaches zero.

Table 7.1 shows that the value of λ changes as N increases until convergence is obtained. The natural frequency becomes closer to the published frequency with N=25 the natural frequency where $\lambda = 10.2294$. The published value is $\lambda = 10.215$, and the difference between the computed and the published value is 0.14%.

It should be noted that the strain energy and the kinetic energy of the square plate are used in this case. The result shows that the difference between using energies of the square plate and that of the circular plate in the case of internal clamped circular boundaries and simply supported boundaries along the edges of the square plate have very small effect on the result and can be neglected. The frequency error between using the kinetic energy of the whole plate and that of circular plate is very small. Also the deflection error is close to 0.001%.

Table 7.1 The first natural frequency of circular plate generated from rectangular plate for different N terms, $a/b = 1, r = 0.5a$.

N	λ	Published result λ	Difference
15	10.4293		
20	10.2565		
25	10.2294	10.215[16]	0.14%

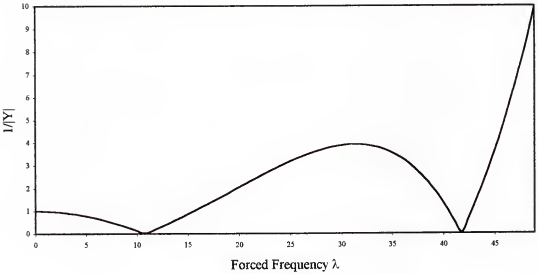

Figure 7.3 The inverse of maximum absolute deflection versus forced frequency for circular plate generated from rectangular plate, a/b=1, r=0.5a, for N=25.

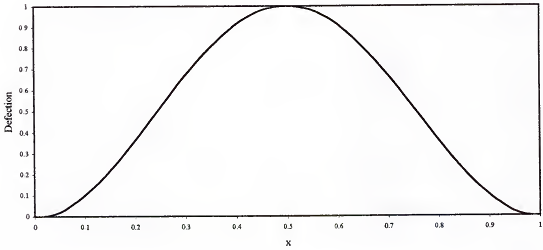

Figure 7.4 The mode shape of circular plate for N=25

Table 7.2 The displacement parameters for circular plate generated from a rectangular plate $r = 0.5a$, $a/b = 1$

n	m						
	1	2	3	4	5	6	7
1	-0.00107	-1.6E-07	0.000239	-1.9E-08	3.4E-05	-9.8E-09	1.01E-05
2	-1.6E-07	-9.8E-20	8.13E-08	-5.5E-20	-2.7E-08	-3.4E-20	9.17E-09
3	0.000239	8.13E-08	-4.7E-07	3.62E-08	-1.4E-05	1.46E-08	-6.2E-06
4	-1.9E-08	-2E-20	3.62E-08	-3.7E-20	-2.7E-08	-3.1E-20	1.18E-08
5	3.4E-05	-2.7E-08	-1.4E-05	-2.7E-08	-9.2E-06	-1.8E-08	-1.3E-06
6	-9.8E-09	2.06E-20	1.46E-08	1.89E-20	-1.8E-08	6.31E-21	1.03E-08
7	1.01E-05	9.17E-09	-6.2E-06	1.18E-08	-1.3E-06	1.03E-08	2.71E-06
8	-5.6E-09	3.98E-21	7.68E-09	5.51E-21	-9.7E-09	2.71E-21	8E-09
9	3.61E-06	-2.9E-09	-3.6E-06	-4.6E-09	1.8E-07	-4.4E-09	1.85E-06
10	-3.7E-09	-3.3E-21	4.45E-09	-2E-21	-5.6E-09	-6.6E-22	5.34E-09
11	1.4E-06	8.7E-10	-1.9E-06	1.23E-09	4.86E-07	1.6E-09	1E-06
12	-2.7E-09	-1.9E-21	2.73E-09	-9.6E-22	-3.4E-09	7.56E-22	3.35E-09
13	8.47E-07	-3.2E-11	-1E-06	-3.4E-10	9.63E-07	-2.8E-10	8.94E-07
14	-2E-09	-1.3E-21	1.92E-09	-1.5E-21	-2.1E-09	-7.8E-22	2.15E-09
15	1.13E-07	2.35E-11	-1.2E-06	-2E-10	-3.7E-07	-1.5E-11	-5.6E-07
16	-1.6E-09	8.3E-23	1.42E-09	-6.9E-23	-1.3E-09	3.35E-22	1.28E-09
17	3.14E-07	-8.1E-12	-2.4E-07	-3.1E-10	4.32E-07	-2.8E-10	-8.5E-08
18	-1.3E-09	8.67E-22	1.12E-09	6.7E-22	-8.2E-10	7.95E-22	7.56E-10
19	2.77E-07	3.45E-10	1.96E-07	3.21E-10	4.99E-07	4.77E-10	-1.9E-07
20	-1E-09	3.54E-22	9.07E-10	-2.8E-22	-4.7E-10	-5.2E-22	4.65E-10
21	1.66E-07	-2.2E-11	9.78E-08	-3.2E-10	2.87E-07	-3.7E-10	-4.5E-07
22	1.68E-08	3.46E-22	-1.6E-08	-2.5E-22	1.57E-08	-3.1E-22	-1.4E-08
23	1.87E-08	1.58E-10	8E-09	7.04E-11	1.7E-07	1.86E-10	-3.9E-07
24	-7.9E-10	3.58E-22	5.05E-10	-6.4E-23	-2.1E-10	1.63E-23	9.85E-11
25	-6.1E-08	3.04E-11	-8.1E-08	-1.3E-10	1.53E-07	-8.5E-11	-3.1E-07

Table 7.3 Displacement parameters for circular plate generated from a rectangular plate $r = 0.5a$, $a/b = 1$ (continuation of table 7.2)

n	m					
	8	9	10	11	12	13
1	-5.6E-09	3.61E-06	-3.7E-09	1.4E-06	-2.7E-09	8.47E-07
2	-8.4E-21	-2.9E-09	-1E-21	8.7E-10	-7.5E-22	-3.2E-11
3	7.68E-09	-3.6E-06	4.45E-09	-1.9E-06	2.73E-09	-1E-06
4	-8.8E-21	-4.6E-09	9.1E-22	1.23E-09	1.43E-21	-3.4E-10
5	-9.7E-09	1.8E-07	-5.6E-09	4.86E-07	-3.4E-09	9.63E-07
6	5.41E-21	-4.4E-09	4.11E-21	1.6E-09	1.21E-21	-2.8E-10
7	8E-09	1.85E-06	5.34E-09	1E-06	3.35E-09	8.94E-07
8	1.93E-21	-3.5E-09	1.52E-22	1.65E-09	-1.9E-21	-2.9E-10
9	-3.5E-09	4.62E-07	-3E-09	-4.5E-07	-2.4E-09	3.05E-07
10	3.79E-22	-3E-09	-1E-22	1.22E-09	-3.8E-22	-5.9E-10
11	1.65E-09	-4.5E-07	1.22E-09	-1.1E-06	1.06E-09	-2.9E-07
12	1.27E-21	-2.4E-09	3.77E-22	1.06E-09	2.34E-22	-6E-10
13	-2.9E-10	3.05E-07	-5.9E-10	-2.9E-07	-6E-10	4.17E-07
14	-5.7E-22	-1.7E-09	-1.3E-21	1.07E-09	-1.2E-21	-4.9E-10
15	1.72E-10	-5.4E-07	9.96E-11	-4.9E-07	2.46E-10	1.08E-08
16	4.08E-22	-1.3E-09	-8E-23	9.3E-10	1.02E-22	-5.5E-10
17	-2.1E-10	2.27E-07	-3.4E-10	2.24E-07	-2.4E-10	4.78E-07
18	7.86E-22	-9.4E-10	3.4E-22	8.41E-10	3.82E-22	-5.4E-10
19	5.55E-10	6.76E-08	4.07E-10	1.02E-07	4.26E-10	6.27E-08
20	-4.9E-22	-6.5E-10	-6.1E-22	7.73E-10	-3.1E-22	-5.1E-10
21	-4E-10	-7.7E-08	-5.2E-10	-2.1E-08	-4.2E-10	-3.4E-08
22	-1.2E-22	1.25E-08	-4.2E-23	-1.1E-08	3.75E-22	9.22E-09
23	2.79E-10	2.46E-08	2.25E-10	1.4E-07	3.26E-10	3.77E-08
24	1.69E-22	-3.7E-10	7.59E-23	5.6E-10	3.15E-22	-5E-10
25	-5.8E-11	1.16E-07	-1.6E-10	1.53E-07	-1E-10	3.53E-08

Table 7.4 Displacement parameters for circular plate generated from rectangular plate $r = 0.5a$, $a/b = 1$ (continuation of table 7.3)

n	m					
	14	15	16	17	18	19
1	-2E-09	1.13E-07	-1.6E-09	3.14E-07	-1.3E-09	2.77E-07
2	-8.9E-22	2.35E-11	-1.2E-21	-8.1E-12	-9.8E-22	3.45E-10
3	1.92E-09	-1.2E-06	1.42E-09	-2.4E-07	1.12E-09	1.96E-07
4	1.23E-21	-2E-10	1.3E-21	-3.1E-10	1.58E-21	3.21E-10
5	-2.1E-09	-3.7E-07	-1.3E-09	4.32E-07	-8.2E-10	4.99E-07
6	-1.1E-22	-1.5E-11	-4.2E-22	-2.8E-10	-2E-22	4.77E-10
7	2.15E-09	-5.6E-07	1.28E-09	-8.5E-08	7.56E-10	-1.9E-07
8	-2E-21	1.72E-10	-1.8E-21	-2.1E-10	-1.4E-21	5.55E-10
9	-1.7E-09	-5.4E-07	-1.3E-09	2.27E-07	-9.4E-10	6.76E-08
10	5.35E-22	9.96E-11	9.66E-22	-3.4E-10	9.76E-22	4.07E-10
11	1.07E-09	-4.9E-07	9.3E-10	2.24E-07	8.41E-10	1.02E-07
12	8.29E-22	2.46E-10	7.52E-22	-2.4E-10	3.21E-22	4.26E-10
13	-4.9E-10	1.08E-08	-5.5E-10	4.78E-07	-5.4E-10	6.27E-08
14	-4.4E-22	3.7E-10	-4.3E-22	-1.7E-10	-6.1E-22	3.73E-10
15	3.7E-10	-1.9E-07	2.99E-10	8.95E-08	3.07E-10	-2.1E-07
16	5.24E-22	2.99E-10	4.12E-22	-2.5E-10	4.11E-22	2.01E-10
17	-1.7E-10	8.95E-08	-2.5E-10	2.63E-07	-2E-10	-7.8E-08
18	3.24E-22	3.07E-10	-1.3E-22	-2E-10	-1.8E-22	1.77E-10
19	3.73E-10	-2.1E-07	2.01E-10	-7.8E-08	1.77E-10	-2.6E-07
20	-2.9E-22	3.17E-10	-6.1E-22	-1.5E-10	-4.7E-22	1.48E-10
21	-3.7E-10	-2E-07	-3.9E-10	3.43E-08	-2.7E-10	-8.6E-08
22	4.48E-22	-8E-09	1.73E-22	6.81E-09	3.94E-22	-5.8E-09
23	3.45E-10	-2.3E-08	2.61E-10	1.18E-07	3.03E-10	-3.1E-08
24	2.22E-22	2.87E-10	-1.1E-22	-9.6E-11	1.01E-23	5.73E-11
25	-1.1E-10	5.15E-09	-2.1E-10	1.19E-07	-1.7E-10	-1E-07

Table 7.5 Displacement parameters for circular plate generated from rectangular plate $r = 0.5\,a$, $a/b = 1$ (continuation of table 7.4)

n	m					
	20	21	22	23	24	25
1	-1E-09	1.66E-07	1.68E-08	1.87E-08	-7.9E-10	-6.1E-08
2	-9.3E-22	-2.2E-11	-1.1E-21	1.58E-10	-1.2E-21	3.04E-11
3	9.07E-10	9.78E-08	-1.6E-08	8E-09	5.05E-10	-8.1E-08
4	1.73E-21	-3.2E-10	1.32E-21	7.04E-11	9.25E-22	-1.3E-10
5	-4.7E-10	2.87E-07	1.57E-08	1.7E-07	-2.1E-10	1.53E-07
6	9.39E-23	-3.7E-10	-1.1E-22	1.86E-10	-2.6E-22	-8.5E-11
7	4.65E-10	-4.5E-07	-1.4E-08	-3.9E-07	9.85E-11	-3.1E-07
8	-1E-21	-4E-10	-1E-21	2.79E-10	-8.9E-22	-5.8E-11
9	-6.5E-10	-7.7E-08	1.25E-08	2.46E-08	-3.7E-10	1.16E-07
10	1.04E-21	-5.2E-10	8.7E-22	2.25E-10	8.55E-22	-1.6E-10
11	7.73E-10	-2.1E-08	-1.1E-08	1.4E-07	5.6E-10	1.53E-07
12	4.82E-23	-4.2E-10	-2.4E-22	3.26E-10	-2.3E-22	-1E-10
13	-5.1E-10	-3.4E-08	9.22E-09	3.77E-08	-5E-10	3.53E-08
14	-6.4E-22	-3.7E-10	-6.8E-22	3.45E-10	-5.1E-22	-1.1E-10
15	3.17E-10	-2E-07	-8E-09	-2.3E-08	2.87E-10	5.15E-09
16	5.06E-22	-3.9E-10	5.37E-22	2.61E-10	6.98E-22	-2.1E-10
17	-1.5E-10	3.43E-08	6.81E-09	1.18E-07	-9.6E-11	1.19E-07
18	-1.2E-22	-2.7E-10	-1.8E-22	3.03E-10	-1.2E-22	-1.7E-10
19	1.48E-10	-8.6E-08	-5.8E-09	-3.1E-08	5.73E-11	-1E-07
20	-2.7E-22	-1.8E-10	-3.2E-22	2.95E-10	-2.4E-22	-1.9E-10
21	-1.8E-10	1.64E-07	4.7E-09	1.43E-07	-1E-10	5.09E-08
22	5.3E-22	4.7E-09	4.57E-22	-3.8E-09	4.05E-22	3.14E-09
23	2.95E-10	1.43E-07	-3.8E-09	6.96E-08	2.21E-10	-5E-08
24	3.85E-23	-1E-10	-1.6E-22	2.21E-10	-1.8E-22	-2.1E-10
25	-1.9E-10	5.09E-08	3.14E-09	-5E-08	-2.1E-10	-1.2E-07

Elliptical Plate

Another illustrative example is the case of an elliptical plate fixed at the boundaries. The solution is generated by utilizing a rectangular plate with its sides tangential to the ellipse as shown in figure 7.5. the center of the elliptical plate is the center of the rectangular plate. The length of the major axis is 2a while the length of minor axis is 2b. The semiaxes of the ellipse along the major axis and the minor axis are a_x and a_y respectively. The elliptical plate is clamped at its boundaries.

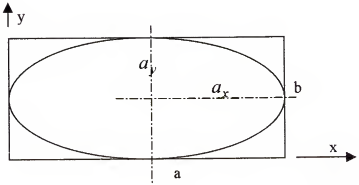

Figure 7.5 Elliptical plate generated from rectangular plate.

The same strain energy and kinetic energy expressions of the rectangular plate as in chapter 4 are used. The external work is calculated due to the uniform load on the elliptical plate only. Since it is difficult to make double integration to find the external work on the elliptical surface, a numerical integration can be used. First the integration along one axis can be performed. Then the numerical integration along the other axis can be performed. The integration in this study is done by the computer using Simpson's rule. The same procedure as in previous cases is used and the result is given in table 7.6.

Result

The result is shown in table 7.6 and figure 7.6. Figure 7.7shows the mode shape along x-axis. Tables 7.7–7.10 show the natural modes for the elliptical plate. The dimension used in this illustration are: $a_x / a_y = 1.25$, $a = 2a_x$ $b = 2a_y$, $a_y = 1$, $= 0.3$. N=25 is also considered in this case. The number of discrete points is 20 points along the elliptical boundary.

Table 7.6 shows how the convergence occurs as the number of terms N increases. The result shows an excellent agreement with the published data. The natural frequency parameter is found when 1/|Y| approaches zero as shown in figure 7.6. Table 6.7 shows the convergence as N increases. Using 20 discrete points along the elliptical boundary the natural frequency parameter is found to be 13.1794 for N=25 and M=25 since it is assumed previously that M=N. The published result for the date given above is λ=13.1.

Table 7.6 The first natural frequency of an elliptical plate generated from a rectangular plate for different N terms, $a_x / a_y = 1.25$, $a = 2a_x$ $b = 2a_y$, $a_y = 1$, N=25, $= 0.3$

N	λ	Published result λ	Difference
15	14.0333		
20	13.5617		
25	13.1794	13.1[13]	0.61%

It can be seen that the solution converges to the published value for λ=13.1 at N=25 by using 20 discrete points along the elliptical boundary.

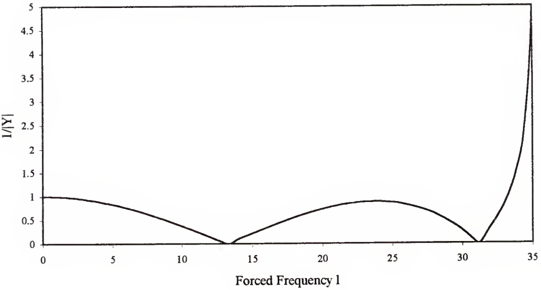

Figure 7.6 The inverse of normalized maximum absolute deflection versus forced frequency for elliptical plate generated from rectangular plate, $a_x / a_y = 1.25$, $a = 2a_x$, $b = 2a_y$, b=1 for N=25.

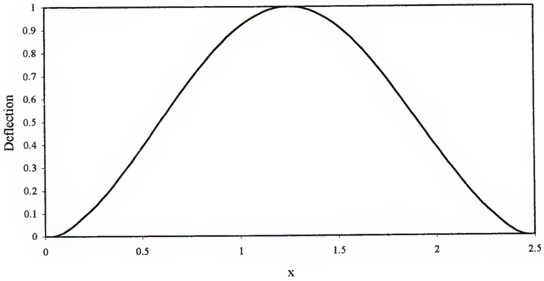

Figure 7.7 Mode shape of elliptical plate generated from rectangular plate at y=b/2.

Table 7.7 Displacement parameters for elliptical plate generated from rectangular plate $a_x / a_y = 1.25$, $a = 2a_x$ $b = 2a_y$, $a_y = 1$

n	m					
	1	2	3	4	5	6
1	-0.00202	6.4E-18	0.000402	-3.4E-18	5.22E-05	1.11E-18
2	1.06E-05	2.02E-18	1.57E-06	-1.3E-18	-1.36E-06	3.79E-19
3	0.000465	1.5E-18	3.29E-06	-2.3E-18	-1.41E-05	1.98E-18
4	-2.6E-06	2.92E-19	-2.7E-06	-5.9E-19	-1.37E-06	4.2E-19
5	7.38E-05	5.02E-19	-2.2E-05	-8.6E-19	-1.02E-05	1.23E-18
6	-1.2E-06	6.14E-20	-1.5E-06	-1.1E-19	-4.01E-07	3.23E-19
7	1.88E-05	1.89E-19	-1.8E-05	-2.7E-19	-7.67E-06	5.62E-19
8	-4.1E-07	-3.7E-20	-3.3E-07	-7.4E-21	2.29E-07	2E-19
9	8.08E-06	2.19E-20	-5.2E-06	-7.5E-20	2.67E-06	1.73E-19
10	-1.1E-07	-6.1E-20	6.06E-08	1.07E-20	3.08E-07	9.87E-20
11	2.88E-06	-2.8E-20	-2.9E-06	4.04E-20	1.67E-06	2.23E-20
12	-6.4E-08	-6.2E-20	4.05E-08	1.55E-20	1.53E-07	1.97E-20
13	1.17E-06	-5.4E-20	-2.4E-06	9.19E-20	8.54E-07	-4.4E-20
14	-6.4E-08	-5.1E-20	-2.8E-08	2.64E-20	3.62E-08	-1.2E-20
15	8.46E-08	-6.9E-20	-1.7E-06	1.11E-19	-4.18E-07	-7.5E-20
16	-4.6E-08	-3.8E-20	-2.4E-08	4.01E-20	1.88E-08	-2.7E-20
17	1.95E-07	-8.1E-20	-3.3E-07	1.08E-19	4.58E-07	-1E-19
18	-1.9E-08	-2.8E-20	1.37E-08	4.7E-20	3.77E-08	-3E-20
19	8.94E-08	-8.3E-20	5E-07	1.06E-19	7.84E-07	-1.2E-19
20	-5.5E-09	-2.5E-20	2.84E-08	4.64E-20	3.40E-08	-3.4E-20
21	-4.4E-08	-7.7E-20	5.4E-07	1.08E-19	8.20E-07	-1.2E-19
22	2.42E-08	-2.5E-20	-1.7E-08	4.28E-20	3.71E-08	-3.7E-20
23	-3.7E-07	-6.8E-20	1.49E-07	1.12E-19	2.87E-07	-1.2E-19
24	-1.2E-08	-2.6E-20	-4E-09	3.86E-20	-1.14E-08	-3.8E-20
25	-5.1E-07	-6.2E-20	-7.6E-08	1.12E-19	1.23E-07	-1.1E-19

Table 7.8 Displacement parameters for elliptical plate generated from rectangular plate $a_x / a_y = 1.25$, $a = 2a_x$ $b = 2a_y$, $a_y = 1$ (continuation of table 7.7)

n	m					
	7	8	9	10	11	12
1	1.57E-05	-3.9E-19	4.74E-06	-9.9E-21	3.26E-06	4.95E-20
2	-1.9E-06	-3.9E-19	-7.6E-07	6.19E-20	-3.9E-07	4.64E-20
3	-6E-06	-6.7E-19	-6.4E-06	3.61E-20	-1.4E-06	1.56E-19
4	-1.1E-06	-4.4E-19	-5.2E-08	7.41E-20	9.34E-08	4.43E-20
5	1.34E-06	-6.2E-19	1.39E-08	1.81E-20	3.2E-06	1.65E-19
6	-1.2E-07	-2.7E-19	5.77E-07	7.35E-20	5.35E-07	2.07E-20
7	-2.2E-07	-4.1E-19	-2.2E-06	3.23E-20	-6.4E-07	1.54E-19
8	1.52E-07	-1.4E-19	4.08E-07	5.67E-20	3.64E-07	-9.5E-21
9	5.41E-06	-2.5E-19	1.56E-06	1.65E-20	2.52E-07	1E-19
10	3.46E-08	-6.6E-20	2.77E-08	5.13E-20	1.76E-08	-1.7E-20
11	2.93E-06	-1E-19	1.27E-07	1.6E-20	-9.5E-07	4.56E-20
12	-8.5E-08	-3.5E-20	-1.3E-07	3.69E-20	-1.1E-07	-2.2E-20
13	8.89E-07	-6.8E-21	5.13E-07	7.78E-21	1.32E-07	-1.1E-20
14	-9.3E-08	-1.5E-20	-8E-08	2.92E-20	-4.6E-08	-2.1E-20
15	-8.7E-07	4.92E-20	-5.1E-07	7.51E-21	6.12E-08	-4.3E-20
16	-4.3E-08	-4E-21	4.45E-09	1.92E-20	2.45E-08	-2.5E-20
17	-7.6E-07	6.97E-20	-7.1E-08	4.64E-21	3.15E-07	-6.1E-20
18	-6.6E-09	6.82E-21	3.46E-08	1.53E-20	2.94E-08	-2.5E-20
19	-5.9E-07	7.73E-20	-1.6E-07	4.62E-21	-2.7E-08	-6.6E-20
20	-8.4E-09	1.09E-20	2.23E-08	1.06E-20	5.27E-09	-2.5E-20
21	-4.5E-07	7.78E-20	1.31E-07	2.93E-21	5.2E-09	-6.9E-20
22	-5.3E-08	1.38E-20	3.5E-08	8.97E-21	-2.6E-08	-2.3E-20
23	-6.2E-07	7.63E-20	5.05E-08	2.7E-21	-1.4E-07	-6.8E-20
24	-2.9E-08	1.49E-20	1.22E-08	6.21E-21	8.86E-09	-2.3E-20
25	-5.2E-07	7.1E-20	2.39E-07	1.92E-21	-1.5E-07	-6.5E-20

Table 7.9 Displacement parameters for elliptical plate generated from rectangular plate $a_x / a_y = 1.25$, $a = 2a_x$ $b = 2a_y$, $a_y = 1$ (continuation of table 7.8)

n	m					
	13	14	15	16	17	18
1	1.43E-06	-4.9E-20	9.03E-07	9.63E-21	5.79E-07	-4.3E-21
2	-4.1E-07	-2.1E-21	-6.1E-08	1.84E-20	2.09E-08	-1.2E-20
3	-1.8E-06	-1E-19	-1.1E-06	3.62E-20	-9E-07	-3.2E-21
4	-3.1E-07	-1.5E-20	-2.8E-08	2.57E-20	-9.1E-08	-2.1E-20
5	1.64E-06	-1.3E-19	1.77E-06	2.82E-20	1.22E-06	-1.5E-20
6	-6.2E-08	-2.3E-20	4.24E-08	2.63E-20	-2.4E-07	-2E-20
7	-1.3E-06	-8.5E-20	-3E-08	2.67E-20	3.43E-07	-1.1E-20
8	-5.4E-08	-2.8E-20	8.95E-08	1.71E-20	-2.7E-07	-2E-20
9	-9.7E-07	-4.3E-20	1.67E-07	1.06E-20	1.02E-06	-9.9E-21
10	-1.4E-07	-1.4E-20	1.32E-07	1.33E-20	-1.8E-07	-1.3E-20
11	-1.9E-06	-8.6E-22	-9.2E-07	-2.4E-21	1.5E-07	1.4E-22
12	-1.4E-07	-5.6E-23	1.77E-07	4.97E-21	-9.3E-08	-9.5E-21
13	-3.5E-08	1.9E-20	4.53E-08	-2.5E-20	8.58E-07	4.69E-21
14	-6E-08	1.44E-20	1.89E-07	-5E-23	-7.5E-08	-3.3E-21
15	2.14E-07	4.2E-20	-6.6E-08	-3.7E-20	3.31E-07	1.46E-20
16	-1.9E-08	1.89E-20	1.52E-07	-9.7E-21	-9.4E-08	-3.2E-21
17	7.04E-07	5.99E-20	-4.8E-08	-4.6E-20	2.74E-07	2.25E-20
18	-3.4E-08	2.41E-20	9.46E-08	-1.6E-20	-9.7E-08	-5.3E-22
19	2.57E-07	7.52E-20	-5.7E-07	-5.1E-20	-3.4E-07	3.06E-20
20	-5.7E-08	2.64E-20	5.71E-08	-2E-20	-7.4E-08	1.46E-22
21	4.41E-07	8.19E-20	-4E-07	-5.9E-20	-1.9E-07	3.24E-20
22	-3.3E-08	3.02E-20	2.82E-08	-2E-20	-2.9E-08	3.99E-21
23	3.92E-07	8.42E-20	-2.6E-07	-6.6E-20	-1.5E-07	3.29E-20
24	-3.4E-08	3.08E-20	4.54E-08	-2.1E-20	-3.3E-08	6.02E-21
25	4.81E-07	8.49E-20	-2.8E-08	-7.2E-20	9.67E-08	3.25E-20

Table 7.10 Displacement parameters for elliptical plate generated from rectangular plate $a_x / a_y = 1.25$, $a = 2a_x$ $b = 2a_y$, $a_y = 1$ (continuation of table 7.9)

n	m						
	19	20	21	22	23	24	25
1	2.91E-07	-7.38E-22	6.48E-07	-2E-21	4.11E-07	-3.8E-21	2.98E-07
2	2.42E-07	4.12E-21	1.65E-07	-3.4E-21	8.47E-09	1.35E-22	-1.5E-08
3	-1.2E-06	6.26E-21	5.72E-08	2.07E-21	-2.7E-07	-4E-21	-2.5E-07
4	2.36E-07	8.68E-21	1.47E-07	-8.9E-21	-4.9E-08	4.3E-22	-2E-08
5	-2.2E-07	3.32E-21	8.6E-07	3.2E-22	1.01E-07	-7.1E-21	9.1E-08
6	8.57E-08	1.56E-20	2.8E-08	-6.9E-21	-1.2E-07	3.13E-21	-4.1E-09
7	-1E-06	7.20E-21	1.12E-07	1.96E-21	-5.7E-07	-3.8E-21	-3.3E-07
8	2.19E-08	1.70E-20	-1.2E-08	-1.4E-20	-1.2E-07	3.67E-21	3.16E-08
9	-2.1E-07	4.41E-21	6.59E-07	-3.7E-21	-3.2E-08	-3.3E-21	2.53E-07
10	6.73E-08	1.89E-20	3.47E-08	-1.3E-20	-6.8E-08	5.4E-21	6.45E-08
11	-6.1E-07	7.10E-21	5.72E-08	-5.3E-21	-3.8E-07	4.36E-21	-7.4E-09
12	9.52E-08	1.64E-20	5.89E-08	-2.1E-20	-3.5E-08	4.3E-21	7.61E-08
13	1.83E-09	4.99E-21	3.32E-07	-1.1E-20	-1.5E-07	1.09E-20	1.94E-07
14	5.33E-08	1.71E-20	2.08E-08	-1.6E-20	-4.6E-08	7.17E-21	7.07E-08
15	-1.8E-07	5.88E-21	-1.1E-07	-1.5E-20	-3.9E-07	1.88E-20	-1.5E-07
16	5.84E-10	1.43E-20	-2E-08	-1.9E-20	-6.1E-08	9.63E-21	6.29E-08
17	6.13E-08	3.72E-21	1.51E-07	-2.2E-20	1.21E-08	2.31E-20	1.61E-07
18	-5.6E-09	1.35E-20	-1.6E-08	-1.4E-20	-5.1E-08	1.43E-20	5.62E-08
19	-1.3E-07	4.01E-21	-5.3E-08	-2.7E-20	6.86E-08	2.85E-20	1.35E-07
20	2.31E-08	1.02E-20	1.6E-08	-1.7E-20	-2.9E-08	1.55E-20	4.48E-08
21	9.4E-08	3.05E-21	4.82E-08	-3E-20	2.33E-07	3.39E-20	2.9E-07
22	2.86E-08	9.27E-21	4.43E-08	-1.4E-20	-3.1E-08	1.69E-20	3.8E-08
23	1.24E-07	3.50E-21	-2.1E-07	-2.9E-20	1.25E-08	4.13E-20	6E-08
24	3.57E-08	7.19E-21	2.03E-08	-1.8E-20	-2.6E-08	1.66E-20	1.63E-08
25	3.16E-07	2.74E-21	-2E-07	-3E-20	3.34E-09	4.6E-20	7.99E-08

CHAPTER 8
PLATES WITH HOLES

A plate with arbitrarily shaped holes is a common problem in structural design and is extremely difficult to handle in the general case by the classical theory of plates. The finite element method, so far, is the approach that analysts prefer to use. The proposed approach can determine the vibratory response of any type of plate with any shape of hole as we will be seen in the next section.

Rectangular Plate with Circular Hole

As an illustration, let us consider a rectangular plate with circular free hole at its center. The outer edges of the rectangular plate are simply supported.

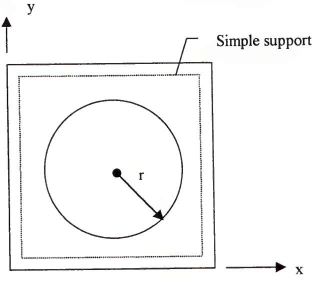

Figure 8.1 Simply supported square plate with a circular hole at the center.

Consider a square plate of width a, and the radius of the hole is 0.3a. The deflection function of the plate used is the same as in equation 5.1. The strain energy of the plate with the hole is the difference between the entire plate and the pseudo plate in the hole.

$$U = U_p - U_h \tag{8.1}$$

where U_p is the strain energy for the whole plate, and U_h is the strain energy for the pseudo plate in the hole.

Also, the kinetic energy of the plate with the hole is the difference between the whole plate and the pseudo plate in the hole.

$$T = T_p - T_h \tag{8.2}$$

where T_p is the kinetic energy for the whole plate, and T_h is the kinetic energy for the pseudo plate in the hole.

Since the plate is subjected to a uniform distributed load, the external work is only related to that surface subjected to the load. Therefore:

$$W = W_p - W_h \tag{8.3}$$

where W_p is the external work for the whole plate, and W_h is the external work for the pseudo plate in the hole.

Since it is difficult to perform double integration on the circular hole, a numerical integration can be used. First the integration along one axis can be performed. Then the numerical integration along the other axis can be performed. The integration in this study is done by the computer using Simpson's rule.

Each discrete point on the boundary of the hole has two components of the shear and the moment as a boundary condition.

$$G_i = V_x(x_i, y_i) + V_y(x_i, y_i) \tag{8.4}$$

$$G_{i+1} = M_x(x_i, y_i)\cos^2(\theta_i) + M_y(x_i, y_i)\sin^2(\theta_i) -$$

$$2M_{xy}\cos(\theta_i)\sin(\theta_i) \tag{8.5}$$

where $i = 1,2,\ldots\ldots I$ and I is the number of discrete points at the boundary of the circle. $2I$ equations are needed to define the constraints along the boundary of the hole.

Result

Figure 8.2 shows the inverse of the normalized maximum of the absolute deflection versus the frequency. Table 8.1 shows the rate of convergence of the value of λ as a function of the number of terms N. The result is compared to the published result for a/b=1, r=0.15a. The computed result approaches the published value when N=51. The frequency corresponds to $\lambda = 21.1441$, and the difference with the published result is 2.1%.

Table 8.1 Natural frequency of rectangular plate with circular hole for different N terms, $a/b = 1, r = 0.15a$, $\omega_n = \lambda = \omega_n a^2 \sqrt{\rho h/D}$

N	λ	Published result λ	Difference
10	30.0194		
20	24.8639		
30	22.3187		
51	21.1441	20.7[17]	2.1%

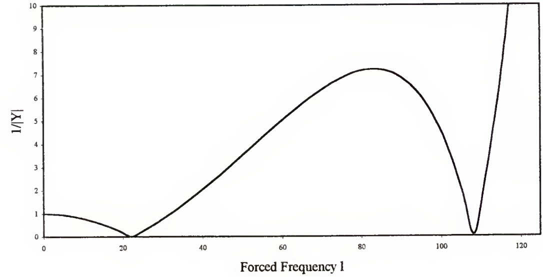

Figure 8.2 The inverse of the maximum absolute deflection versus forced frequency for Simply Supported rectangular plate with free circular hole, a/b=1

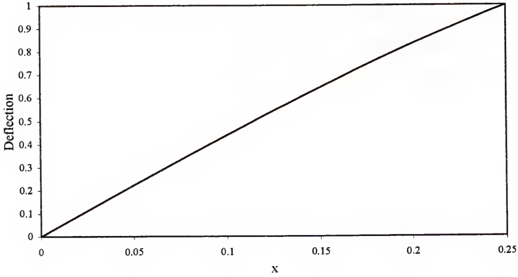

Figure 8.3 Mode shape of rectangular plate with free circular hole, a/b=1, r=0.15a

Table 8.2 Displacement parameters for rectangular plate with circular hole of radius $r = 0.15a$, $a/b = 1$

n	m						
	1	3	5	7	9	11	13
1	-0.006	-1.7E-05	-3.2E-07	2.52E-06	-1.7E-06	4.94E-07	1.67E-07
3	-1.7E-05	3.8E-06	1.44E-06	-2.1E-06	1.14E-06	-1.5E-07	-3.3E-07
5	-3.2E-07	1.44E-06	-2E-06	1.46E-06	-5.1E-07	-2.2E-07	4.86E-07
7	2.52E-06	-2.1E-06	1.46E-06	-7E-07	-2.2E-08	4.49E-07	-5.1E-07
9	-1.7E-06	1.14E-06	-5.1E-07	-2.2E-08	3.75E-07	-4.9E-07	3.72E-07
11	4.94E-07	-1.5E-07	-2.2E-07	4.49E-07	-4.9E-07	3.67E-07	-1.6E-07
13	1.67E-07	-3.3E-07	4.86E-07	-5.1E-07	3.72E-07	-1.6E-07	-3.8E-08
15	-2.7E-07	3.33E-07	-3.7E-07	3.03E-07	-1.4E-07	-4.4E-08	1.65E-07
17	6.99E-08	-1E-07	1.05E-07	-4.1E-08	-7.1E-08	1.66E-07	-1.9E-07
19	1.37E-07	-1.1E-07	9.05E-08	-1.2E-07	1.57E-07	-1.7E-07	1.34E-07
21	-2E-07	1.63E-07	-1.3E-07	1.19E-07	-1.1E-07	8.76E-08	-3.4E-08
23	1.24E-07	-8.9E-08	5.04E-08	-2.4E-08	6.62E-09	1.61E-08	-4.8E-08
25	-7.1E-09	-1.9E-08	5.09E-08	-7.2E-08	7.76E-08	-7.5E-08	7.33E-08
27	-5.8E-08	7.52E-08	-9.6E-08	1.05E-07	-9.4E-08	6.75E-08	-3.9E-08
29	4.36E-08	-5.6E-08	6.99E-08	-7.1E-08	5.14E-08	-1.6E-08	-1.9E-08
31	1.39E-08	-3E-09	-8.3E-09	9.95E-09	4.17E-09	-3.1E-08	5.91E-08
33	-5.7E-08	4.89E-08	-3.9E-08	3.16E-08	-3.1E-08	4E-08	-5.5E-08
35	5.4E-08	-5.2E-08	4.65E-08	-3.5E-08	1.96E-08	-9.1E-09	1.11E-08
37	-9.5E-09	1.9E-08	-2.5E-08	1.57E-08	9.67E-09	-3.5E-08	4.27E-08
39	-4.3E-08	1.93E-08	3.28E-09	-3E-09	-2.5E-08	6.08E-08	-7.7E-08
41	7.43E-08	-3.7E-08	-2.9E-09	1.57E-08	9.03E-09	-5.2E-08	7.8E-08
43	-7.5E-08	2.93E-08	2.34E-08	-4.8E-08	2.92E-08	1.76E-08	-5.5E-08
45	5.83E-08	-1.1E-08	-4.6E-08	7.76E-08	-6.5E-08	1.83E-08	2.6E-08
47	-4.2E-08	-2.3E-10	5.16E-08	-8.3E-08	7.46E-08	-3.5E-08	-8.6E-09
49	3.3E-08	-2.8E-09	-3.5E-08	5.79E-08	-5.4E-08	2.61E-08	5.63E-09
51	-2.7E-08	1.21E-08	5.76E-09	-1.6E-08	1.44E-08	-2.8E-09	-9.6E-09

Table 8.3 Displacement parameters for rectangular plate with circular hole of radius $r = 0.15\,a$, $a/b = 1$ (continuation of table 8.2)

n	m						
	15	17	19	21	23	25	27
1	-2.7E-07	6.98E-08	1.37E-07	-2E-07	1.23E-07	-7.1E-09	-5.8E-08
3	3.34E-07	-1E-07	-1.1E-07	1.63E-07	-8.9E-08	-1.9E-08	7.52E-08
5	-3.7E-07	1.05E-07	9.05E-08	-1.3E-07	5.04E-08	5.09E-08	-9.6E-08
7	3.03E-07	-4.1E-08	-1.2E-07	1.19E-07	-2.4E-08	-7.2E-08	1.05E-07
9	-1.4E-07	-7.1E-08	1.57E-07	-1.1E-07	6.62E-09	7.76E-08	-9.4E-08
11	-4.4E-08	1.66E-07	-1.7E-07	8.76E-08	1.61E-08	-7.5E-08	6.75E-08
13	1.65E-07	-1.9E-07	1.34E-07	-3.4E-08	-4.8E-08	7.33E-08	-3.9E-08
15	-2E-07	1.49E-07	-5.7E-08	-3.2E-08	7.88E-08	-6.8E-08	1.58E-08
17	1.49E-07	-6.2E-08	-2.5E-08	8.04E-08	-8.7E-08	5.18E-08	3.37E-09
19	-5.7E-08	-2.5E-08	7.96E-08	-9.1E-08	6.49E-08	-2E-08	-2E-08
21	-3.2E-08	8.04E-08	-9.1E-08	6.47E-08	-2E-08	-1.9E-08	3.38E-08
23	7.88E-08	-8.7E-08	6.49E-08	-2E-08	-2.6E-08	5.08E-08	-4.3E-08
25	-6.8E-08	5.18E-08	-2E-08	-1.9E-08	5.08E-08	-6.1E-08	4.29E-08
27	1.58E-08	3.37E-09	-2E-08	3.38E-08	-4.3E-08	4.29E-08	-3.2E-08
29	4.35E-08	-5E-08	3.98E-08	-2.2E-08	7.06E-09	-2.8E-09	9.23E-09
31	-7.5E-08	6.78E-08	-3.7E-08	-4.5E-09	3.71E-08	-4.4E-08	2.01E-08
33	6.42E-08	-5.5E-08	2.24E-08	2.55E-08	-6.6E-08	7.65E-08	-4.7E-08
35	-2.2E-08	2.65E-08	-1.1E-08	-2.5E-08	6.4E-08	-8.2E-08	6.19E-08
37	-2.6E-08	-1.1E-10	1.41E-08	-1.8E-09	-2.9E-08	5.64E-08	-5.8E-08
39	5.75E-08	-1.3E-08	-2.9E-08	4.13E-08	-2.1E-08	-1.4E-08	3.77E-08
41	-6.4E-08	1.33E-08	4.28E-08	-7.2E-08	6.25E-08	-2.6E-08	-1.2E-08
43	5.31E-08	-1.2E-08	-4.3E-08	7.79E-08	-7.5E-08	4.3E-08	-4.4E-09
45	-3.9E-08	1.54E-08	2.55E-08	-5.5E-08	5.57E-08	-3.3E-08	4.86E-09
47	3.03E-08	-2.3E-08	5.34E-10	1.71E-08	-1.8E-08	4.51E-09	8.17E-09
49	-2.5E-08	2.66E-08	-1.9E-08	1.39E-08	-1.7E-08	2.32E-08	-2.4E-08
51	1.64E-08	-1.7E-08	1.8E-08	-2.3E-08	3.05E-08	-3.5E-08	2.94E-08

Table 8.4 Displacement parameters for rectangular plate with circular hole of radius $r = 0.15\,a$, $a/b = 1$ (continuation of table 8.3)

n	m						
	29	31	33	35	37	39	41
1	4.36E-08	1.39E-08	-5.7E-08	5.4E-08	-9.5E-09	-4.3E-08	7.43E-08
3	-5.6E-08	-3E-09	4.89E-08	-5.2E-08	1.9E-08	1.93E-08	-3.7E-08
5	6.99E-08	-8.3E-09	-3.9E-08	4.65E-08	-2.5E-08	3.28E-09	-2.9E-09
7	-7.1E-08	9.95E-09	3.16E-08	-3.5E-08	1.57E-08	-3E-09	1.57E-08
9	5.14E-08	4.17E-09	-3.1E-08	1.96E-08	9.67E-09	-2.5E-08	9.03E-09
11	-1.6E-08	-3.1E-08	4E-08	-9.1E-09	-3.5E-08	6.08E-08	-5.2E-08
13	-1.9E-08	5.91E-08	-5.5E-08	1.11E-08	4.27E-08	-7.7E-08	7.8E-08
15	4.35E-08	-7.5E-08	6.42E-08	-2.2E-08	-2.6E-08	5.75E-08	-6.4E-08
17	-5E-08	6.78E-08	-5.5E-08	2.65E-08	-1.1E-10	-1.3E-08	1.33E-08
19	3.98E-08	-3.7E-08	2.24E-08	-1.1E-08	1.41E-08	-2.9E-08	4.28E-08
21	-2.2E-08	-4.5E-09	2.55E-08	-2.5E-08	-1.8E-09	4.13E-08	-7.2E-08
23	7.06E-09	3.71E-08	-6.6E-08	6.4E-08	-2.9E-08	-2.1E-08	6.25E-08
25	-2.8E-09	-4.4E-08	7.65E-08	-8.2E-08	5.64E-08	-1.4E-08	-2.6E-08
27	9.23E-09	2.01E-08	-4.7E-08	6.19E-08	-5.8E-08	3.77E-08	-1.2E-08
29	-1.8E-08	1.98E-08	-8.4E-09	-1.2E-08	3.01E-08	-3.7E-08	3.18E-08
31	1.98E-08	-5.3E-08	6.21E-08	-4.3E-08	9.6E-09	1.94E-08	-3.1E-08
33	-8.4E-09	6.21E-08	-8.7E-08	7.45E-08	-3.7E-08	-2.2E-09	2.16E-08
35	-1.2E-08	-4.3E-08	7.45E-08	-6.9E-08	3.6E-08	1.31E-10	-1.8E-08
37	3.01E-08	9.6E-09	-3.7E-08	3.6E-08	-1.3E-08	-1.3E-08	2.29E-08
39	-3.7E-08	1.94E-08	-2.2E-09	1.31E-10	-1.3E-08	2.72E-08	-2.9E-08
41	3.18E-08	-3.1E-08	2.16E-08	-1.8E-08	2.29E-08	-2.9E-08	2.68E-08
43	-2E-08	2.39E-08	-1.7E-08	1.1E-08	-1.2E-08	1.5E-08	-1.4E-08
45	1.06E-08	-8.9E-09	-1.9E-09	1.01E-08	-1E-08	5.58E-09	-2.4E-09
47	-8.9E-09	-3.1E-09	1.89E-08	-2.8E-08	2.66E-08	-1.8E-08	1.07E-08
49	1.22E-08	7.03E-09	-2.4E-08	3.12E-08	-2.6E-08	1.49E-08	-5.6E-09
51	-1.4E-08	-5.5E-09	1.86E-08	-2E-08	1.05E-08	1.58E-09	-8.8E-09

Table 8.5 Displacement parameters for rectangular plate with circular hole of radius $r = 0.15a$, $a/b = 1$ (continuation of table 8.4)

n	m				
	43	45	47	49	51
1	-7.5E-08	5.83E-08	-4.2E-08	3.3E-08	-2.7E-08
3	2.93E-08	-1.1E-08	-2.3E-10	-2.7E-09	1.21E-08
5	2.34E-08	-4.6E-08	5.16E-08	-3.5E-08	5.76E-09
7	-4.8E-08	7.77E-08	-8.3E-08	5.78E-08	-1.6E-08
9	2.92E-08	-6.5E-08	7.46E-08	-5.4E-08	1.44E-08
11	1.76E-08	1.83E-08	-3.5E-08	2.61E-08	-2.8E-09
13	-5.5E-08	2.6E-08	-8.6E-09	5.63E-09	-9.6E-09
15	5.31E-08	-3.9E-08	3.03E-08	-2.5E-08	1.64E-08
17	-1.2E-08	1.54E-08	-2.3E-08	2.66E-08	-1.7E-08
19	-4.3E-08	2.55E-08	5.33E-10	-1.9E-08	1.8E-08
21	7.79E-08	-5.5E-08	1.71E-08	1.39E-08	-2.3E-08
23	-7.5E-08	5.57E-08	-1.8E-08	-1.7E-08	3.05E-08
25	4.3E-08	-3.3E-08	4.51E-09	2.32E-08	-3.5E-08
27	-4.4E-09	4.86E-09	8.17E-09	-2.4E-08	2.94E-08
29	-2E-08	1.06E-08	-8.9E-09	1.22E-08	-1.4E-08
31	2.39E-08	-8.9E-09	-3.1E-09	7.03E-09	-5.5E-09
33	-1.7E-08	-1.9E-09	1.89E-08	-2.4E-08	1.86E-08
35	1.1E-08	1.01E-08	-2.8E-08	3.12E-08	-2E-08
37	-1.2E-08	-1E-08	2.66E-08	-2.6E-08	1.05E-08
39	1.5E-08	5.58E-09	-1.8E-08	1.49E-08	1.58E-09
41	-1.4E-08	-2.4E-09	1.07E-08	-5.6E-09	-8.8E-09
43	5.75E-09	4.01E-09	-7.7E-09	2.06E-09	8.63E-09
45	4.01E-09	-7.6E-09	7.86E-09	-2.8E-09	-4.1E-09
47	-7.7E-09	7.86E-09	-7.1E-09	3.67E-09	2.39E-10
49	2.06E-09	-2.8E-09	3.67E-09	-2.2E-09	-3.4E-11
51	8.63E-09	-4.1E-09	2.39E-10	-3.4E-11	2.2E-09

CHAPTER 9
PLATE WITH STIFFENERS

The considered approach can be readily used to solve the problem of the vibratory response of stiffened plate. The stiffened plate is consisting of plate stiffened by number of stiffeners. A stiffener is considered in the form of a beam. Its strain energy U_{sj} and kinetic energy T_{sj} are formulated as discussed earlier using the same type of function. The example of a rectangular plate with J stiffeners will be discussed in this chapter.

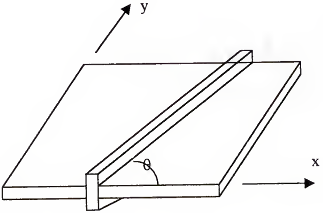

Figure 9.1 Rectangular plate with a stiffener forming an angle θ with the x-axis and its length is $b/\sin(\theta)$.

The general deflection function of the stiffener is assumed as

$$u(\eta) = \sum_{k=1}^{N_k} d_k \sin(\frac{k\pi\eta}{L}) \tag{9.1}$$

The deflection function of the plate is considered to be the same as in equation 5.1 and the strain energy U_e and kinetic energy T of the plate and the external work W on the plate will be the same as given in chapter 5.

Rectangular Plate with J Stiffeners

As an illustrative example, let us consider the case of a simple supported square plate reinforced by three stiffeners each having a length of a placed equidistance parallel to the y-axis of the plate. The compatibility requirement for the deflection of the stiffener and plate can be written as

$$x_{ji} = \eta_{ji} \cos\theta_j + x_{j0} \tag{9.2}$$

$$y_{ji} = \eta_{ji} \sin\theta_j + y_{j0} \tag{9.3}$$

where $i = 1,2,......I$, $j = 1,2,......J$, I is the number of constraints, and J is the number of stiffeners if several stiffeners are used. The constraints are the compatibility between the plate and the stiffeners. The unsatisfied constraints are

$$G_{ji} = w(x_{ji}, y_{ji}) - u(\eta_{ji}) = 0 \tag{9.4}$$

The strain energies for the plate and all stiffeners should be added to each other. Also the kinetic energy should be added to each other. The external work is due to the uniformly distributed load applied on the plate.

The Lagrangian function is

$$L = U_e + \sum_{j=1}^{J} U_{sj} - T - \sum_{j=1}^{J} T_{sj} - W + \sum_{j=1}^{J}\sum_{i=1}^{I} \lambda_{ji} G_{ji} \tag{9.5}$$

where U_{sj} is the strain energy of the stiffener j and T_{sj} is the kinetic energy of the stiffener j. The same procedure as in the previous examples is applied and the result is given in figure 9.2 and table 9.1

Result

Table 9.1 shows the natural frequency parameter for different values of N. The table shows the convergence is relatively fast after few terms. It can be seen that for N=10 the value of λ becomes 8.07042, and it converges at N=15 to a value of 8.06317.

Figure 9.2 shows that the value of the natural frequency parameter is obtained as 1/|Y| approaches zero. Figure 9.3 shows the mode shape of the square plate with three stiffeners at relative Rigidity of 5.088E-4 placed parallel to the y-axis at $x = 0.25a$, $x = 0.5a$ and $x = 0.75a$

Table 9.1 Natural frequency of rectangular plate with 3 stiffeners parallel to y-axis for different N terms, $a/b = 1$ $\omega_n = \lambda = \omega_n a^2 \sqrt{\rho h/D}$

N	8	10	15	20
λ	8.08492	8.07042	8.06317	8.06317

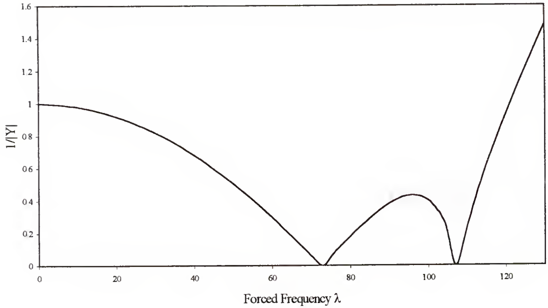

Figure 9.2 The inverse of normalized maximum absolute deflection versus forced frequency for Simply Supported square plate with three stiffeners, N=20.

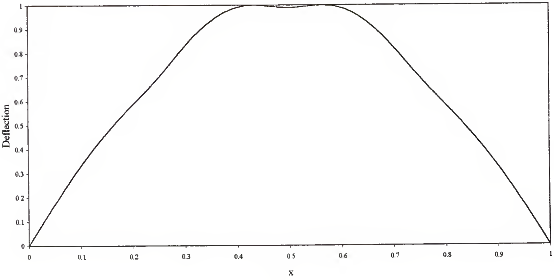

Figure 9.3 Mode shape at y=b/2 for square plate with three stiffeners parallel to the y-axis with R.G.=5.088E-4.

Table 9.2 Displacement parameters for rectangular plate with three stiffeners, $a/b = 1$

n	m						
	1	2	3	4	5	6	7
1	-1.90E-02	-1.39E-18	1.36E-07	2.06E-19	2.11E-08	-3.06E-20	-0.000389363
2	-6.49E-19	-7.18E-19	1.45E-18	1.38E-34	-2.22E-19	4.62E-21	-3.1458E-21
3	7.58E-09	7.81E-19	5.22E-09	-2.41E-24	4.59E-09	-4.55E-20	4.0781E-09
4	8.64E-19	3.64E-18	1.70E-18	1.48E-34	-5.85E-19	-4.75E-19	-5.13345E-20
5	2.04E-09	-9.52E-19	1.16E-09	-3.95E-25	1.06E-09	2.04E-19	1.29778E-09
6	6.65E-19	1.08E-18	7.35E-19	9.79E-35	-3.92E-19	-3.25E-19	-1.22846E-19
7	7.08E-10	-1.44E-18	3.37E-10	-8.57E-26	3.05E-10	5.55E-19	4.40067E-10
8	2.76E-19	-3.22E-19	5.04E-19	1.61E-34	-3.38E-19	1.48E-19	-9.02114E-20
9	2.76E-10	1.25E-18	1.20E-10	-2.40E-26	1.07E-10	-6.56E-19	1.64611E-10
10	-1.16E-18	-1.90E-18	-5.11E-19	9.19E-36	3.88E-19	1.11E-18	5.30902E-19
11	1.41E-10	4.19E-19	5.29E-11	-6.61E-27	4.10E-11	-2.65E-19	5.83276E-11
12	5.79E-19	2.37E-19	9.15E-20	2.40E-35	-7.46E-20	-1.60E-19	-3.26229E-19
13	7.68E-11	-7.33E-19	2.63E-11	-1.74E-27	1.76E-11	5.22E-19	2.06538E-11
14	2.86E-19	5.75E-19	-1.91E-19	-1.03E-34	1.64E-19	-4.27E-19	-1.84634E-19
15	4.75E-11	2.01E-33	1.48E-11	3.07E-37	7.76E-12	-1.54E-33	4.61419E-12
16	-1.65E-19	-3.40E-19	1.14E-19	6.26E-35	-1.01E-19	2.70E-19	1.17138E-19
17	3.24E-11	2.55E-19	9.17E-12	6.40E-28	3.31E-12	-2.07E-19	-2.41327E-12
18	-1.14E-19	-4.83E-20	-1.91E-20	-5.20E-36	1.74E-20	4.01E-20	8.65337E-20
19	2.38E-11	-4.89E-20	6.20E-12	8.71E-28	1.15E-12	4.13E-20	-5.57694E-12
20	7.41E-20	1.26E-19	3.63E-20	-7.01E-37	-3.35E-20	-1.08E-19	-5.90564E-20

Table 9.3 Displacement parameters for rectangular plate with three stiffeners, $a/b = 1$ (continuation of table 9.2)

n	m						
	8	9	10	11	12	13	14
1	-1.35E-19	1.43E-04	2.97E-20	-1.74E-10	6.91E-21	3.01E-10	9.06E-21
2	-8.22E-36	-2.77E-21	-6.63E-22	1.07E-20	4.93E-36	-5.03E-21	1.79E-22
3	1.37E-24	-1.30E-09	7.59E-21	-9.07E-11	-1.77E-25	1.13E-10	-2.14E-21
4	1.43E-35	2.25E-20	9.40E-20	5.15E-20	1.65E-35	-2.78E-20	-2.81E-20
5	4.66E-25	-4.64E-10	-4.81E-20	-2.28E-11	-6.77E-26	4.54E-11	1.54E-20
6	-2.74E-35	6.42E-20	9.03E-20	5.85E-20	2.42E-35	-3.44E-20	-3.10E-20
7	1.66E-25	-1.71E-10	-1.80E-19	-4.99E-12	-2.88E-26	2.14E-11	6.63E-20
8	-8.08E-35	5.47E-20	-5.48E-20	7.79E-20	7.09E-35	-4.90E-20	2.18E-20
9	6.38E-26	-6.67E-11	2.73E-19	-4.00E-13	-1.33E-26	1.11E-11	-1.17E-19
10	9.46E-35	-3.60E-19	-5.13E-19	-1.24E-19	5.94E-36	8.36E-20	2.34E-19
11	2.16E-26	-2.07E-11	1.34E-19	1.53E-12	-5.29E-27	5.53E-12	-6.49E-20
12	-1.42E-34	2.40E-19	8.71E-20	3.04E-20	2.20E-35	-2.17E-20	-4.48E-20
13	6.52E-27	-4.33E-12	-3.03E-19	1.82E-12	-1.82E-27	2.77E-12	1.64E-19
14	-1.82E-36	1.44E-19	2.62E-19	-7.98E-20	-1.20E-34	6.02E-20	-1.50E-19
15	-2.49E-36	2.88E-12	9.96E-34	1.84E-12	3.92E-37	1.20E-12	-5.92E-34
16	-6.19E-38	-9.60E-20	-1.81E-19	5.64E-20	8.68E-35	-4.44E-20	1.13E-19
17	-2.84E-27	5.98E-12	1.45E-19	1.76E-12	9.52E-28	3.01E-13	-9.31E-20
18	4.03E-35	-7.34E-20	-2.89E-20	-1.07E-20	-8.32E-36	8.73E-21	1.92E-20
19	-4.08E-27	7.29E-12	-3.06E-20	1.66E-12	1.46E-27	-2.26E-13	2.10E-20
20	-1.22E-35	5.15E-20	8.20E-20	2.23E-20	-1.13E-36	-1.87E-20	-5.77E-20

Table 9.4 Displacement parameters for rectangular plate with three stiffeners, $a/b = 1$ (continuation of table 9.3)

n	m					
	15	16	17	18	19	20
1	-1.87E-05	-1.71E-20	1.13E-05	5.33E-21	-3.03E-11	8.94E-21
2	-2.82E-22	-1.11E-36	2.97E-23	-6.64E-23	1.20E-21	2.11E-36
3	2.30E-10	2.06E-25	-1.25E-10	8.10E-22	-1.46E-11	-1.49E-25
4	-3.87E-21	2.45E-36	2.42E-21	1.09E-20	6.77E-21	3.77E-37
5	1.04E-10	9.28E-26	-5.65E-11	-6.16E-21	-5.12E-12	-6.75E-26
6	-1.27E-20	-6.40E-36	8.29E-21	1.29E-20	9.12E-21	6.33E-36
7	5.07E-11	4.54E-26	-2.76E-11	-2.86E-20	-2.04E-12	-3.43E-26
8	-1.37E-20	-2.58E-35	9.23E-21	-9.77E-21	1.47E-20	5.81E-35
9	2.63E-11	2.36E-26	-1.43E-11	5.45E-20	-8.75E-13	-1.89E-26
10	1.11E-19	4.01E-35	-7.78E-20	-1.14E-19	-2.84E-20	5.87E-35
11	1.20E-11	1.04E-26	-6.05E-12	3.29E-20	-1.58E-13	-8.86E-27
12	-8.91E-20	-7.66E-35	6.47E-20	2.37E-20	8.39E-21	3.98E-35
13	4.95E-12	3.92E-27	-1.99E-12	-9.01E-20	1.63E-13	-3.57E-27
14	-6.25E-20	-1.20E-36	4.71E-20	8.50E-20	-2.58E-20	-1.69E-34
15	7.98E-13	-1.79E-36	5.40E-13	3.49E-34	3.71E-13	1.36E-36
16	4.71E-20	-4.84E-38	-3.67E-20	-6.83E-20	2.10E-20	1.40E-34
17	-1.66E-12	-2.38E-27	2.12E-12	5.83E-20	5.06E-13	2.43E-27
18	3.99E-20	3.60E-35	-3.20E-20	-1.24E-20	-4.52E-21	-2.21E-35
19	-3.15E-12	-3.87E-27	3.13E-12	-1.39E-20	5.97E-13	4.15E-27
20	-3.05E-20	-1.22E-35	2.51E-20	3.91E-20	1.04E-20	-2.25E-35

CHAPTER 10
HONEYCOMB STRUCTURE

Sandwich Plate with Four Stiffeners

Another illustrative example for the application of the undetermined multipliers approach is the honeycomb sandwich structure as illustrated in figure 10.1

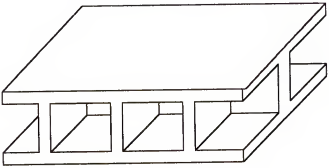

Figure 10.1 Honeycomb sandwich structure

A sandwich structure is a combination of two plates with stiffeners between them. The top and bottom plates have local and global deflections. Therefore the local deflections for the top and bottom plates respectively are assumed as

$$w_t(x,y)=\sum_{m=1}^{M}\sum_{n=1}^{N}B_{mn}\sin(\frac{n\pi x}{a})\sin(\frac{m\pi y}{b}) \tag{10.1}$$

$$w_b(x,y)=\sum_{m=1}^{M}\sum_{n=1}^{N}C_{mn}\sin(\frac{n\pi x}{a})\sin(\frac{m\pi y}{b}) \tag{10.2}$$

The global deflection is

$$w_g(x,y)=\sum_{m=1}^{M}\sum_{n=1}^{N}A_{mn}\sin(\frac{n\pi x}{a})\sin(\frac{m\pi y}{b}) \tag{10.3}$$

The deflection function of the stiffeners is the same as in equation 3.12. Both of the two plates have local strain energy, and global strain energy. The local strain energy of the top plate is

$$U_{tl}=\frac{D}{2}\sum_{m=1}^{M}\sum_{n=1}^{N}B_{mn}^2 Q_{mn} \tag{10.4}$$

The local strain energy of the bottom plate is

$$U_{bl}=\frac{D}{2}\sum_{m=1}^{M}\sum_{n=1}^{N}C_{mn}^2 Q_{mn} \tag{10.5}$$

The global strain energy of the top plate is

$$U_{tg}=\frac{D_c}{2}\sum_{m=1}^{M}\sum_{n=1}^{N}A_{mn}^2 Q_{mn} \tag{10.6}$$

The global strain energy of the bottom plate is

$$U_{bg}=\frac{D_c}{2}\sum_{m=1}^{M}\sum_{n=1}^{N}A_{mn}^2 Q_{mn} \tag{10.7}$$

where $Q_{mn}=\frac{ab}{4}[(\frac{n\pi}{a})^2+(\frac{m\pi}{b})^2]^2$ (10.8)

The kinetic energy is formulated in a way similar to the case of strain energy. The local kinetic energy of the top plate is

$$T_{tl} = \sum_{m=1}^{M} \sum_{n=1}^{N} B_{mn}^{2} \overline{\omega} \tag{10.10}$$

The local kinetic energy of the bottom plate is

$$T_{bl} = \sum_{m=1}^{M} \sum_{n=1}^{N} C_{mn}^{2} \overline{\omega} \tag{10.11}$$

The global kinetic energy based on the full structure for the top plate is

$$T_{tg} = \sum_{m=1}^{M} \sum_{n=1}^{N} A_{mn}^{2} \overline{\omega} \tag{10.12}$$

The global kinetic energy based on the full structure for the bottom plate is

$$T_{bg} = \sum_{m=1}^{M} \sum_{n=1}^{N} A_{mn}^{2} \overline{\omega} \tag{10.13}$$

where $\overline{\omega} = \omega^{2} \dfrac{\rho abh}{8}$ (10.14)

The external work is caused by the uniformly distributed load applied on the top plate due to the global and local deflection of the plate. Therefore the external work is obtained by adding the external work calculated for the global deflection to that calculated for the local deflection. Hence, the external work is

$$W = \int_{0}^{b}\int_{0}^{a} p[w_{g}(x,y) + w_{t}(x,y)]dxdy \tag{10.15}$$

$$W = \sum_{m=1}^{M} \sum_{n=1}^{N} (A_{mn} + B_{mn}) S_{mn} \tag{10.16}$$

where $S_{mn} = \dfrac{ab}{nm\pi^2} p[\cos(n\pi) - 1][\cos(m\pi) - 1]$ (10.17)

There is no external work for the bottom plate because it is not subjected to external load. The stiffeners are treated as beams therefore the deflection function, the strain energy, and the kinetic energy are the same as that given in equations 3.13, 3.14. Each stiffener is expected to have a different deflection function. The deflection of each stiffener is assumed to be

$$u(\eta_j) = \sum_{k=1}^{K} d_k \sin(\frac{k\pi\eta_j}{L_j}) \tag{10.18}$$

where η_j is the coordinate along the stiffener j and L_j is the length of stiffener j and K is the number of approximation terms. The strain energy of the stiffener is

$$U_{sj} = \frac{EI\pi^4}{4L_j^3} \sum_{k=1}^{K} k^4 d_{jk}^2 \tag{10.19}$$

The kinetic energy stiffener is

$$T_{sj} = \frac{\gamma\omega^2 L_j}{4} \sum_{k=1}^{K} d_{jk}^2 \tag{10.20}$$

The unsatisfied constraints are that the global deflection should equal the stiffener deflection at every discrete point. In other words, the difference between them should be zero. Another constraint is formulated by making the local deflection of the top plate at the stiffeners equal to zero. The last constraint is to make the local deflection of the bottom plate at the stiffeners equal to zero. These constraints are given respectively as follows

$$G_{1,ji} = \sum_{m=1}^{M}\sum_{n=1}^{N} A_{mn}Q_{mn,1i} - \sum_{k=1}^{K} u_k(\eta_j) \tag{10.21}$$

$$G_{2,ji} = \sum_{m=1}^{M}\sum_{n=1}^{N} A_{mn}Q_{mn,2i} \tag{10.22}$$

$$G_{3,ji} = \sum_{m=1}^{M}\sum_{n=1}^{N} A_{mn}Q_{mn,3i} \tag{10.23}$$

where $i = 1,2,3,..........I$ and I is the number of discrete points for one stiffener, $j = 1,2,3,..........J$, and J is the number of stiffeners.

The Lagrangian function can therefore be formulated as:

$$\begin{aligned} L = {} & U_{tl} + U_{bl} + U_{tg} + U_{bg} - T_{tl} - T_{bl} - T_{tg} - T_{bg} - W + \\ & \sum_{j=1}^{J} U_{sj} - \sum_{j=1}^{J} T_{sj} + \sum_{i=1}^{I} \lambda_i G_{1i} + \sum_{i=1}^{I} \mu_i G_{2i} + \sum_{i=1}^{I} \zeta_i G_{3i} \end{aligned} \tag{10.24}$$

The displacement parameters of the plates and stiffeners are A_{mn}, B_{mn}, C_{mn} and d_k. Taking derivative with respect to these parameters gives equations that can be solved simultaneously to give the values of these parameters.

Result

The honeycomb used in this example has a/b=3, hight 0.1b and plate thickness of 0.01b. Four stiffeners are used. Three of are parallel to y-axis placed at equal distances from each other and from the edges. The fourth is parallel to the x-axis at y=b/2. The number of discrete points for each of the first three stiffeners is 4. The number of discrete points for the last one is 9. Figure 10.2 shows the first natural frequency. Table 10.1 shows the progression of the convergence process with increasing the number of terms. Figure 10.4 shows the mode shape of the honeycomb at the first natural frequency. Table 10.1 shows how the convergence occurs as N increases. At N=10, the natural frequency becomes $\lambda = 84.5763$. At N=20, the natural frequency becomes $\lambda = 80.5302$.

Table 10.1 Natural frequency of Honeycomb plate with 4 stiffeners for different N terms, $a/b = 1$, $\lambda = \omega_n a^2 \sqrt{\rho h/D}$

N	λ_1	λ_2
10	84.5763	127.595
15	81.9659	111.803
20	80.5302	111.248

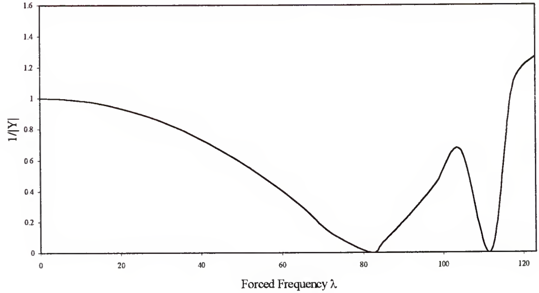

Figure 10.2 Inverse of the normalized maximum absolute deflection versus the forced frequency for Honeycomb sandwich plate, a/b=1, N=15.

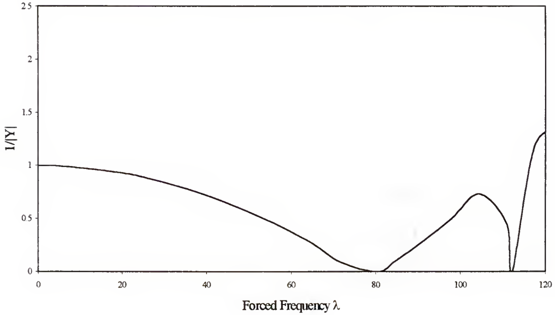

Figure 10.3 The inverse of the normalized maximum absolute deflection versus the forced frequency for Honeycomb sandwich plate, a/b=1, N=20.

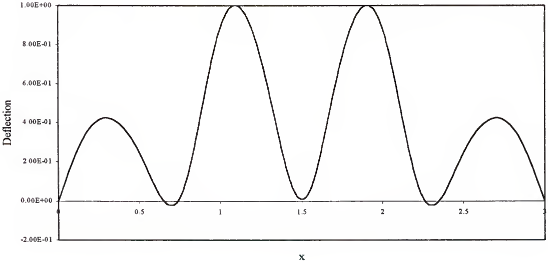

Figure 10.4 Mode shape of honeycomb sandwich plate at y=b/4 for N=20

Table 10.2 Displacement parameters for Honeycomb sandwich plate with four stiffeners; $a/b = 1$

n	m						
	1	2	3	4	5	6	7
1	-4.16E-05	5.50E-19	-1.41E-06	-2.07E-19	2.14E-06	5.53E-19	-3.01137E-05
2	8.39E-21	-1.81E-21	-2.70E-20	-5.34E-35	5.14E-20	3.30E-20	3.53567E-20
3	-3.29E-05	5.47E-19	2.01E-07	-2.44E-19	2.47E-07	4.54E-19	-2.06427E-05
4	2.24E-20	2.65E-20	6.53E-21	-1.18E-35	-5.06E-21	-1.62E-20	-1.3087E-20
5	3.50E-06	-6.29E-20	5.11E-07	1.89E-20	-4.77E-07	-2.86E-20	1.74488E-06
6	-2.73E-21	-4.24E-21	-1.07E-21	3.34E-36	9.19E-22	3.49E-21	2.86846E-21
7	-1.45E-06	2.55E-20	-2.59E-07	-4.96E-21	2.50E-07	-8.21E-22	-2.39711E-08
8	-1.02E-22	-2.08E-23	-3.23E-22	-1.47E-36	3.03E-22	1.86E-23	-2.6626E-22
9	1.88E-07	-5.72E-21	8.04E-08	1.82E-21	-8.05E-08	-2.96E-21	3.03546E-07
10	3.92E-23	-1.83E-36	2.99E-23	7.30E-37	-3.03E-23	-1.64E-36	1.57161E-22
11	-8.40E-08	2.56E-21	-3.61E-08	-8.24E-22	3.67E-08	1.37E-21	-1.41195E-07
12	-1.01E-22	4.09E-24	3.27E-23	-4.15E-37	-2.91E-23	-3.89E-24	-2.28218E-23
13	1.19E-07	-2.12E-21	2.18E-08	4.28E-22	-2.22E-08	7.54E-23	2.28847E-09
14	1.84E-22	1.41E-22	4.86E-23	2.72E-37	-4.77E-23	-1.36E-22	-1.00888E-22
15	-3.90E-08	7.19E-22	-6.11E-09	-2.39E-22	6.48E-09	4.23E-22	-2.83016E-08
16	-8.40E-23	-8.15E-23	-2.72E-23	-1.80E-37	2.62E-23	7.93E-23	3.13451E-23
17	6.49E-09	-1.48E-22	-7.87E-11	1.43E-22	-2.08E-10	-5.42E-22	3.38525E-08
18	2.17E-23	-8.08E-25	-1.06E-23	1.23E-37	9.87E-24	7.90E-25	1.44692E-23
19	-2.09E-08	2.72E-22	-6.71E-10	-9.27E-23	8.49E-10	1.73E-22	-5.61836E-09
20	-2.53E-23	3.29E-37	-9.81E-25	-9.31E-38	1.16E-24	1.15E-37	-1.2328E-24

Table 10.3 Displacement parameters for Honeycomb sandwich plate with four stiffeners, $a/b = 1$ (continuation of table 10.2)

n	m						
	8	9	10	11	12	13	14
1	5.30E-27	9.75E-06	3.11E-20	1.39E-06	1.67E-20	-3.94E-06	4.65E-20
2	7.21E-36	-6.73E-21	5.25E-22	4.68E-21	3.58E-36	-2.66E-21	-1.42E-22
3	-6.60E-21	7.20E-06	-7.42E-20	-2.36E-07	-5.74E-21	1.68E-06	3.52E-21
4	-3.77E-36	8.78E-21	8.07E-21	1.81E-21	-8.37E-37	-9.98E-22	-3.97E-21
5	4.40E-22	-3.87E-07	9.66E-22	2.99E-07	2.30E-21	-8.11E-07	1.02E-20
6	8.53E-37	-2.19E-21	-2.49E-21	-5.60E-22	5.69E-37	3.19E-22	1.64E-21
7	1.38E-22	-3.06E-07	6.39E-21	-1.93E-07	-1.02E-21	4.02E-07	-9.38E-21
8	-1.02E-37	1.40E-22	-1.52E-23	-2.32E-22	-4.50E-37	2.81E-22	1.17E-23
9	1.10E-22	-1.45E-07	-1.95E-23	7.29E-08	4.16E-22	-1.74E-07	2.12E-21
10	6.12E-38	-9.11E-23	3.67E-37	2.89E-23	1.72E-37	-7.34E-23	5.96E-37
11	-5.20E-23	6.94E-08	8.20E-24	-3.58E-08	-2.08E-22	8.86E-08	-1.09E-21
12	-1.66E-39	-1.31E-23	3.54E-24	2.10E-23	-8.79E-38	8.78E-24	-3.10E-24
13	-1.37E-23	3.20E-08	-6.99E-22	2.23E-08	1.24E-22	-5.17E-08	1.28E-21
14	-3.62E-38	1.19E-22	1.27E-22	4.51E-23	8.11E-38	-6.21E-23	-1.15E-22
15	-7.90E-24	7.70E-09	-2.15E-23	-7.42E-09	-6.41E-23	2.53E-08	-3.57E-22
16	4.91E-39	-4.53E-23	-7.51E-23	-2.59E-23	-4.85E-38	3.84E-23	6.94E-23
17	1.45E-23	-2.09E-08	2.79E-22	1.13E-09	3.45E-23	-1.25E-08	-3.21E-23
18	5.51E-39	-3.04E-24	-7.57E-25	-8.24E-24	2.51E-38	-1.97E-24	7.11E-25
19	-2.56E-30	-2.38E-09	-1.83E-23	-1.41E-09	-2.62E-23	8.86E-09	-1.44E-22
20	2.51E-39	-6.70E-24	3.60E-38	-1.71E-24	-2.75E-38	9.21E-24	-1.99E-37

Table 10.4 Displacement parameters for Honeycomb sandwich plate with four stiffeners, $a/b = 1$ (continuation of table 10.3)

n	m					
	15	16	17	18	19	20
1	-6.74E-07	-1.71E-20	4.23E-07	2.78E-20	-1.35E-06	-2.53E-21
2	9.31E-22	-9.04E-37	-5.97E-22	5.54E-23	4.25E-22	4.95E-37
3	-1.62E-06	8.33E-21	1.07E-06	-2.97E-20	9.77E-07	3.09E-21
4	-3.01E-21	-5.44E-38	2.17E-21	2.05E-21	6.60E-22	2.17E-39
5	1.38E-07	-4.60E-21	-9.75E-08	9.45E-21	-4.73E-07	-1.17E-21
6	1.16E-21	-5.17E-37	-9.26E-22	-1.05E-21	-3.79E-22	8.07E-38
7	2.03E-07	2.45E-21	-1.72E-07	-1.55E-21	2.10E-07	2.94E-22
8	-8.86E-23	6.88E-37	7.22E-23	-8.55E-24	-2.07E-23	7.88E-38
9	9.70E-08	-1.01E-21	-8.32E-08	2.42E-21	-1.20E-07	-3.89E-22
10	6.58E-23	-4.20E-37	-5.80E-23	1.35E-36	-5.60E-23	-2.09E-37
11	-5.10E-08	5.38E-22	4.53E-08	-1.34E-21	6.76E-08	2.23E-22
12	1.44E-23	3.41E-37	-1.32E-23	2.63E-24	6.80E-23	1.50E-37
13	-2.92E-08	-3.73E-22	2.77E-08	2.64E-22	-3.79E-08	-5.60E-23
14	-1.04E-22	-2.96E-37	9.83E-23	1.01E-22	-1.39E-24	-9.06E-38
15	-5.38E-09	2.00E-22	4.72E-09	-5.07E-22	2.81E-08	7.69E-23
16	4.13E-23	1.79E-37	-3.91E-23	-6.28E-23	6.31E-24	9.91E-38
17	1.79E-08	-1.11E-22	-1.69E-08	5.51E-22	-2.12E-08	-7.75E-23
18	2.34E-24	-1.12E-37	-2.04E-24	-6.56E-25	-2.67E-23	-7.20E-38
19	2.76E-09	9.02E-23	-2.82E-09	-2.30E-22	1.37E-08	3.08E-23
20	6.78E-24	9.58E-38	-6.72E-24	-1.87E-37	1.36E-23	2.52E-38

CHAPTER 11
PLATE WITH ARBITRARY SHAPE AND BOUNDARY CONDITIONS

The proposed approach is readily applicable to the case of plates with arbitrary shapes and support conditions.

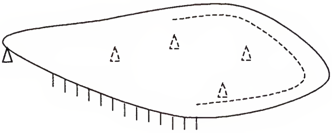

Figure 11.1 Plate with arbitrarily shape with arbitrarily support conditions

Triangular Plate with Internal Support

A study of the literature revealed that exact or highly accurate solutions exist for the rectangular thin plate free vibration problem. The situation pertaining to straight-edged thin flat plates, which do not have rectangular shapes, is quite different [18]. Adding an internal support to this kind of problem makes it more difficult. Special treatment to the problem is needed. Using superposition method in conjunction with the proposed approach can solve the problem in a convenient way.

The example of a simply supported $30^\circ - 60^\circ - 90^\circ$ triangular plate along the edges is considered with an additional internal point support at ξ and η.

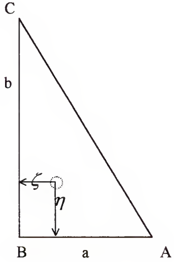

Figure 11.2 Triangular plate simply supported with internal discrete support

Using the proposed approach and the superposition method in a way that been reported by Gorman [18-25] gives a deflection function for the specified problem. The superposition procedure is described in publications by Gorman [18-25]. Four rectangular plates [25] are considered in the superposition method. Each two rectangular plates are simply supported at three edges and free at the fourth edge parallel to x-axis. The fourth edge for the first rectangular is subjected to forced rotation while for the second rectangular it is exposed to forced displacement. Similarly, the other two rectangular plates are the same except that the fourth edge is parallel to y-axis. The deflection function of each of the first two plates can be assumed as

$$w_1(x,y)=\sum_{m=1}^{M}\sum_{n=1}^{N}A_{mn}\sin(n\pi x/a)\sinh(m\pi y/b) \tag{11.1}$$

The function of each of the other two plates can be assumed as

$$w_2(x,y)=\sum_{m=1}^{M}\sum_{n=1}^{N}B_{mn}\sinh(n\pi x/a)\sin(m\pi y/b) \tag{11.2}$$

The strain energy of each rectangular plate can be found as described in chapter 5. Also, the kinetic energy and the external work for each rectangular plate can be found in the same way described in chapter 5.

The unsatisfied constraints for the first rectangular plate having rotation at the edge y=b are

$$G_i=\frac{\partial w_1(x_i,b)}{\partial y}-\sum_{m=1}^{M}\sum_{n=1}^{N}A_{mn}\sin(\frac{n\pi x_i}{a}) \tag{11.3}$$

The unsatisfied constraints for the second rectangular plate having forced displacement at the edge y=b are

$$G_i=w_1(x_i,b)-\sum_{m=1}^{M}\sum_{n=1}^{N}A_{mn}\sin(\frac{n\pi x_i}{a}) \tag{11.4}$$

The unsatisfied constraint for the internal support at each of the first two rectangular plates is

$$G_{I+1}=w_1(\zeta,\eta) \tag{11.5}$$

The unsatisfied constraints for the third rectangular plate having rotation at the edge x=a are

$$G_i=\frac{\partial w_2(a,y_i)}{\partial x}-\sum_{m=1}^{M}\sum_{n=1}^{N}B_{mn}\sin(\frac{my_i}{b}) \tag{11.6}$$

The unsatisfied constraints for the fourth rectangular plate having forced displacement at the edge x=a are

$$G_i = w_2(a, y_i) - \sum_{m=1}^{M} \sum_{n=1}^{N} B_{mn} \sin(\frac{m\pi y_i}{b}) \tag{11.7}$$

The unsatisfied constraint for the internal support at each of the other two rectangular plates is

$$G_{I+1} = w_2(\zeta, \eta) \tag{11.8}$$

Following the same solution procedures as in the previous cases for each one of the four rectangular plates gives a deflection function for each of them. Adding these four solutions gives the deflection function of the plate. The solution can be written in the form

$$w(x,y) = \sum_{m=1}^{M} \sum_{n=1}^{N} (C_{mn} \sin(n\pi x/a)\sinh(m\pi y/b) +$$

$$D_{mn} \sinh(n\pi x/a)\sin(m\pi y/b)) \tag{11.9}$$

where C_{mn} is the summation of the coefficients of the first and the second rectangular plates, and D_{mn} is the summation of the coefficients of the third and the fourth rectangular plates.

Result

The illustrative case of a $30^\circ\, 60^\circ\, 90^\circ$ triangular plate with a/b=$1/\sqrt{3}$ is considered. The triangular is simply supported along the edges. The internal support is located at ζ/a=0.25 and η/b=0.5. Nine discrete points along x-axis and also along y-axis are considered to satisfy the support constraint along the diagonal. Figure 11.3 shows the inverse of the normalized maximum deflection versus frequency. Table 11.1 shows that the convergence is relatively fast. As N increases the natural frequency approaches the published value. At N=15 the natural frequency parameter is found to be $\lambda = 101.178$. Compared with a published result, which it is $\lambda = 101.06$, the difference is found to be 0.12%.

Table 11.1 Natural frequency of 30° 60° 90° triangular plate simply supported with internal support for different N terms, $b/a=\sqrt{3}$, $\omega_n = \lambda = \omega_n a^2 \sqrt{\rho h/D}$

N	λ	Published result λ	Difference
5	115.509		
10	103.763		
15	101.178	101.06 [13]	0.12%

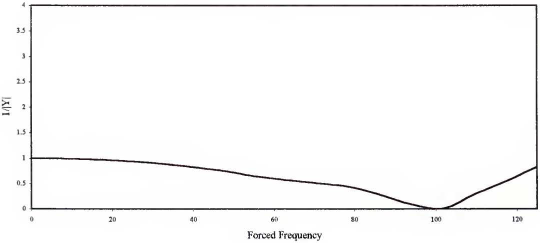

Figure 11.3 Inverse of normalized maximum absolute deflection versus forced frequency for simply supported right triangular plate with internal discrete support

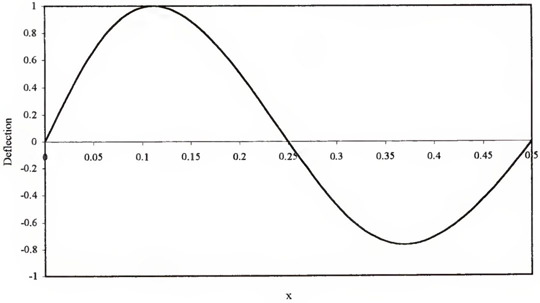

Figure 11.4 Mode shape along x-axis at y=b/2 for simply supported right triangular plate with internal discrete support

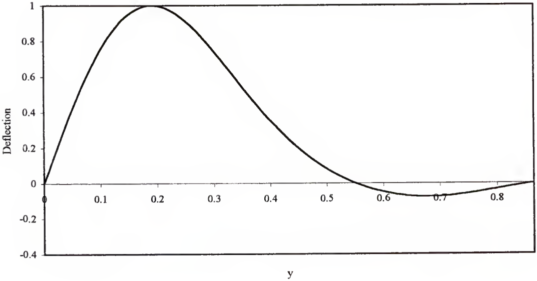

Figure 11.5 Mode shape along y-axis at x=a/4 for simply supported right triangular plate with internal discrete support

Table 11.2 Displacement parameters C_{mn} for Triangular plate with internal support; $a = 1,\ b = \sqrt{3}$

n	m							
	1	2	3	4	5	6	7	8
1	-0.00028	0.000626	5.684E-05	4.16E-21	-4.79E-06	-2.70E-06	-9.09E-07	1.61E-21
2	-1.3E-05	6.18E-06	3.493E-06	3.56E-22	-1.83E-07	-4.84E-08	-1.34E-09	2.54E-22
3	8.08E-06	3.78E-08	2.188E-07	2.65E-23	-1.04E-08	-6.27E-10	1.25E-09	2.24E-23
4	1.78E-08	2.08E-10	1.153E-08	1.65E-24	-6.46E-10	-7.07E-12	1.02E-10	1.59E-24
5	3.86E-10	1.16E-12	5.163E-10	8.44E-26	-3.69E-11	-7.30E-14	6.45E-12	9.89E-26
6	1.07E-11	6.72E-15	2.086E-11	4.02E-27	-1.91E-12	-7.07E-16	3.66E-13	5.74E-27
7	3.29E-13	4.07E-17	7.979E-13	2.21E-28	-9.15E-14	-6.51E-18	1.93E-14	3.12E-28
8	1.07E-14	2.56E-19	2.976E-14	6.65E-30	-4.12E-15	-5.74E-20	9.64E-16	1.60E-29
9	3.6E-16	1.66E-21	1.100E-15	2.93E-31	-1.77E-16	-4.89E-22	4.60E-17	7.87E-31
10	1.25E-17	1.11E-23	4.064E-17	1.11E-32	-7.37E-18	-4.06E-24	2.11E-18	3.71E-32
11	4.41E-19	7.65E-26	1.507E-18	4.26E-34	-3.00E-19	-3.30E-26	9.41E-20	1.70E-33
12	1.59E-20	5.36E-28	5.622E-20	1.71E-35	-1.21E-20	-2.65E-28	4.09E-21	7.73E-35
13	5.8E-22	3.82E-30	2.111E-21	7.52E-37	-4.80E-22	-2.11E-30	1.75E-22	3.38E-36
14	2.14E-23	2.77E-32	7.977E-23	2.23E-38	-1.90E-23	-1.67E-32	7.34E-24	1.46E-37
15	8.01E-25	2.04E-34	3.034E-24	1.04E-39	-7.49E-25	-1.32E-34	3.05E-25	6.20E-39

Table 11.3 Displacement parameters C_{mn} for Triangular plate with internal support, $a = 1,\ b = \sqrt{3}$ (continuation of table 11.2)

n	m						
	9	10	11	12	13	14	15
1	3.44E-07	3.50E-07	1.84E-07	-3.03E-22	-9.83E-08	-9.11E-08	-3.64E-08
2	2.19E-09	6.35E-09	5.21E-09	-4.90E-23	-3.17E-09	-1.66E-09	7.52E-10
3	-3.14E-10	8.45E-11	2.28E-10	-4.40E-24	-1.59E-10	-2.23E-11	1.29E-10
4	-2.78E-11	9.93E-13	1.39E-11	-3.14E-25	-1.01E-11	-2.64E-13	9.90E-12
5	-1.81E-12	1.09E-14	8.59E-13	-2.02E-26	-6.33E-13	-2.93E-15	6.41E-13
6	-1.06E-13	1.13E-16	5.05E-14	-1.20E-27	-3.75E-14	-3.10E-17	3.82E-14
7	-5.84E-15	1.14E-18	2.82E-15	-6.68E-29	-2.11E-15	-3.19E-19	2.16E-15
8	-3.05E-16	1.11E-20	1.51E-16	-3.58E-30	-1.14E-16	-3.20E-21	1.17E-16
9	-1.53E-17	1.06E-22	7.77E-18	-1.89E-31	-5.97E-18	-3.15E-23	6.18E-18
10	-7.46E-19	9.89E-25	3.89E-19	-9.52E-33	-3.03E-19	-3.04E-25	3.17E-19
11	-3.52E-20	9.07E-27	1.90E-20	-4.66E-34	-1.51E-20	-2.90E-27	1.59E-20
12	-1.62E-21	8.18E-29	9.04E-22	-2.24E-35	-7.34E-22	-2.73E-29	7.84E-22
13	-7.31E-23	7.26E-31	4.23E-23	-1.07E-36	-3.51E-23	-2.55E-31	3.80E-23
14	-3.24E-24	6.37E-33	1.94E-24	-4.90E-38	-1.65E-24	-2.35E-33	1.81E-24
15	-1.41E-25	5.53E-35	8.78E-26	-2.26E-39	-7.64E-26	-2.14E-35	8.54E-26

Table 11.4 Displacement parameters D_{mn} for Triangular plate with internal support, $a = 1,\ b = \sqrt{3}$

n	m							
	1	2	3	4	5	6	7	8
1	-0.00014	4.35E-06	9.6E-09	1.05E-10	1.17E-12	-3.54E-15	-1.14E-15	-6.76E-17
2	-0.00016	1.01E-05	8.37E-08	1.48E-09	3.28E-11	8.23E-13	2.25E-14	6.54E-16
3	-0.00084	1.54E-06	2.78E-08	4.87E-10	9.04E-12	1.62E-13	2.17E-15	-1.42E-17
4	-0.00015	-5.7E-06	-1.4E-07	-3.14E-09	-7.72E-11	-2.04E-12	-5.75E-14	-1.70E-15
5	1.75E-05	-2.3E-08	-4.2E-09	-1.13E-10	-2.66E-12	-5.99E-14	-1.27E-15	-2.21E-17
6	4.18E-06	2.72E-07	1.1E-08	3.50E-10	1.03E-11	2.99E-13	8.92E-15	2.73E-16
7	-4.5E-06	-1.2E-08	1.02E-09	3.95E-11	1.14E-12	2.99E-14	7.19E-16	1.52E-17
8	-4.4E-06	-3.2E-07	-1.6E-08	-6.54E-10	-2.30E-11	-7.57E-13	-2.44E-14	-7.88E-16
9	1.68E-06	7.54E-09	-3.3E-10	-1.61E-11	-5.54E-13	-1.66E-14	-4.47E-16	-1.06E-17
10	3.82E-07	2.98E-08	1.66E-09	7.64E-11	3.08E-12	1.14E-13	4.00E-15	1.38E-16
11	-7.5E-07	-3.4E-09	1.72E-10	9.29E-12	3.60E-13	1.21E-14	3.59E-16	9.34E-18
12	-1.3E-06	-1E-07	-6.1E-09	-3.02E-10	-1.33E-11	-5.38E-13	-2.05E-14	-7.53E-16
13	3.76E-07	8.09E-10	-1.5E-10	-7.93E-12	-3.29E-13	-1.20E-14	-3.85E-16	-1.08E-17
14	3.25E-07	2.64E-08	1.6E-09	8.27E-11	3.86E-12	1.67E-13	6.78E-15	2.64E-16
15	-2E-07	1.03E-09	1.73E-10	9.02E-12	3.89E-13	1.48E-14	5.02E-16	1.47E-17

Table 11.5 Displacement parameters D_{mn} for Triangular plate with internal support, $a = 1,\ b = \sqrt{3}$ (continuation of table 11.4)

n	m						
	9	10	11	12	13	14	15
1	-3.25E-18	-1.44E-19	-6.20E-21	-2.61E-22	-1.09E-23	-4.54E-25	-1.88E-26
2	1.99E-17	6.28E-19	2.04E-20	6.80E-22	2.31E-23	8.01E-25	2.82E-26
3	-3.12E-18	-1.94E-19	-9.76E-21	-4.51E-22	-2.00E-23	-8.68E-25	-3.71E-26
4	-5.24E-17	-1.67E-18	-5.46E-20	-1.83E-21	-6.24E-23	-2.17E-24	-7.63E-26
5	-1.23E-19	1.63E-20	1.27E-21	6.96E-23	3.39E-24	1.56E-25	6.93E-27
6	8.61E-18	2.78E-19	9.21E-21	3.11E-22	1.07E-23	3.73E-25	1.32E-26
7	2.19E-19	-2.64E-21	-4.49E-22	-2.87E-23	-1.49E-24	-7.13E-26	-3.26E-27
8	-2.57E-17	-8.53E-19	-2.87E-20	-9.82E-22	-3.41E-23	-1.20E-24	-4.27E-26
9	-1.91E-19	-3.27E-22	2.19E-22	1.62E-23	8.97E-25	4.43E-26	2.06E-27
10	4.70E-18	1.61E-19	5.56E-21	1.94E-22	6.81E-24	2.42E-25	8.68E-27
11	1.92E-19	1.39E-21	-1.57E-22	-1.34E-23	-7.81E-25	-3.97E-26	-1.89E-27
12	-2.71E-17	-9.63E-19	-3.42E-20	-1.22E-21	-4.37E-23	-1.57E-24	-5.71E-26
13	-2.41E-19	-2.34E-21	1.71E-22	1.63E-23	9.87E-25	5.14E-26	2.49E-27
14	9.97E-18	3.70E-19	1.36E-20	4.96E-22	1.81E-23	6.65E-25	2.44E-26
15	3.30E-19	2.46E-21	-3.21E-22	-2.87E-23	-1.74E-24	-9.11E-26	-4.45E-27

CHAPTER 12
BOX STRUCTURE

An Open Structure with Four Rectangular Plates

Another example for applying the considered approach is that of a box structure consisting of four walls and is open in the z-direction. All the walls are rectangular plates. The plates are located in x-y and z-y planes. Each of the four plates is assumed to be subjected to the same uniformly distributed load but in an opposite direction to the one parallel to it.

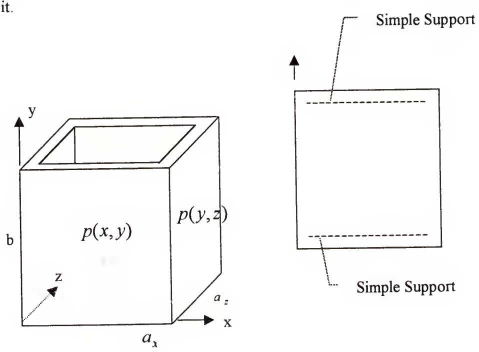

Figure 12.1 Box Structure of plates simply supported at y=0 along the lower edges and at y=b along the upper edges.

The deflection of the plate in the x-y plane is

$$w_1(x,y)=\sum_{m=1}^{M}\sum_{n=1}^{N}A_{mn}(1-\frac{x}{a_x}+\frac{x^2}{a_x^2})\cos(\frac{n\pi x}{a_x})\sin(\frac{m\pi y}{b}) \tag{12.1}$$

The deflection of the plate in the z-y plane is

$$w_2(y,z)=\sum_{m=1}^{M}\sum_{n=1}^{N}B_{mn}(1-\frac{z}{a_z}+\frac{z^2}{a_z^2})\cos(\frac{n\pi z}{a_z})\sin(\frac{m\pi y}{b}) \tag{12.2}$$

The strain energies, kinetic energies and external work of the plates are formulated in the same manner as in chapter 5. The strain energy, the kinetic energy and the external work can be calculated by the same procedure used in chapter 5.

The strain energies of the four plates are added to obtain the total strain energy of the structure. Also the kinetic energy of the four plates, are added to obtain the total kinetic energy of the structure. The external work for the four plates is added to obtain the total external work for the structure.

Since the structure is simply supported along the edges at $y=0$ and at $y=b$, the boundary conditions at $y=0$ and $y=b$ are satisfied. The deflection and moment along the edges parallel to y-axis for the two intersecting plates should be equal. Hence, the unsatisfied constraints are

$$G_{ji}=w_1(x_{ji},y_{ji})-w_2(y_{ji},z_{ji}) \tag{12.3}$$

$$G_{ji+I}=-D[w_{1xx}(x_{ji},y_{ji})+\nu w_{1yy}(x_{ji},y_{ji})]+$$

$$D[w_{2zz}(y_{ji},z_{ji})+\nu w_{2yy}(y_{ji},z_{ji})] \tag{12.4}$$

where $i = 1,2,........I$, I is the number of discrete points at each edge, $j = 1,2,...J$, and J is the number of the welded edges.

The Lagrangian function is

$$L = 2U_1 + 2U_2 - 2W_1 - 2W_2 - 2T_1 - 2T_2 + \sum_{j=1}^{J}\sum_{i=1}^{2I} \lambda_{ji} G_{ji} \tag{12.5}$$

where U_1 is the strain energy of the x-y plate, U_2 is the strain energy of the y-z plate, T_1 is the kinetic energy of the x-y plate, T_2 is the kinetic energy of the y-z plate, W_1 is the external work of the x-y plate and W_2 is the external work of the y-z plate. Applying the same procedure as in the previous cases, the vibratory response, natural frequencies, and natural modes can be determined.

Result

The dimensions of the considered structure are $a_x/b = 0.5$ and $a_z/b = 1$. Four discrete points are selected along each of the edges parallel to the y-axis. Figure 12.2 shows the natural frequency result at N=15. Figures 12.3 and 12.4 show the mode shape for the two plates in the structure. Table 12.1 shows the fundamental frequency parameter result for the structure, while tables 12.2-12.5 show the coefficients of the assumed deflection function corresponding to the fundamental frequency.

Table 12.1 Fundamental frequency of a box structure made from four welded plates for different N terms, $a_x/b = 0.5$, $a_z/b = 0.5$

N	5	10	15
λ	151.681	151.681	151.6802

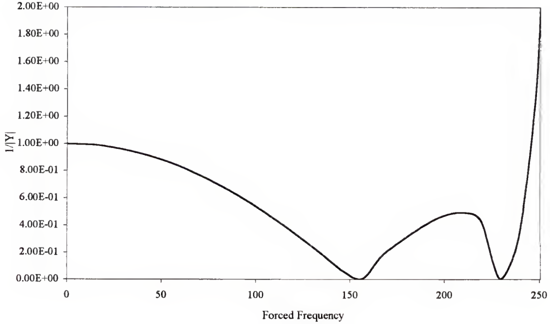

Figure 12.2 The inverse of normalized maximum absolute deflection versus forced frequency for box structure, N=15, $a_x = a_z = 1$, b=2

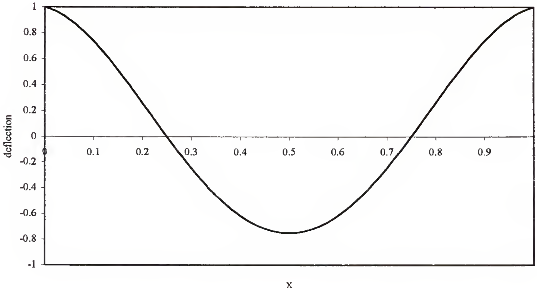

Figure 12.3 Mode shape of x-y plate of box structure along x-axis at y=b/2, a_x=1,b=2, a_z=1, N=15.

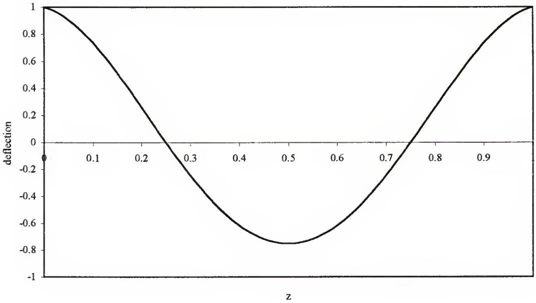

Figure 12.4 Mode shape of y-z plate of box structure along z-axis at y=b/2, ax=1,b=2, az=1, N=15

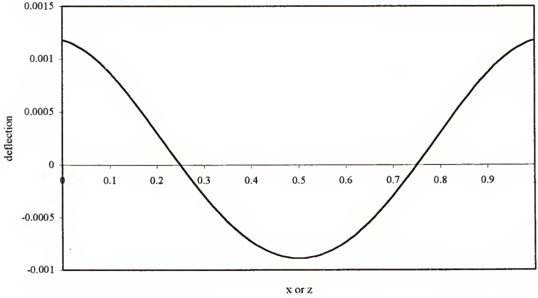

Figure 12.5 Deflection of x-y plate or y-z plate in Box Structure along x-axis or z-axis at y=b/2, N=15, a_x=1,b=2, a_z=1

Table 12.2 Displacement parameters A_{mn} for x-y plate of Box Structure; $a_x = 1$, $b = 2$, $a_z = 1$

n	m							
	1	2	3	4	5	6	7	8
1	-1.6E-22	0.173169	4.84E-23	4.35E-09	5.21E-24	3.61E-10	1.33E-24	6.35E-11
2	0	0	0	0.00E+00	0.00E+00	0.00E+00	0.00E+00	0.00E+00
3	-1.4E-22	6.48E-08	9.84E-24	1.12E-09	1.48E-24	1.08E-10	4.10E-25	1.99E-11
4	0	0	0	0.00E+00	0.00E+00	0.00E+00	0.00E+00	0.00E+00
5	1.25E-23	9.33E-09	2.93E-24	4.40E-10	6.68E-25	5.26E-11	2.11E-25	1.06E-11
6	0	0	0	0.00E+00	0.00E+00	0.00E+00	0.00E+00	0.00E+00
7	2.04E-24	2.34E-09	1.03E-24	1.91E-10	3.32E-25	2.87E-11	1.22E-25	6.41E-12
8	0	0	0	0.00E+00	0.00E+00	0.00E+00	0.00E+00	0.00E+00
9	5.8E-25	7.85E-10	4.1E-25	8.88E-11	1.74E-25	1.63E-11	7.41E-26	4.08E-12
10	0	0	0	0.00E+00	0.00E+00	0.00E+00	0.00E+00	0.00E+00
11	2.15E-25	3.16E-10	1.84E-25	4.43E-11	9.47E-26	9.59E-12	4.62E-26	2.66E-12
12	0	0	0	0.00E+00	0.00E+00	0.00E+00	0.00E+00	0.00E+00
13	9.4E-26	1.45E-10	9.07E-26	2.35E-11	5.39E-26	5.80E-12	2.94E-26	1.77E-12
14	0	0	0	0.00E+00	0.00E+00	0.00E+00	0.00E+00	0.00E+00
15	4.63E-26	7.4E-11	4.83E-26	1.32E-11	3.19E-26	3.61E-12	1.91E-26	1.19E-12

Table 12.3 Displacement parameters A_{mn} for x-y plate of Box Structure; $a_x = 1$, $b = 2$, $a_z = 1$ (continuation of table 12.2)

n	m						
	1	2	3	4	5	6	7
1	4.86E-25	1.66E-11	7.91E-25	5.55E-12	-1.37E-25	2.20E-12	1.84E-25
2	0.00E+00	0.00E+00	0.00E+00	0.00E+00	0.00E+00	0.00E+00	0.00E+00
3	1.54E-25	5.31E-12	2.55E-25	1.80E-12	-4.47E-26	7.18E-13	6.04E-26
4	0.00E+00	0.00E+00	0.00E+00	0.00E+00	0.00E+00	0.00E+00	0.00E+00
5	8.41E-26	2.95E-12	1.44E-25	1.02E-12	-2.56E-26	4.14E-13	3.50E-26
6	0.00E+00	0.00E+00	0.00E+00	0.00E+00	0.00E+00	0.00E+00	0.00E+00
7	5.25E-26	1.89E-12	9.34E-26	6.75E-13	-1.71E-26	2.79E-13	2.37E-26
8	0.00E+00	0.00E+00	0.00E+00	0.00E+00	0.00E+00	0.00E+00	0.00E+00
9	3.46E-26	1.28E-12	6.46E-26	4.75E-13	-1.22E-26	2.01E-13	1.73E-26
10	0.00E+00	0.00E+00	0.00E+00	0.00E+00	0.00E+00	0.00E+00	0.00E+00
11	2.34E-26	8.90E-13	4.61E-26	3.45E-13	-8.99E-27	1.50E-13	1.30E-26
12	0.00E+00	0.00E+00	0.00E+00	0.00E+00	0.00E+00	0.00E+00	0.00E+00
13	1.61E-26	6.31E-13	3.34E-26	2.55E-13	-6.76E-27	1.15E-13	1.01E-26
14	0.00E+00	0.00E+00	0.00E+00	0.00E+00	0.00E+00	0.00E+00	0.00E+00
15	1.13E-26	4.53E-13	2.46E-26	1.91E-13	-5.15E-27	8.86E-14	7.87E-27

CHAPTER 13
SUMMARY, CONCLUSIONS AND RECOMMENDATIONS

Summary

The work undertaken in this study can be summarized as follows:

1) The use of the undetermined multipliers method in evaluating the vibratory response of elastic structures with general shapes boundary conditions have been successfully investigated.
2) The method is then utilized to determine the natural frequencies and natural modes for several illustrative cases of structures.
3) Numerical examples for beam problems are considered for a variety of end conditions. These are:
    a) Simple Supported Ends (chapter 4)
    b) Clamped-Simple Supported Ends (chapter 4)
    c) Clamped-Clamped Ends (chapter 4)
    d) Clamped-Free Edges (chapter 4)
    e) Multi Span Beam (chapter 4)
4) The method has also been applied to plate problems with the following boundary conditions:
    a) Simply Supported Edges (chapter 6)

b) Two Clamped Edges in the y direction and Simply Supported in the x-direction. (Chapter 6)

c) Clamped Edges in the y direction at x=0 and Simply Supported at the other edges (chapter 6)

d) Clamped Edges (chapter 6)

e) Mixed Boundary Conditions (chapter 6)

f) Plates with Arbitrary Shapes (chapter 7)

g) Plates with Holes (chapter 8)

h) Plate with arbitrarily shape with arbitrarily support conditions (chapter 11)

i) The vibratory response of reinforced plates and evaluation of their natural frequencies and natural modes is also investigated in chapter 9.

j) The procedure for applying the method to honeycomb structures is developed and presented in chapter 10.

k) The method is also applied to box-type structures as presented in chapter 12.

Conclusion

The following can be concluded from the reported investigation:

1) The proposed approach shows excellent promise in extending the Rayleigh-Ritz method to deal with the dynamic response of elastic structures with arbitrary shapes, loading and boundary conditions.

2) The procedure does not require pre or post processing and is very efficient computationally.

3) The vibratory response and the natural modes are evaluated as a finite series. The coefficients of the series functions give physical insight into the contribution of each term in the function to the response and the shape of the natural modes.
4) The calculated results for the natural frequencies are in excellent agreement for all the considered cases, which have analytical or numerical solution in the published literature.
5) The convergence of the solution can be accelerated by the selection of the series type and terms (odd or even or both), which should be appropriate to each problem based on inspection of the shape and boundary conditions. In situations where this is difficult to judge, a full series should be considered and the number of terms increased successively until convergence occurs.

Recommendations

The following are some recommendations for future studies:

1. Since convergence of the result is the only criterion used to determine the number of terms required to reach the solution, it would be interesting to compare the obtained results with finite element solutions for several examples of complex structures. In this case, a comparison of the CPU time required to achieve the same level of accuracy by both methods can shed light on the generality of the proposed approach and the areas where it can be used to advantage.
2. Whenever a significant difference exists between the proposed method and the FE method, it is recommended that an experimental test on an actual structure or a scale

model of it should be conducted to determine which method gives a closer answer to the experimental results.

3. A study of the type of function which speeds the convergence for different types of structures should be undertaken to provide a guide for the user instead of simply using a full series of a particular type and running the risk of requiring large number of terms to reach convergence.

REFERENCES

1. Sheikh, Abdul Hamid, and Mukhopadhyay, Madhujit, "Transverse Vibration of Plate Structures With Elastically Restrained Edges by the Spline/Finite Strip Method," Journal of Vibration and Acoustics, vol. 115, July 1993, pp. 295-301.

2. Grossi, Ricardo O., Arenas, Blanca del V., and Laura, P. A. A., "Free Vibration of Rectangular Plates With Circular Openings," Ocean Engng., vol 24, No. 1, 1997, pp. 19-24.

3. Chang, T.–P., and Liang, J.–Y., "Vibration of Postbuckled Delaminated Beam-plates," Int. J. Solids Structures, vol. 35, No. 12, 1998, pp. 1199-1217.

4. Malik, Moinuddin, and Bert, Charles W., "Three Dimensional Elasticity Solutions For Free Vibrations of Rectangular Plates By The Differential Quadrature Method," Int. J. Solids Structures, vol. 35, Nos. 3-4, 1997, pp. 299-318.

5. Bambill, Diana V., Rossi, Raul E., Jederlinic, Veronica, and Rossit, Carlos A., "Vibrations of Rectangular Plates With a Free Edge in The Case of Discontinuously Varying Thickness," Int. J. Solids Structures, vol. 24, No. 1, 1997, pp. 45-49.

6. Liew, K. M., and Wang, C. M., "Flexible Vibration of In-Plane Loaded Plates with Straight Line/Curved Internal Supports," Journal of Vibration and Acoustics, vol. 115, 1993, pp. 441-447.

7. Al-Shareedah, E. M., and Seireg, A. A., "Use of Undetermined Multipliers in the Design of Stiffened Plate," Computers in Mechanical Engineering, vol. 4, No. 5, 1986, pp. 57-64.

8. Al-Shareedah, E. M., and Seireg, A. A., "Use of Undetermined Multipliers in the Solution of Plate Problems," Computers in Mechanical Engineering, vol. 4, No. 3, 1985, pp. 59-68.

9. Al-Shareedah, E. M., and Seireg, A. A., "The Design of Slabs With Constraining Columns Using the Undetermined Multipliers Method," Computers in Mechanical Engineering, vol. 4, No. 4, 1986, pp. 59-68.

10. Chen, Tzu-Yang, Ph.D dissertation, "The Use of Undetermined Multipliers in The Analysis and Opimum Design of Elastic Structures," Gainesville, Florida, University of Florida, 1989.

11. Soedel, Werner, "Vibrations of Shells and Plates," New York, Marcel Dekker, Inc, 1993.

12. Troitsky, M. S., "Stiffned Plates, Bending, Stabillity and Vibrations," Amsterdam, Elsevier Scientific Publishing Company, 1976.

13. Rao, Singiresu S., "Mechanical Vibrations," New York, Addison-Wesley Publishing Company, 1995.

14. James, M. L., Smith, G. M., Wolford, J. C., and Whaley, P. W., "Vibration of Mechanical and Structural Systems," New York, HarperCollines College Publishers, 1994.

15. Leissa, Arthur W., "Vibration of Plates," Washington, D. C., National Aeronautics and Space Administration, 1969.

16. Rao, J. S., "Dynamics of Plates," New York, Marcel Dekker, Inc., 1999.

17. Laura, P. A. A., Futierrez, R. H., Sonzogni, V., and Idelsohn, S., "Transverse Vibrations of Rectangular Plates of Non-Uniform Thickness with a Free, Concentric Circular Hole,"Journal of Sound and Vibration, vol. 199, No. 4, 1997, pp. 704-710.

18. Gorman , D. J., "A Highly Accurate Analytical Solution for Free Vibration Analysis of Simply Supprted Right Triangular," Journal of Sound and Vibration, vol. 89, No. 1, 1983, pp. 107-118.

19. Gorman , D. J., "A Note on Bending Moment Distributions in Cantilever Plates in Fundamental Mode Vibration," Journal of Sound and Vibration, vol. 122, No. 1, 1988, pp. 185-187.

20. Gorman, D. J., "Free Vibration Analysis of Right Triangular Plates with Combinations of Clamped-Simply Supported Boundary Conditions," Journal of Sound and Vibration, vol. 106, No. 3, 1986, pp. 419-431.

21. Gorman, D. J., "Free Vibration Analysis of Cantilever Plates by the Method of Superposition," Journal of Sound and Vibration, vol. 49, No. 4, 1976, pp. 453-467.

22. Gorman, D. J., "Accurate Analytical Solution for Free Vibration of the Simply Supported Triangular Plate," Journal of Sound and Vibration, vol. 27, No. 5, 1989, pp. 647-651.

23. Gorman, D. J., "Accurate Free Vibration Analysis of Right Triangular Plate with One Edge," Journal of Sound and Vibration, vol. 131, No. 1, 1989, pp. 115-125.

24. Gorman, D. J., "Free Vibration Analysis of the completely Free Rectangular Plate by the Method of Superposition," Journal of Sound and Vibration, vol. 57, No. 3, 1978, pp. 647-651.

25. Gorman, D. J., "Modified Superposition Method for the Free Vibration Analysis of Right Triangular Plates," Journal of Sound and Vibration, vol. 112, No. 1, 1987, pp. 173-176

BIOGRAPHICAL SKETCH

Mahmoud Kaoud was born in Dhuba, Saudi Arabia in 1960. He finished his high school education in the same city. After getting his Mechanical Engineering Bachelor's degree from King Saud University in 1985, he worked as an engineer in quality assurance in Saudi Telecom until 1987. He worked in Education Ministry until 1991. Then he worked as a teacher at the college of Technology.

He received a government scholarship to pursue education in Mechanical Engineering in the USA. He got his M. S. degree from Western Michigan University in 1995. He was given another scholarship to continue his Ph.D. in the same field at the University of Florida in Gainesville.

I certify that I have read this study and that in my opinion it conforms to acceptable standards of scholarly presentation and is fully adequate, in scope and quality, as a thesis for the degree of Doctor of Philosophy.

Ali Seireg

Ali A. Seireg, Chairman
Ebaugh Professor of Mechanical
Engineering

I certify that I have read this study and that in my opinion it conforms to acceptable standards of scholarly presentation and is fully adequate, in scope and quality, as a thesis for the degree of Doctor of Philosophy.

Joseph Duffy

Joseph Duffy
Graduate Research Professor of
Mechanical Engineering

I certify that I have read this study and that in my opinion it conforms to acceptable standards of scholarly presentation and is fully adequate, in scope and quality, as a thesis for the degree of Doctor of Philosophy.

John Ziegert
Associate Professor of
Mechanical Engineering

I certify that I have read this study and that in my opinion it conforms to acceptable standards of scholarly presentation and is fully adequate, in scope and quality, as a thesis for the degree of Doctor of Philosophy.

Carl Crane
Professor of Mechanical
Engineering

I certify that I have read this study and that in my opinion it conforms to acceptable standards of scholarly presentation and is fully adequate, in scope and quality, as a dissertation for the degree of Doctor of Philosophy.

Fazil T Najafi

Fazil T. Najafi
Professor of Civil and Coastal
Engineering

This dissertation was submitted to the Graduate Faculty of the College of Engineering and to the Graduate School and was accepted as partial fulfillment of the requirements for the degree of Doctor of Philosophy.

August 2000

M. J. Ohanian
Dean, College of Engineering

Winfred M. Phillips
Dean, Graduate School